Changes in Functional Connectivity Due to Modulation by Task and Disease

Sasidhar Madugula

The Queen's College

Trinity Term 2013

FMRIB Centre

Nuffield Department of Clinical Neurosciences

Changes in Functional Connectivity Due to Modulation by Task and Disease

Sasidhar Madugula

Trinity Term 2013
The Queen's College
Nuffield Department of Clinical Neurosciences

A thesis submitted for the requirements of the degree of Master of Science by Research at the University of Oxford

Abstract

Soon after the advent of signal-recording techniques in the brain, functional connectivity (FC), a measure of interregional neural interactions, became an important tool to assess brain function and its relation to structure. It was discovered that certain groups of regions in the brain corresponding to behavioural domains are organized into intrinsic networks of connectivity (ICNs). These networks were shown to exhibit high FC during rest, and also during task. ICNs are not only delineated by areas which correspond to various behaviours, but can be modulated in the long and short-term in their connectivity by disease conditions, learning, and task performance. The significance of changes in FC, permanent and transient, is poorly understood with respect to even the simplest ICNs corresponding to motor and visual regions. A better grasp on how to interpret these changes could elucidate the mechanisms and implications of patterns in FC changes during therapy and basic tasks. The aim of this work is to examine long-term changes in the connectivity of several ICNs as a result of modulation by stroke and rehabilitation, and to assess short term changes due to simple, continuous task performance in healthy volunteers.

To explore long-term changes in ICN connectivity, fifteen hemiparetic stroke patients underwent resting state scanning and behavioural testing before and after a two-week session of Constraint Induced Movement Therapy (CIMT). It was found that therapy led to localized increases in FC within the sensorimotor ICN.

To assess transient changes in FC with task, sixteen healthy volunteers underwent a series of scans during rest, continuous performance of a non-demanding finger-tapping task, viewing of a continuous visual stimulus, and a combined (but uncoupled) visual and motor task. Group Independent Component Analysis (ICA) revealed that canonical ICNs remained robustly connected during task conditions as well as during rest, and dual regression/seed analyses showed that visual and sensorimotor ICNs showed divergent patterns of changes in FC, with the former showing increased intra-network connectivity and the latter decreased intra-network connectivity. Additionally, it was found that task activation within ICNs has a relationship to these changes in FC.

Overall, these results suggest that modulation of functional connectivity is a valuable and informative tool in the study of disease recovery and task performance.

This thesis contains approximately 22,000 words.

Table of Contents

i. Abbreviations v

ii. List of Figures vii

iii. List of Tables ix

iv. List of Equations x

iv. Acknowledgements xi

1 INTRODUCTION 1

1.1 General Principles of Functional Connectivity 1
1.2 Intrinsic Connectivity Networks 3
1.3 Analysing and interpreting ICNs 6

2 MODULATION OF ICNS WITH STROKE AND REHABILITATION 12

2.1 Introduction 12
2.2 CIMT-Therapy Experiment Methods 19
2.2.1 Participants and Intervention 19
2.2.2 Scanning 22
2.2.3 Image pre-processing 23
2.2.4 ICA 23
2.2.5 Seed Analysis 24
2.3 Results for Stroke Rehabilitation Study 25
2.3.1 Differences in ICNs between patients and controls 25
2.3.2 Changes in connectivity with Constraint-Induced Movement Therapy 27
2.3.3 Correlation with clinical scores 29
2.4 Discussion of CIMT stroke rehabilitation results 29
2.4.1 Changes in FC associated with CIMT 31
2.4.2 Future Directions 34

3 STEADY-STATE TASKS 35

3.1 Introduction 35
3.2 Steady-State Task Experiment Methods 40
3.2.1 Participants and Experimental Design 40
3.2.2 Data Acquisition 42
3.2.3 Image pre-processing 42
3.2.4 Activation & Seed Analysis 43
3.2.5 Parcellation and Matrix ROI Analysis 45
3.2.6 Covariance vs. Correlation 47
3.2.7 Power, Correlation, and Activation Comparison 48
3.3 Steady-State Experiment Results 49
3.3.1 Task-localiser scans 49
3.3.2 ICN Extent and Shape during steady-state task conditions 51
3.3.3 Relationship of Activation to Correlation 56
3.3.4 Whole-brain changes in connectivity during steady-state tasks 58
3.3.4.1 Visual Task Condition-Seed Analysis 59
3.3.4.2 Visual Task Condition-Connectivity Matrices 61
3.3.4.3 Motor Task Condition-Seed Analysis 65

3.3.4.4 Motor Task Condition-Connectivity Matrices 68
3.3.4.5 Combined Visual and Motor Task Steady-State 73
3.4 DISCUSSION 75
3.4.1 ICN ROBUSTNESS AND TASK-ACTIVATION PATTERNS 76
3.4.2 CHANGES IN FC DURING VISUAL AND MOTOR TASKS—RELATIONSHIP TO ACTIVATIONS 77
3.4.2.1 Visual Steady-State Condition 78
3.4.2.2 Motor Steady-State Condition & Activation-Connectivity Relationship 79
4 OVERALL SUMMARY & FUTURE DIRECTIONS 83
Appendix 86
References 89

i. Abbreviations

BOLD	Blood Oxygen Level Dependent
CIMT	Constraint Induced Movement Therapy
CSF	Cerebrospinal Fluid
CST	Corticospinal Tract
DTI	Diffusion Tensor Imaging
EEG	Electroencephalography
EXCITE	Extremity Constraint Induced Therapy Evaluation
FAST	FMRIB's Automated Segmentation Tool
FC	Functional Connectivity
FLIRT	FMRIB's Linear Image Registration Tool
fMRI	Functional Magnetic Resonance Imaging
FMRIB	Centre for Functional MRI of the Brain
FNIRT	FMRIB's Non-linear Image Registration Tool
FSL	FMRIB Software Library

ICA	Independent Component Analysis
M1	Primary Motor Cortex
MPRAGE	Magnetization Prepared Rapid Gradient Echo
MRI	Magnetic Resonance Imaging
MRS	Magnetic Resonance Spectroscopy
PCA	Principle Component Analysis
PPI	Psychophysiological Interactions
SMA	Supplementary Motor Area
TMS	Transcranial Magnetic Stimulation
WMFT	Wolf Motor Function Test

ii. List of Figures

1.1 Ten robust, canonical ICNs corresponding to behavioural domains

1.2 Comparison of Voxel-Based-Seed Analysis and PICA

1.3 Changes in DMN spatial maps in patients with Alzheimer's disease

2.1 Neural activation during motor task in stroke patients

2.2 Group sensorimotor ICNs in healthy controls and stroke patients

2.3 Changes in FC with stroke and rehabilitation, seed maps

3.1 Schematic representation of steady-state scans and localizer scan

3.2 Task Localiser

3.3 Correlation of Smith 10 to Steady-State ICN maps

3.4 Correlation of Smith 10 to Steady-State ICN maps-Diagonal only

3.5 Spatial maps of Steady-State ICN maps overlain on Smith 10

3.6 Activation-Correlation Histograms

3.7 Visual Steady-State seed maps

3.8 Changes in FC during Visual Steady-State in activated/deactivated visual areas

3.9 Changes in FC during Visual Steady-State across 10 ICNs

3.10 Motor Steady-State seed maps

3.11 Changes in FC during Motor Steady-State in activated/flipped motor areas

3.12 Symmetrical changes in FC for flipped and un-flipped motor activation loci

3.13 Changes in FC during Motor Steady-State across 10 ICNs

3.14 Visual & Motor combined Steady-State Interaction seed maps

A.1 Extended Activation-Correlation Histograms

A.2 Large parcellation matrices for visual, motor, and combined visuo-motor conditions

iii. List of Tables

2.1 Patient details

3.1 Parcellations

iv. List of Equations

2.1 Correlation
2.2 Covariance

iv. Acknowledgements

I would like to thank the people without whom the completion of this thesis would not have been possible: My supervisors Tamar Makin, Eugene Duff, and Heidi Johansen-Berg, who not only gave me a world-class education in the field of imaging neuroscience, but trained me in the arts of critical thinking and analysis. Another thanks to Eugene and Tamar as it was they who collected the steady-state task data which forms one of the subjects of this thesis. Thanks to Dr. Jakob Blicher for providing us with resting-state stroke data. I would also like to thank the participants in the various studies covered by this thesis, and everyone at FMRIB for making the past year a wonderfully memorable one. Finally, I would like to thank my family for all their loving support.

1 Introduction

The aim of this work is to contribute to the current knowledge on the interaction between perturbations in functional connectivity (FC) and functional states of the brain. This section surveys the existing literature regarding task and disease state modulation of FC.

1.1 General Principles of Functional Connectivity

With the emergence of functional Magnetic Resonance Imaging (fMRI) as an important tool for diagnosis and research in the last two decades, functional scans have been used in a variety of applications ranging from mapping of functional areas to assessment of stroke. In the course of some early fMRI experiments it was found that low frequency fluctuations in Blood Oxygen Dependent Levels (BOLD) signal correlate spatially in patterns reminiscent of those derived from task activation (Achard, Salvador, Whitcher, Suckling, & Bullmore, 2006; Cordes et al., 2001; Lowe, Dzemidzic, Lurito, Mathews, & Phillips, 2000). Since then, the assessment of temporal coupling between brain regions (Functional Connectivity) has been a primary means of investigating brain activity patterns. Functional Connectivity (FC) is defined as a measure of spatiotemporal synchrony of fMRI signal between anatomically distinct brain regions, and is reflective of global patterns in slow brain-wave fluctuations at a given time during a given task, resting, or disease condition (Jafri, Pearlson, Stevens, & Calhoun, 2008). FC was observed in modalities other than fMRI very early on; this was especially true of EEG (G L Gerstein, Bedenbaugh, & Aertsen, 1989; George L . Gerstein & Perkel, 1969). In a pioneering study, Friston et al. (1993) used Principle Component Analysis to resolve spatial maps of

temporally correlated regions in PET data into functional networks. Six volunteers were scanned in a PET scanner during verbal tasks (eyes closed). PCA revealed two major components explaining 86% of the variance in the data; these two components were comprised of areas such as the Anterior Cingulate Cortex (common to both), left dorsolateral prefrontal cortex, and Broca's area (first component only). While the brain regions in the first component, which stayed constant in correlation throughout the task, were known to have dense and reciprocal anatomic connections with one another, the second seemed to diminish with time. This was dubbed an "attentional network" by the authors and demonstrated the power of FC not only to identify networks of anatomically connected areas, but also areas which become associated due to particular external circumstances.

While there is some macroscopic understanding of the structure which leads to FC, the microscopic origin of spontaneous fluctuation has yet to be well understood (J. Damoiseaux & Rombouts, 2006). During task-activation the BOLD signal only changes by 1-5%--this means that the vast majority of the signal is made up of baseline activity and also implies that spontaneous fluctuations play important, uninterruptable roles in brain function (J. S. Damoiseaux & Greicius, 2009). Originally in the field, there was some confusion as to the precise origin of these fluctuations. Studies showing that BOLD fluctuations occur at much lower frequencies (.01-.1 Hz) than cardiac and respiratory oscillations (Cordes et al., 2000, 2001) and a correspondence between electrophysiological recordings and functional fluctuations as well as correlations (Nir et al., 2008; Shmuel & Leopold, 2008; Shmuel et al., 2002) strongly suggest neuronal

origins. Additionally, because FC is measured mostly in grey matter, it is widely agreed that it represents processes of neuronal modulations of brain signal (J. Damoiseaux & Rombouts, 2006). The driving force behind this neuronal activity is still unknown, and is thought to be due to common signal inputs to functionally connected areas from neurotransmitter systems (Karl J. Friston, 1994; Van Dijk et al., 2010).

1.2 Intrinsic Connectivity Networks

Owing to the fact that functional networks have distinct temporal characteristics, separate functional networks can be identified from a single series of resting fMRI data (Vahdat, Darainy, Milner, & Ostry, 2011). From the time it was first noticed that, during rest, the motor cortex remained temporally correlated to other regions in its functional network—i.e. cortical regions also activated during motor tasks (Biswal, Yetkin, Haughton, & Hyde, 1995), the study of spontaneous BOLD fluctuations has served to reveal other intrinsically correlated regions originally dubbed Resting State Networks (RSNs). More recently the term Intrinsic Connectivity Networks (ICNs) has been used in light of the fact that these networks remain coherent during not only rest, but also task conditions (Beckmann, DeLuca, Devlin, & Smith, 2005; J. Damoiseaux & Rombouts, 2006; Hutchison et al., 2013; Pettersson-Yeo, Allen, Benetti, McGuire, & Mechelli, 2011). These networks are robust and can be identified reliably in resting FMRI acquisitions due to their unique frequency characteristics (Beckmann et al., 2005; Cordes et al., 2000; Xiong, Parsons, Gao, & Fox, 1999). This reliability in ICN extraction from fMRI data has resulted in the classification of canonical networks associated with various behavioural domains

including vision, motor function, cognition, and auditory function, as shown below in Figure 1.1:

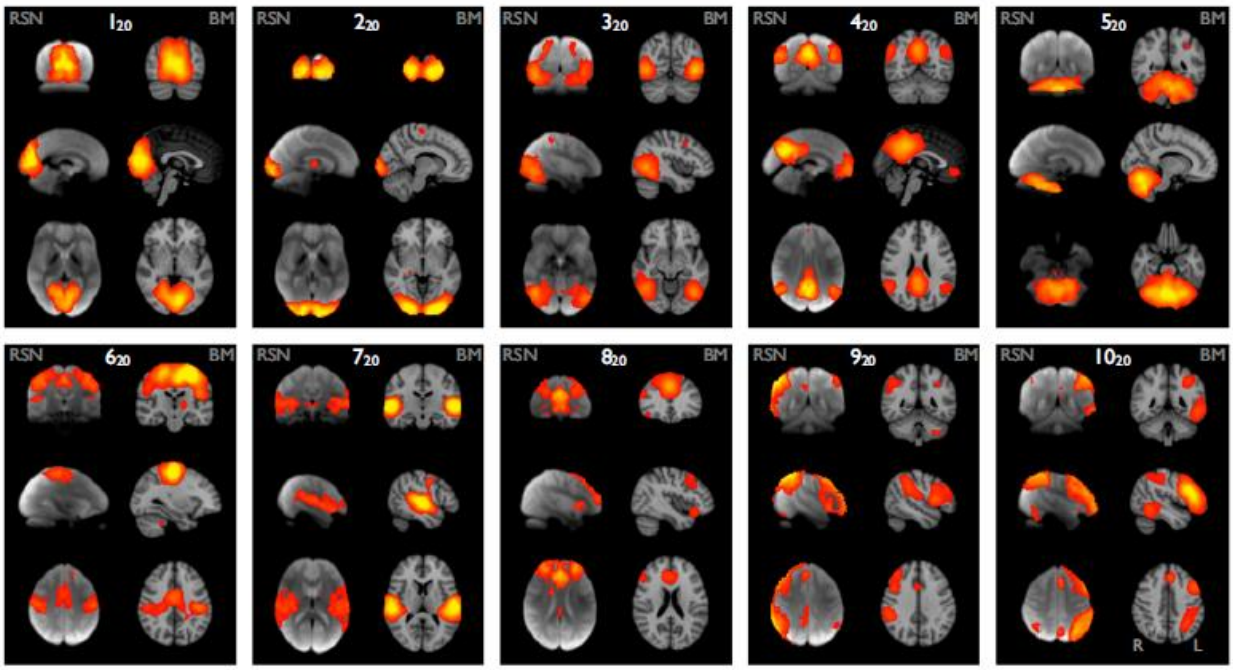


Figure 1.1: Ten well-matched pairs of networks from the 20-component analysis of the 29,671-subject BrainMap activation database and (a completely separate analysis of) the 36-subject resting FMRI dataset. This figure shows the 3 most informative orthogonal slices for each pair. (Left column of each pair) Resting FMRI data, shown superimposed on the mean FMRI image from all subjects. (Right column of each pair) Corresponding network from BrainMap, shown superimposed on the MNI152 standard space template image. The networks were paired automatically by using spatial cross-correlation, with mean r=0.53 (0.25:0.79); the weakest of these correlations thus has a significance of $P<10^{-5}$ (corrected). All ICA spatial maps were converted to z statistic images via a normalized mixture–model fit, and then thresholded at Z=3. *Taken from* (Smith et al., 2009).

The set of ten networks shown in Figure 1.1 have become well-established in the literature as the "Smith 10". The functional significance of each of these is given below (Smith et al., 2009).

1) Medial Visual. Involved in low-level visual processing of peripheral areas. Includes portions of V1 and V2 (Eickhoff et al., 2005; Kandel, Schwartz, Jessell, Siegelbaum, & Hudspeth, 2012) in higher-level visual areas and motion processing

2) Occipital Visual. Includes lower-level visual areas associated with foveal (central) visual-field inputs. Primarily covers V1 and V2, though parts of V3 and V4 are included as well (Eickhoff et al., 2005).
3) Lateral Visual. Involved in higher order visual processing-dorsal and ventral streams (Eickhoff et al., 2005).
4) Default Mode Network. Includes medial parietal (precuneus and posterior cingulate), bilateral inferior–lateral– parietal and ventromedial frontal cortex. This network has been the most widely studied in the context of resting state networks and is more active at rest than during task (Greicius & Menon, 2004).
5) Cerebellum. Plays major role in motor feedback and control, and is implicated in brain functions ranging from attention regulation to fear response.
6) Sensorimotor. Includes supplementary motor area, primary sensorimotor cortex, and secondary somatosensory cortex (though this can vary across datasets). Involved in voluntary movement and somatosensory processing and perception (Biswal et al., 1995; K J Friston, Frith, Fletcher, Liddle, & Frackowiak, 1996).
7) Auditory. Includes the superior temporal gyrus, Heschl's gyrus, and posterior insular. Involved in sound and language processing, as well as cognition and attention. Also includes the secondary somatosensory cortex (S2) which plays a role in pain processing and tactile attention (Bolognini et al., 2011).
8) Executive Control. This network is based in medial-frontal areas such as the paracingulate and anterior cingulate cortices, as well as parietal areas. It is active during cognitive paradigms of executive control (Seeley et al., 2007; Sridharan, Levitin, & Menon, 2008; White, Joseph, Francis, & Liddle, 2010).

9) Right Lateral and 10) Left Lateral. These maps include several fronto-parietal regions such as Broca's and Wernicke's areas, as well as parts of the superior parietal cortex. They are lateralized and for the most part spatially mirror one another. Despite this, they are associated with different sets of functions involving language, spatial awareness (right network only), and perception of pain and touch--this is expected as these functions are known to be lateralized (Kandel et al., 2012).

The roles that these networks play in brain function and an understanding of their potential is crucial to understanding changes in their functional connectivity patterns.

1.3 Analysing and interpreting ICNs

Methods used to analyse changes in FC and in ICNs take advantage of various statistical techniques. One prominent technique is Independent Component Analysis (ICA), used to identify generalizable ICNs. ICA is a computational method that assumes various time-courses are statistically independent of one another and thereby extracts temporal and spatial maps, robustly in the case of fMRI (Beckmann et al., 2005). The advantage of this technique is that it is somewhat resistant to physiological noise caused by respiration and the cardiac pulse, as those frequencies are often isolated as separate components (J. S. Damoiseaux & Greicius, 2009). A disadvantage is that ICA is somewhat stochastic and can sometimes group anatomically diverse networks into the same component if parameters are not carefully chosen. After generating ICA components, average time signals across all the underlying voxels in each component (or parcellations of each component) are taken and correlated with one another. Another very pervasive method is seed analysis, which involves averaging the time-series of the voxels in a particular

region of interest (ROI, or seed) and correlating that with every other voxel in the brain, or other ROI time-courses. This correlational approach can be extended to a General Linear Model analysis which correlates voxels to multiple time series at once, and can factor in time-series from white matter (WM) and cerebro-spinal fluid (CSF; thus accounting for global physiological noise) as regressors of no interest. Seed analysis yields brain maps (for detailed visualization of one seed) and the latter connectivity matrices (for simultaneous conceptualization of many seeds). The methodological differences between the two approaches can result in different characterizations of connectivity patterns, and care must be taken to apply the appropriate analysis. These differences result from the nature of the parcels used in the connectivity matrices—average time-series over a group of voxels may exhibit significant changes while those of the individual voxels may not. One common issue to consider when weighing the two in a particular analysis, for example, is that both regression analyses often involves regressing out the mean global signal of the brain. This can result in false negative correlations (Murphy, Birn, Handwerker, Jones, & Bandettini, 2009)—the ICA-parcellation may avoid this difficulty (J. S. Damoiseaux & Greicius, 2009). An illustrative figure from their study is shown below (Fig. 1.2).

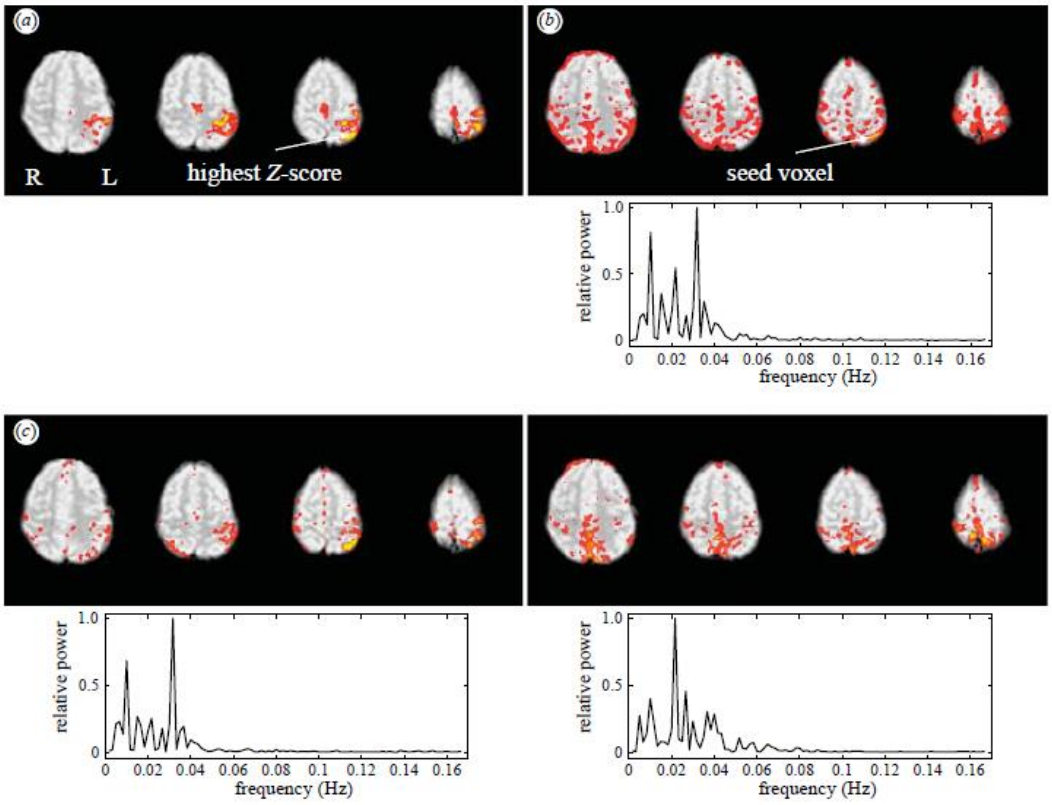


Figure 1.2: Comparison of seed-voxel-based correlation analysis and Probabilistic Independent Component Analysis (PICA): for seed-voxel based analysis, an activation dataset is first analysed to identify the location of most significant response to external stimulation (a). The time-course of the coinciding voxel in the resting data is used as a reference time-course for a correlation analysis of all other time-courses acquired under rest. The resulting correlation map (b) shows significant resting correlation in similar motor areas as the activation map, but also identifies part of the ipsi-lateral motor cortex. In addition, other regions outside of these motor areas were also found, including medial and lateral posterior parietal areas and prefrontal regions. In a PICA decomposition of the resting data (c), similar cortical regions are identified by two (out of 40) separate spatial maps. The multiple regression framework implicit in a PICA decomposition separates resting correlations in motor areas (left) from other cortical areas. This separation is induced by the fact that the associated time-courses are significantly different: the associated normalized power spectra show different peak frequencies. All spatial maps were thresholded using mixture modeling (at p=0.5) and are shown in radiological convention. *Taken from* (Beckmann et al., 2005)

Employing these methods, resting-state fMRI has been used to identify the architecture of healthy brain organization, as well as reorganization (Smith et al., 2009; Vincent et al., 2007). One network, the default mode network (DMN), has generated particular interest in this context, as it is usually not active while participants are engaged with their environment (i.e. it is more active during rest). Alterations in DMN connectivity have

been implicated in a large range of neuropathologies. For instance, in Alzheimer's disease the Posterior Cingulate, Hippocampus, and Entorhinal Cortex show robust, group-level changes in intrinsic functional connectivity patterns, illustrating the potential utility of observing FC change as a means of diagnosis (Greicius, Srivastava, Reiss, & Menon, 2004). Figure 1.3 shows these effects in elderly patients:

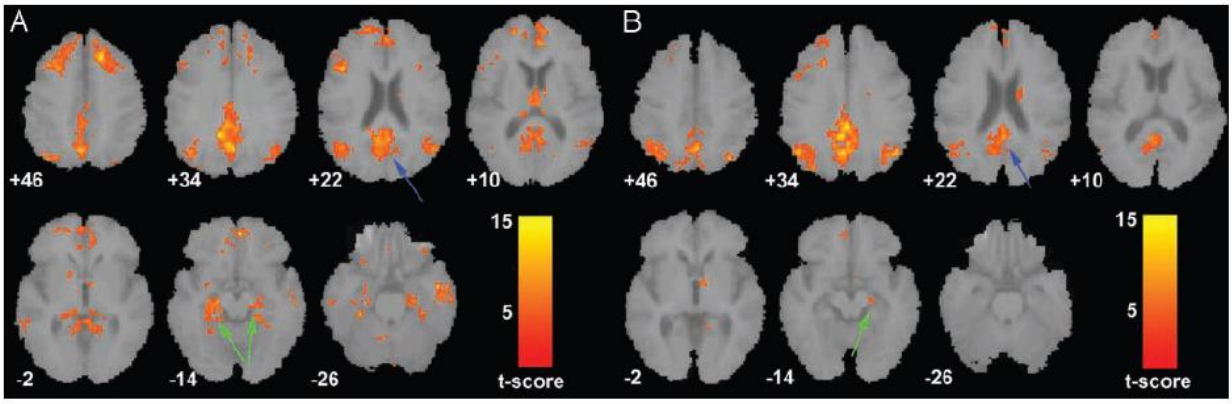


Figure 1.3: Default-mode network in healthy elderly and AD subjects (Washington University data). Axial images showing the default-mode network for the healthy elderly (A) and AD (B) groups. The blue arrows indicate the PCC. The hippocampus and underlying entorhinal cortex (green arrows) were detected bilaterally in healthy elderly subjects (A) but only in the right hemisphere in the AD group (B). Joint height and extent thresholds of P _ 0.0001 were used to determine significant clusters.

Other networks, such as the sensory-motor ICN, have been shown to change in their FC with long-term motor learning (Vahdat et al., 2011). There is also evidence that robust ICNs reflect the underlying structural connectivity of the brain. Diffusion Tensor Imaging (DTI) studies investigating the paths of white matter tracts have found connections between various regions connected to the DMN, as well as between areas in the sensory-motor ICN (Buckner, Krienen, & Yeo, 2013; Greicius, Supekar, Menon, & Dougherty, 2009). Furthermore, they can be mapped to coherent behavioural domains (Smith et al., 2009) and functional topographies (Yeo et al., 2011) suggesting that the intrinsic organization of ICNs corresponds to function in addition to underlying brain structure.

However, FC is not always compatible with structural phenomena in the brain (as seen above in the example from Friston et al. (1993)). For example, non-congenital sectioning of the corpus callosum disrupts inter-hemispheric functional connectivity (Johnston et al., 2008), but studies in adults with congenital agenesis of the corpus callosum show FC patterns identical to those in normal subjects (Tyszka, Kennedy, Adolphs, & Paul, 2011). To corroborate this, it was shown in a modelling study that imperfect correlation between DTI and FC is not an artefact of limitations in fMRI resolution—however the same study reported that inter-session connectivity amongst nodes is more consistent when they have stronger structural links (C J Honey et al., 2009). These intriguing results highlight the fact that there is much to be learned about the physiological origins and organizational principles of ICNs. The remainder of this work explores the modulation of ICNs by two different mechanisms, task performance and incidence of stroke, in the hopes of adding to our understanding of patterns of intrinsic connectivity and how changes in networks can be interpreted.

Long-term and non-dynamic changes in ICNs can result from learning or disease. The influence of stroke on brain anatomy and functional activation during motor task has been widely reported and analysed in the literature, but changes in networks of functional connectivity have not been so well characterized, especially over the course of therapy. The fruitful application of ICN analysis as a means to assess neurological conditions ranging from schizophrenia to Alzheimer's disease suggests that there is much to be gained from an understanding of how networks can recover from the ravages of a stroke incident, both in terms of the effectiveness of a particular therapy and in

terms of the importance of ICNs on behaviour. Chapter 2 summarizes the literature on this topic and describes an experiment and analysis pertaining to changes in resting-state functional connectivity over the course of Constraint-Induced Movement Therapy for stroke.

Shifting focus to dynamic changes, changes in our understanding of the relationship of ICNs to task modulation has shifted views on the roles of these networks. Initially thought to become dissolved during task performance, it has since been established—first notably in the DMN (Greicius & Menon, 2004)—that Intrinsic Connectivity Networks in fact persist during task conditions. Understanding dynamic changes in ICN connectivity with task could shed light on the role of these networks in behaviour and their relationship to task activation. However, most studies have looked at higher-level cognitive networks when exploring this phenomenon (e.g. Greicius & Menon, 2004; Keeser et al., 2011; Newton, Morgan, Rogers, & Gore, 2011; Shirer, Ryali, Rykhlevskaia, Menon, & Greicius, 2012), leaving ICNs corresponding to basic visual and motor function relatively unstudied. In addition, the relationship between BOLD activation and connectivity changes during modulation is very poorly understood. The specific questions to be addressed are motivated by an extensive literature review in Section 3.1, and an experiment to help answer some of these questions is detailed in Chapter 3.

2 Modulation of ICNs with stroke and rehabilitation

The work in this chapter analyses and interprets the changes in ICN connectivity with rehabilitation, and is derived from a unique dataset comprising of resting state scans from stroke patients before and after a very popular stroke therapy called Constraint-Induced Movement Therapy (Steven L Wolf, Winstein, Miller, & Morris, 2006). The goal of the analysis is to further understanding of ways in which this prevalent therapy alters ICNs, and to assess the usefulness of resting-state measures in investigating recovery progress and predicting behavioural outcomes.

2.1 Introduction

Plasticity in motor maps has been shown to occur in response to a variety of manipulation types, including motor learning. One of the earliest fMRI studies on this topic showed that practised finger-tapping sequences showed larger areas of activation after 4 weeks than unpractised sequences (Ungerleider, 1995). Subsequent studies have confirmed and built upon this first study, finding that while adults do not exhibit as much plasticity as children, their motor cortices are capable of undergoing extensive reorganization (Doyon & Benali, 2005).

Motor reorganization is especially important in motor-related stroke recovery: the lesions resulting from ischemia in the brain cause *paresis,* a term that denotes weakness or paralysis of side of the body contralateral to the lesion. Longitudinal research into natural recovery has demonstrated that functional activation patterns, as assessed by

fMRI, become hyper-activated and shifted to the contralesional motor areas for a variety of motor tasks which would normally activate the ipsilesional side, and move back to the ipsilesional side over time (Kim et al., 2006; Tombari et al., 2004). This was shown directly to be a compensatory mechanism by Johansen-Berg et al. (2002). Tombari et al. (2004) also noted that in addition to the contralesional motor area, stroke patients recruit a number of auxiliary areas such as the Supplementary Motor Area (SMA) and Posterior Cingulate Cortex (PCC), and that these areas are often hyper-activated just like the contralesional motor areas. These types of changes in inter-hemispheric activations imply disruption of cortico-cortico and cortico-spinal structural pathways linking the two hemispheres (Westlake & Nagarajan, 2011). Therefore, given the relationship of functional connectivity to structural elements and symmetry it can be expected that structural connectivity may also be affected by stroke. An illustration of abnormal activation in stroke patients is shown below in Figure 2.1:

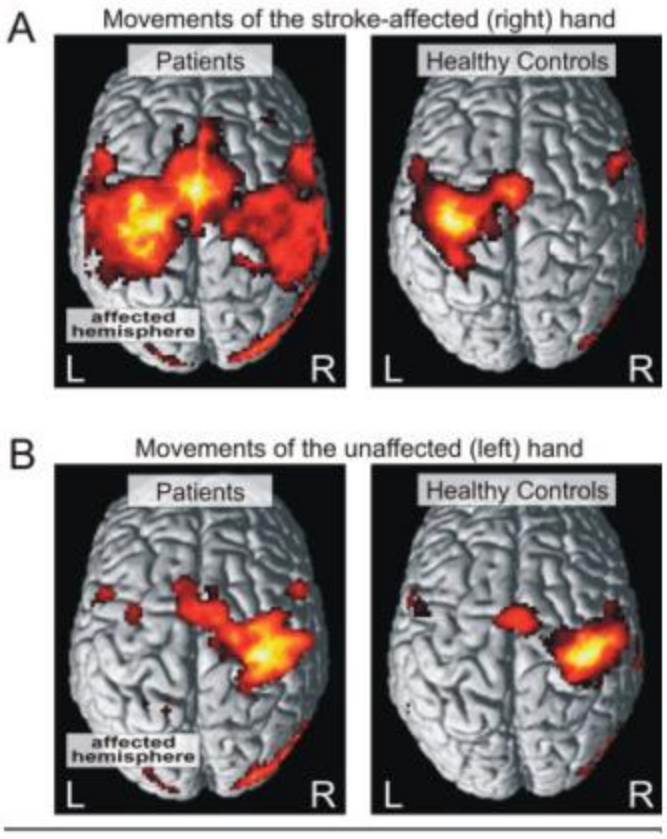


Figure 2.1 Neural activity during movements of the left or right hand in healthy subjects and in stroke patients with left-sided subcortical lesions ($p < 0.05$, corrected on the cluster level). Activation clusters were surface rendered onto a canonical brain shown from above. In stroke patients, movements of the impaired hand were associated with significant activations also in ipsilateral (ie, contralesional) motor areas, which were absent in the healthy control subjects (A) or during movements of the hand unaffected by the stroke (B). *Taken from* (Grefkes et al., 2008)

Resting-state data has been used in several studies to assess motor recovery after stroke (see papers described below). This was spurred largely due to its independence from task-based design (J. Damoiseaux & Rombouts, 2006), which is of a particular advantage when dealing with patients with paresis. Another major reason for the utilization of FC is that abnormalities in regions outside of the task-activated regions can be observed (Sharma, Baron, & Rowe, 2009). Seitz et al. (1999) conducted one of the first studies to assess FC in chronic stroke patients using PET data. After running principle component

analysis (PCA) on their scans, they were able to extract eight components, two of which differed significantly in the patients. Surprising results of the experiment included that the components showed very widespread abnormalities despite the localized nature of the lesion, and that the strength of one of the networks was correlated to behavioural performance. Since then, researchers have attempted to characterize these network abnormalities. Grefkes et al. (2008) found not only that subacute (34-55 days) stroke patients show less connectivity between contralesional and ipsilesional M1 areas, but also that the degree of inhibition between the two was negatively correlated with task performance.

Similarly, Wang et al. (2010) ran a longitudinal study with many time points (1 week, 2 weeks, 1 month, 3 months, 1 year) and upon analysing their imaging results with graph-theory methods found that network disruption after stroke can be understood as a "randomization" process, where information is passed more slowly between nodes, which in turn become less clustered. In the same spirit, Honey & Sporns (2008) theoretically assessed the effects of cortical lesions on networks of FC in macaque monkeys. They found that lesions over major structural network nodes such as pre-frontal and parietal areas caused greater disruption. Another notable facet of the literature on resting-state connectivity within the motor cortex is that interhemispheric coupling (connectivity between left M1 and right M1) is consistently found to be correlated to behavioural measures of motor recovery in stroke (Carter et al., 2010; Park et al., 2011; Westlake & Nagarajan, 2011), and even grows stronger immediately after stroke in some cases (Park et al., 2011). The studies detailed above illustrate some of the ways in which FC offers a unique approach to the analysis of the effects of stroke.

Since both fMRI activation and resting-state FC seem to present a powerful means by which to assess the effects of stroke and even to predict behavioural outcomes with natural recovery, it is not surprising that some research in this field has been carried out with respect to systematic stroke rehabilitation. The development of fMRI assessments of various therapy types could aid greatly in their comparison to other therapies and to "spontaneous" recovery (Westlake & Nagarajan, 2011). Current fMRI-assessed stroke rehabilitation studies present some difficulties because the time between the incident of stroke and onset of rehabilitation is very crucial: experiments in rats have shown that there is a significant difference in rehabilitative outcome if treatment is begun one day after incidence of stroke in comparison to one week (Kreisel, Hennerici, & Bäzner, 2007). Another problem lies in the fact that there is a lack of standardization of therapeutic paradigms in the literature, and that many longitudinal studies do not specify whether their patients are undergoing therapy at all. All this makes comparing studies rather difficult, but there have been many dedicated stroke rehabilitation studies assessing changes in functional activation levels using fMRI (Dimyan & Cohen, 2011; Hodics, Cohen, & Cramer, 2006). Hodics et al. (2006) in their review mention 10 papers which assessed therapy outcomes using task-based fMRI, noting that there is a general consensus that activation levels in post-therapy patients trend towards normal levels and patterns, with ipsilesional activation growing in strength while contralesional activation diminishes. They also note, however, that therapy type influenced findings significantly.

The above review is of papers which address the relationship between fMRI activation and stroke rehabilitation, from which the primary consensus seems to be that after stroke 1) Contralesional and peripheral motor area activation during tasks involving the affected limb increases and tends towards normal levels with recovery, 2) functional connectivity between motor hemispheres is decreased but increases with recovery. These increases are correlated with behavioural tests.

There are several papers in the literature exploring resting-state fMRI with regards to longitudinal motor rehabilitation. Sharma et al. (2009) cross-sectionally examined chronic stroke patients undergoing unspecified forms of physical therapy (external to the study), looking at functional activation and connectivity. They found that while return to normal patterns of task-related activation was associated with behavioural normality, resting-state FC remained abnormal. While this is an interesting result, it does not examine how the specific therapies utilized influences recovery in normal ICN structure. Another similar study in the literature by James et al. (2009) examines the effects of Accelerated Skill Acquisition Program therapy on resting state FC before and after a program lasting 3 weeks. They found using an effective connectivity approach that inter-hemispheric connectivity between the dorsal premotor cortices increased. Similar to the previous study, abnormal levels of inter-hemispheric connectivity persisted after therapy. This was a pilot study, so only six subjects and two controls were used and no seed analyses were performed. The remaining papers examine the effects of robot-assisted, brain stimulation, and drug therapies, reporting significant changes in connectivity amongst different sets of regions, mostly trending towards increases over

time (L. Jiang, Xu, & Yu, 2013). Another pilot study (involving two subjects), however, found that after 12 weeks of robot-assisted paretic limb therapy connectivity between hemispheres of the motor cortex *decreased* (Sergi et al., 2011). This illustrates that various therapies effect specific changes in functional connectivity.

The therapy used in our study is Constraint Induced Motion Therapy, or CIMT. This therapy involves intensive physical therapy sessions during which a goal-oriented task is conducted with the patient's paretic hand, while the functional hand is restrained. The purpose of this therapy is to encourage use of the paretic hand in daily life. Experimental assessment of CIMT over large numbers of patients has shown favourable outcomes, with statistically significant improvement in Wolf Motor Function Test (a widely used quantitative measure of upper extremity function comprised of 17 timed and functional tasks (S. L. Wolf et al., 2001)) scores. In fact, the popularity of this therapy is such that of the 10 papers cited by Hodics et al. (2006) in their review of fMRI activation studies, 5 concerned themselves with CIMT. Sawaki et al. (2008) found that the size of motor maps in post-CIMT patients increased using Transcranial Magnetic Stimulation (TMS), and this is a consistent result (Wittenberg & Schaechter, 2009). Johansen-Berg, Dawes, et al., (2002) found that improvement in hand function after CIMT was correlated to increases in activation in premotor cortex, contralesional secondary somatosensory cortex, and superior cerebellum while Laible et al. (2012) found the same correlation with regards to increases in ipsilesional S1 activation instead. This inconsistency may be due to experimental differences in the CIMT regime or motor function tests used. Despite the robustness of FC measures employed in other forms of therapy (as detailed above) and

the popularity of this therapy, there are no papers in the literature examining longitudinal changes in resting-state FC with CIMT. Furthermore, there are no studies which address global changes in ICNs with respect to any sort of rehabilitation. Therefore, the study detailed in this paper is a first attempt at trying to understand the global changes in functional connectivity during CIMT therapy. To this end, 15 patients and 20 controls were scanned during the resting state before and after therapy. Extensive motor test scores were collected before, after, and 3-months post therapy. The nature of the therapy led us to expect that functional connectivity between the sensorimotor network and the affected motor cortex would increase, while connectivity between the unaffected motor cortex and motor network would remain the same or decrease because of disuse. We would also expect that inter-hemispheric connectivity would increase in line with the studies described above.

2.2 CIMT-Therapy Experiment Methods

All data from this experiment, including the MRI scanning and behavioural tests, was collected by Dr. Jakob Udby Blicher of The Department of Neuroradiology, Aarhus University Hospital and his team. We are grateful for his provision of the data and his advice and support in conducting the analysis.

2.2.1 Participants and Intervention

Participants were recruited from all patients at Aarhus University Hospital currently undergoing CIMT using the Extremity Constraint Induced Therapy Evaluation (EXCITE) trials inclusion and exclusion criteria, as described in the work by Steven L Wolf,

Winstein, Miller, & Morris (2006). The EXCITE trial was the first nation-wide, randomized study to test a neurorehabilitation therapy among patients who retained their ability to wholly or partially extend their wrist and fingers. In the trial, patients (mean age 60, range 36-75) who had had a stroke within the previous 3 to 9 months were considered for inclusion, but in this study the outer limit was increased to 12 months post-stroke. Another difference was that no testing of cognitive function was assessed as an inclusion factor. However, assessment as to whether the subject would be able to complete the CIMT was done by a physician and a therapist. 21 age and gender-matched control participants were also recruited from members of the University and from the public (mean age 61, range 41-75). All subjects gave written informed consent, and the study was approved by the De Videnskabsetiske Komitéer for Region Midtjylland ethics committee. CIMT training was completed as described by Steven L Wolf et al. (2006). Participants were instructed to use restraining, protective safety mitt on their unimpaired arm (right arm was impaired for all but 4 analysed subjects) for 90% of their waking time two weeks for a total of 14 days. During weekdays in this period (for a total of 10 sessions) patients practiced adaptive task training (shaping) and standard task training for up to 6 hours a day. Adaptive task training involves discrete tasks which involve motor learning. Standard task training consists of more continuous blocks and involves sessions of "regular" task performance such as eating or writing in blocks between 15 and 20 minutes. After completion of therapy each day, patients were encouraged to try a couple of the tasks learned at home. Therapy was done with one occupational therapist and one physiotherapist per patient group of four.

Below is a list of study patients from whom data was analysed, along with information regarding the site and type of stroke, gender, age, and time since stroke. Of 21 patients three were excluded on the basis of study incompletion, and the remaining three due to their having strokes which coincided with the motor cortex. Excluded patients are highlighted in red.

Table 2.1 Patient Details

Patient	Age	Sex	Time since stroke (months)	Stroke type	Stroke location	Affected Hand	Reason for Exclusion
1	66	Male	12	Hemorrhagic	Left basal ganglia	Right	
2	67	Male	4	Ischemic	Frontal lesion left hemisphere. Old lesion in right putamen (acute MRI)	Right	
3	51	Female	9	Hemorrhagic	Left internal capsula	Right	Stroke location
4	70	Female	5	Ischemic	Right External capsula	Left	
5	67	Male	9	Ischemic	Right basal ganglia	Left	Study Incompletion
6	38	Female	4	Ischemic	Right Pons (acute MRI)	Left	
7	70	Male	9	Ischemic	Right MCA territory infarct affecting anterior and middle temporal lobe	Left	Stroke location
8	70	Male	4	Ischemic	Left Corona Radiata	Right	
9	75	Female	11	Ischemia	Left Corona Radiata and basal ganglia	Right	
10	67	Female	3	Ischemia	Left side of Pons	Right	
11	63	Male	4	Ischemic	Right internal capsula, Right Thalamus	Left	
12	66	Male	8	Ischemic	Left internal capsula and corona radiata	Right	
13	46	Female	5	Ischemic	Left Corona Radiata and basal ganglia	Right	Stroke location
14	61	Female	6	Ischemic	Multiple lesions in left Corona Radiata	Right	
15	71	Male	8	Ischemic	Right basal ganglia and insula	Left	Study Incompletion

16	64	Male	10	Ischemic	Left internal capsula	Right	
17	48	Male	4	Hemorrhagic	Right basal ganglia	Left	
18	36	Female	10	Ischemic	Small lesion on acute DWI in right parietal lobe, not visible on later T1	Left	
19	59	Male	5	ischemic	Left basal ganglia	Right	
20	51	Female	3	Ischemic	Left Corona Radiata	Right	
21	58	Male	11	Ischemic	Left basal ganglia	Right	Study Incompletion

The 21 control participants were age and gender matched, and all were right-handed. One control was excluded based on study incompletion. Both paired—where each patient time-point before and after therapy was matched—and unpaired statistics between patients and controls were run.

In order to assess clinical outcome measures, a range of clinical scores were collected. For the purposes of this chapter, only the primary outcome measure, the Wolf Motor Function Test (WMFT, as described by S. L. Wolf et al., 2001), will be considered. Basic tests of clinical effectiveness of the therapy are not performed here, as these are already reported in previous publications on this dataset (Bilcher et al, submitted). Instead, individual differences in clinical scores are tested for correlations to imaging measures.

2.2.2 Scanning

Participants were scanned on a 3T MR system (Siemens Trio, Erlangen, Germany). Patients were scanned before and after the two weeks of training, whereas healthy subjects were scanned only once. The scan protocol included structural T1 (MPRAGE), GABA-edited MRS, BOLD resting-state MRI (TR/TE 2000/28 ms, 39 slices with slice

thickness 3.0 mm, with partial cerebellum coverage, flip angle: 90°; volumes 180; FOV: 192mm transversal slices) with a total scan time close to 1 hour. A T1 MPRAGE scan (TR/TE 2420/3.7 ms, 1 mm isotropic resolution, scan time 5 ½ minute) was performed and used for voxel placement and posthoc tissue segmentation. GABA-edited MRS was performed using MEGA-PRESS TR/TE=2500/68ms). GABA data were not analysed here.

2.2.3 Image pre-processing

All imaging data was processed using FSL 5.1 (www.fmrib.ox.ac.uk/fsl). EPI volumes were spatially realigned to the mean image and co-registered with the structural T1-weighted image. Scans were corrected for motion using FMRIB's Linear Image Registration Tool (MCFLIRT [21]). Time-series statistical analysis was carried out using FILM (FMRIB's Improved Linear Model) with local autocorrelation correction. Then all images were brain-extracted (using FSL's BET tool [22]) and spatially normalized using a nonlinear registration tool (FNIRT) with the resulting warp fields applied to the functional statistical summary images, to the standard template of the Montreal Neurological Institute (MNI, Canada). Registration of stroke patient scans was inspected in order to ensure that proper alignment was achieved despite presence of lesions. Scans were subjected to spatial smoothing using a Gaussian kernel of FWHM (full width at half maximum) 3mm.

2.2.4 ICA

Resting-state data was analysed using MELODIC (Multivariate Exploratory Linear Optimized Decomposition into Independent Components, part of FSL

http://www.fmrib.ox.ac.uk/fsl/melodic/). Individual scans were temporally concatenated for each group and time-point (controls, patients pre-therapy, and patients post-therapy) and decomposed to 50 independent components. These were then spatially correlated across the whole brain to 10 previously defined network maps (Smith et al., 2009) and the maps with the highest correlation values from each MELODIC output were selected in a winner-takes all paradigm. Of these 10 network maps, the sensorimotor and occipital ICNs were selected and thresholded at Z>3 for figure presentation.

2.2.5 Seed Analysis

Seed analyses were carried out on the resting-state data. This seed analysis was identical to performing a dual regression except that it was univariate instead of multivariate. The ROI used was the thresholded (Z>3) sensorimotor and occipital visual (control) ICN maps from the control dataset as mentioned in the section above. The choice of these seed ROIs was motivated by the fact that stroke patient ICN maps, especially for the sensorimotor network, were quite variable and influenced by lesion location and extent—the control ICN maps were fairly uniform and localised. First, a lower-level analysis was performed for each condition and each subject. In order to test the effects of lesion hemisphere on connectivity, the affected scans were appropriately flipped across the sagittal plane so that the affected hemispheres aligned on the left for every subject--there were a total of four patients with right-sided lesions whose scans had to be flipped, the rest remained the same. The matching controls were also flipped. Time series were extracted from the pre-processed images using the ROI seeds as masks. CSF and WM

time series were also generated for each subject, and further included in the seed analysis as regressors of no interest. Then ROI series were correlated voxel-wise across the brain using a general linear model (GLM) in FSL's FEAT utility (Version 5.98). Spatial smoothing was conducted using a Gaussian kernel at 5 mm. Then, a group seed analysis was performed using the output from the low-level analysis. Statistics were thresholded as in the localizer analysis. Contrasts were generated between controls and post/pre therapy as well as between pre therapy and post therapy. Since numbers of controls and subjects varied, an unpaired group test was used in the contrast between controls and patients while a paired test was used to assess changes between pre and post therapy patient groups.

2.3 Results for Stroke Rehabilitation Study

What follows are results from the analyses performed on resting-state data from 15 stroke patients and 20 controls.

2.3.1 Differences in ICNs between patients and controls

First, to corroborate findings in the literature, the ICNs of patients and controls were extracted by running group ICA for each dataset (pre-therapy, post-therapy, and controls) and finding components with the highest correlation to the Smith 10 (as outlined in Section 2.2.4). This was done for controls, pre-CIMT, and post-CIMT patients. The sensorimotor ICN, which is of primary interest, and the visual ICN, which serves as a control, are shown below for each dataset:

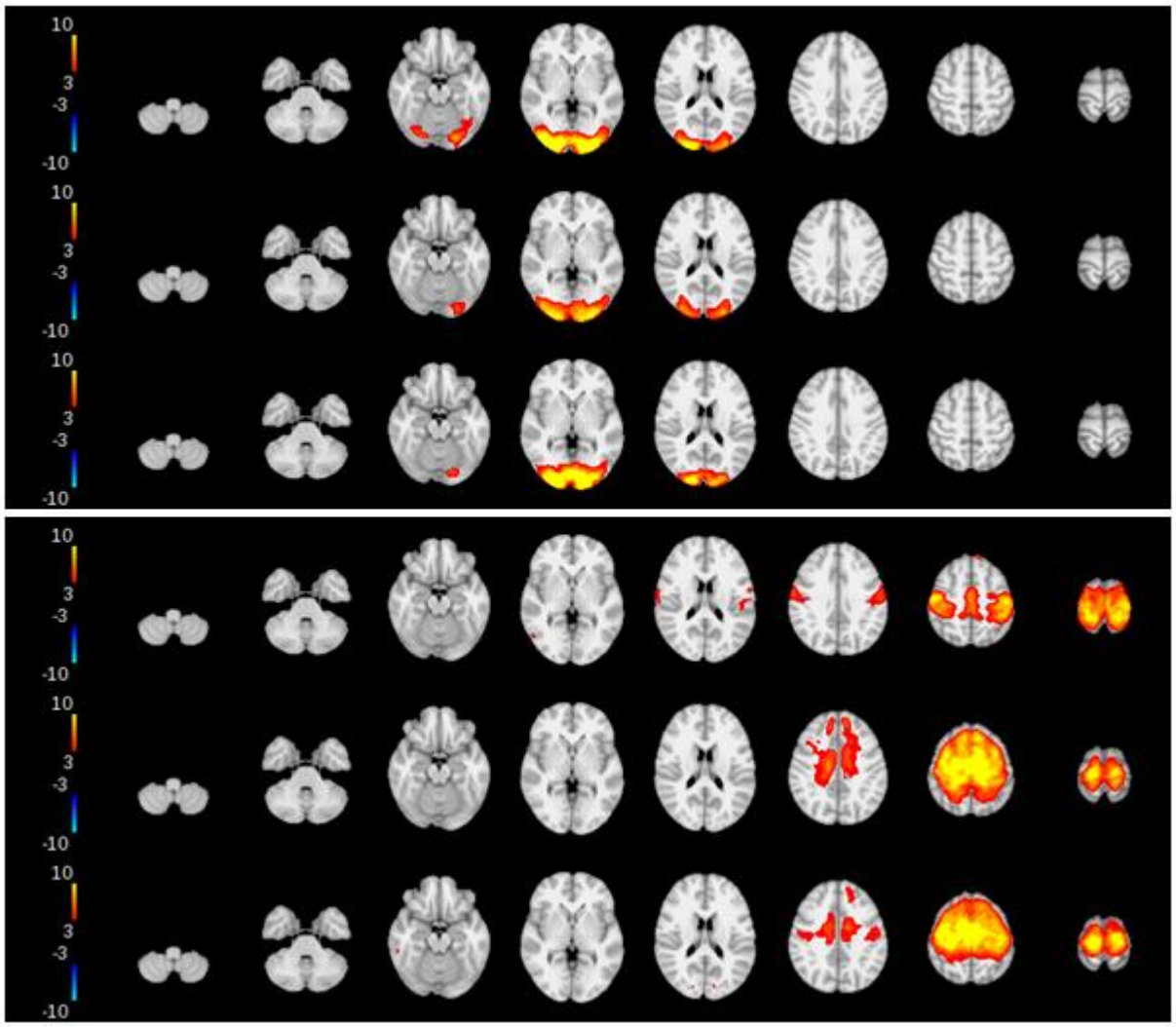


Figure 2.2: Occipital Visual (top) and Sensorimotor (bottom) ICNs for controls (top of each series), pre-CIMT patients (middle), and post-CIMT patients (bottom). Group ICA output was thresholded at Z>3. Shown Right to Left.

In correspondence to the results in the literature (Section 2.1), while the occipital visual ICN remains largely unchanged (as shown in the top panel of Figure 2.2), there are marked spatial differences in the sensorimotor ICNs shown in the bottom panel. Patients have larger sensorimotor ICN maps. The amount of pre-CIMT and post-CIMT occipital ICNs spatially overlapped by the control occipital ICN is 92% and 85% respectively. In

contrast, the amount of pre-CIMT and post-CIMT sensorimotor ICNs overlapped by the control sensorimotor ICN is 39% and 46% respectively. However, it must be noted that it is very difficult to capture particular differences in ICNs at the group level given that lesions in patients vary in location.

Due to the enormous inter-patient variability in lesion location and size resulting in diffuse ICN maps, it was thought best to use group ICNs from the controls only in the seed analysis across all subjects. Though this does bias results towards controls, the fact that the most important comparison is between pre-therapy and post-therapy (neither group here is favoured by using control ICNs) makes this method acceptable.

2.3.2 Changes in connectivity with Constraint-Induced Movement Therapy

To assess changes in FC with therapy, the control sensorimotor and occipital visual ICNs were used as ROIs (shown in Figure 2.2) in a seed analysis where connectivity after therapy was contrasted with connectivity before therapy. The visual ICN served as a control network. In addition, both the pre-therapy and post-therapy scans were contrasted against control scans. The results are shown below in Figure 2.3:

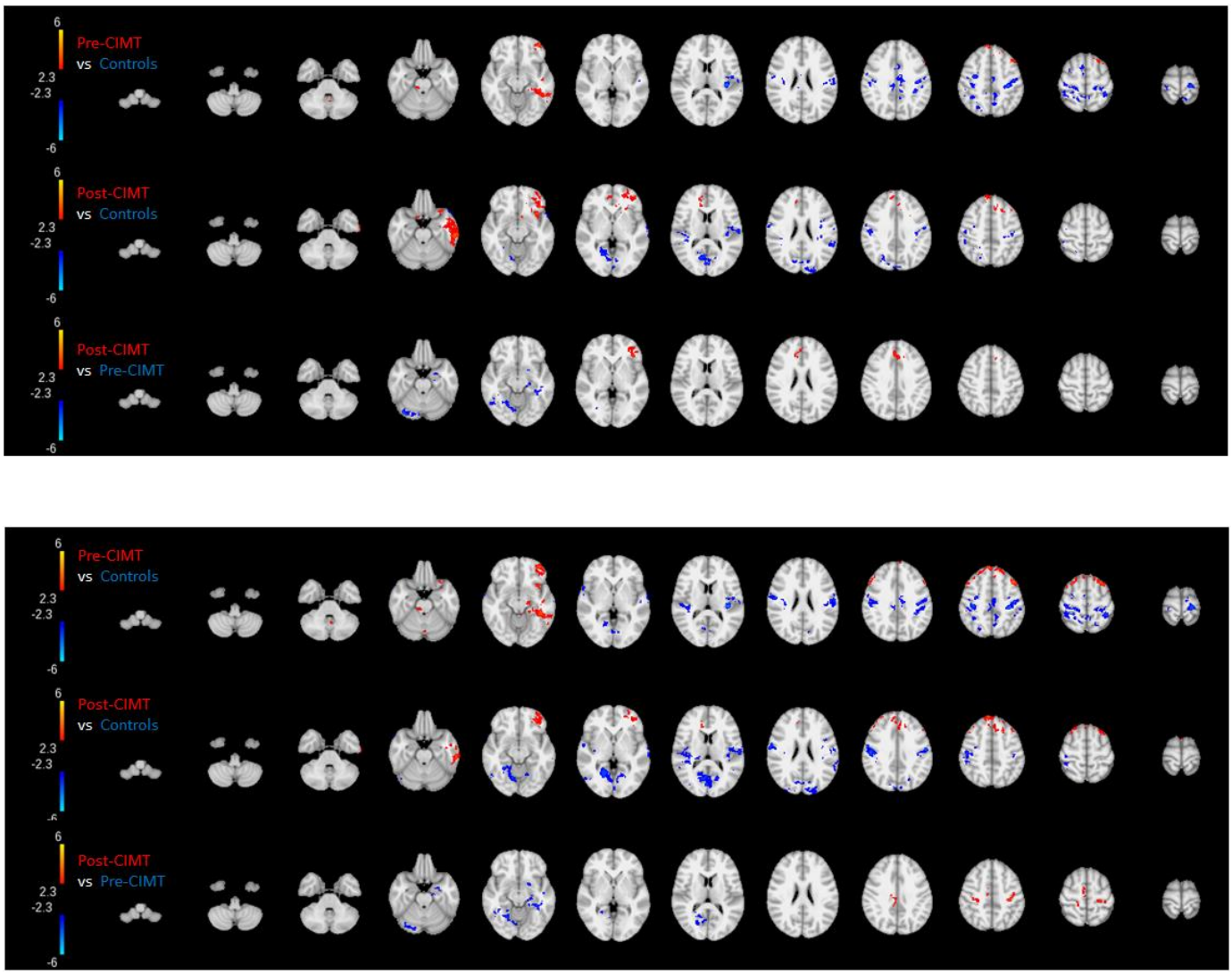


Figure 2.3: Occipital visual (top) and sensorimotor (bottom) ICN seed results for pre-CIMT patients vs. controls (top), post-CIMT patients vs. controls (middle), and post-CIMT patients vs. pre-CIMT patients (bottom). In the top two panels, regions where patients have increased FC to the ICN are given in red, and regions where the controls have increased FC are given in blue. In the bottom panel regions where the post-CIMT patients have increased FC are red, and pre-CIMT blue. Shown Right to Left--the affected hemisphere is on the left.

The bottom-most panel of the figure above shows that connectivity within the motor ICN is increased after stroke patients have undergone CIMT sessions. Most prominently, the hand knobs on both sides and a medial portion of the contralesional SMA increase in their connectivity to the network, as shown by the red clusters. As expected, the affected hand area on the left shows slightly greater increases. In addition, medial visual areas become dissociated from the network, as shown by the blue areas in the bottom-most panel. The occipital visual ICN, on the other hand, does not show any change in FC to motor areas indicating that the effects described above are not global but network-specific. These changes in the motor areas can be interpreted by examining the differences between healthy controls and stroke patients pre and post-therapy: at first controls show greatly increased connectivity in M1. The difference between patients and controls in M1 is reduced after therapy, while conversely the difference between control and patient connectivity between the sensorimotor ICN and medial visual areas increases. This could indicate that CIMT does not drive all connectivity patterns back to normal levels, and that some may become even more abnormal.

2.3.3 Correlation with clinical scores

At baseline, no correlations were found between individual WMFT scores and FC measures for either the sensorimotor or the medial visual network. Similarly, no correlations were found between changes in WMFT score and change in FC over time for either network.

2.4 Discussion of CIMT stroke rehabilitation results

The goal of the above section was to explore how constraint-induced movement therapy affects resting-state functional connectivity in recovering stroke patients. This study is the first of its kind because there is work addressing changes in resting-state FC for robotic (L. Jiang et al., 2013), drug-related and various motor therapies (James et al., 2009; Sharma et al., 2009), but not for Constraint-Induced Movement Therapy (CIMT). It is essential to obtain an understanding of how CIMT affects steady-state functional connectivity in patients because inter and intra-regional coupling patterns are intimately connected to activation profiles and therefore to performance of behaviours. It's also very important to know whether CIMT achieves improvement in motor performance by forming compensatory connections between cortical regions which are recruited to play larger roles in motor task performance, as seen in post-stroke patients by Grefkes et al. (2008), or by re-establishing pre-stroke patterns of connectivity. Ideally one would expect that therapy brings FC patterns back to levels comparable to those in controls, but new FC patterns evoked by the therapy may play a crucial role in its efficacy, providing a means of temporarily rerouting functionality until a full course of healing can take place over time.

An important tool used in our analysis is ICA; to our knowledge this is the first time such a tool has been used to assess a stroke rehabilitation therapy. While ICA is a somewhat stochastic process, we found that it yields consistent and reliable results if parameters are chosen correctly. The main advantage of ICA in this situation is its data-driven identification of networks which can then be used to examine changes in connectivity. Data-driven network definition is crucial in this sort of study because anatomical ROIs

are difficult to apply to damaged brains where structural integrity is compromised due to ischemic lesions.

2.4.1 Changes in FC associated with CIMT

The first major finding in Section 2.3 concerns the nature of ICNs in stroke patients. While the sensorimotor ICN for controls is spatially similar to that reported in the literature (Smith et al., 2009) and that found above in the steady-state dataset, the ICN for the patients is much wider in extent (with an average of 1.6 times more voxels at Z>3 than the control sensorimotor ICN). This may be associated with the phenomenon of hyper-activation in areas of the motor cortex outside the ipsi-lesional M1 seen during task-activation in stroke patients (Grefkes et al., 2008). It could also have to do with variability in lesion location and extent, resulting in spatial spreading during group averaging of ICA outputs. Our experimental dataset lacked viable task-activation scans pre and post-therapy, a robust link between hyper-activation levels and ICA extent could not be established. Additionally, the lack of change in the occipital ICN (and other ICNs not shown) indicates that this is most likely a motor ICN-specific effect, making it possible to concentrate on a specific region of change and utilise the occipital network as a control region.

Pre-therapy patients had less intra-motor ICN connectivity than controls, especially in M1 on the affected side (Fig 2.3). The decrease in connectivity fits with the fact that during stroke in the motor cortex, neuronal connections are physically disrupted by ischemia. The disparity in connectivity between patients and controls largely

disappeared after CIMT, suggesting a return to normal levels of connectivity similar to those in the control patients. A return to normal levels of cortical connectivity, along with increases in motor performance, was also seen after therapeutic pharmacological intervention by L. E. Wang et al. (2011) and as a result of other motor therapies (James et al., 2009; Sharma et al., 2009). In particular in this study, increases are seen in the hand areas and SMA. Increases in cortical connectivity between relevant motor regions have been reported in other studies examining the relationship between resting-state FC and therapy (James et al., 2009; L. Jiang et al., 2013). These increases may be linked to the increases in healthy activation, and therefore motor function, seen by some groups after CIMT therapy in ipsilesional and contralesional areas (Johansen-Berg, Dawes, et al., 2002; Laible et al., 2012).

Post-therapy patients also showed reduced connectivity between the sensorimotor ICN and the foveal and medial visual areas. This effect has not been previously reported in the literature, probably because most studies choose to examine effects between select seed regions confined to motor areas. It is crucial to note that CIMT did not after two weeks cause *all* disruptions in connectivity in patients to trend towards normal levels, implying that in addition to restoring healthy FC levels in the motor cortex, therapy may drive abnormal FC patterns in other areas. It is difficult to interpret these reductions in connectivity because the link between connectivity changes in medial visual areas and behaviour has not been systematically investigated. One potential explanation might lie in the fact that the effects of stroke encompass many aspects of daily living involving

many brain regions. Visual guidance of hand movements, for instance, may become very important in compensating for lost motor function and this compensation may become stronger during the course of objective-driven therapy regimens. Effects such as these may drive trends towards abnormal FC in visual areas.

Despite the results outlined above, there were some limitations to this study. For instance, controls were only scanned at baseline—analysis of changes over time would have been more rigorous if controls had been scanned at two time-points in a similar manner to the stroke patients, especially allowing for a look at the stability of FC measures in the absence of an intervention. Another limitation was the fact that the location and extent of the lesions in the patient group was highly variable. This weakened the statistics of the contrasts during group analysis, perhaps leading to missed effects. Lesions also present challenges during registration to standard space. The final major issue was the lack of correlation between clinical outcomes and levels of FC in the motor cortex. Since in general therapy resulted in both increased FC in the motor cortex and better behavioural outcomes, one might expect that individual patient changes in FC would be correlated to individual WMFT scores. Since this was not the case, it might raise questions regarding the efficacy of FC measures or simply reflect limitations due to small patient numbers, lesion variability, or the clinical scales themselves.

In summary, the well-established behavioural gains seen with CIMT are also associated with changes in sensorimotor cortex connectivity in key areas towards normal levels. Simultaneously, CIMT inspires abnormal changes in medial visual-motor ICN

connectivity, possibly reflecting compensatory mechanisms which form a part of the rehabilitation process. This research also validates the use of ICA as a method for finding ICNs in stroke patients and analysing changes in connectivity.

2.4.2 Future Directions

This analysis suggests a number of new directions to further explore the effects of CIMT on the neuronal recovery process. The novel association between the course of therapy and increase in intra-motor ICN connectivity suggests avenues for correlating connectivity levels to behavioural outcomes directly in CIMT, though no such correlations were found here. Other interesting leads to investigate could include interpreting the effects seen in medial visual areas, and the relationship of activation to both ICN shape and connectivity changes. To achieve this, high-resolution functional localisers taken from stroke patients pre and post-CIMT during a manual task would be needed. Since this is one of the first studies of FC and CIMT, there are a lot of unanswered questions and directions to investigate. One major direction involves linking changes in FC to changes in behaviour—there is no attempt in the literature to connect the two in basic systems such as visual and motor regions. For example, it is not expressly clear what the implications of an increase in hand area connectivity to the hand area as a result of CIMT are for behaviour. Thus, the larger portion of this thesis attempts to elucidate the interpretation of changes in FC to promote greater understanding of ICNs and their role in physiological function.

3 Steady-State Tasks

It is apparent from Chapter 2 that functional connectivity is a good measure for certain long-term changes induced by behavioural modulation. However, these effects are difficult to interpret due to the fact that very little is known about what drives changes in FC. It would be interesting, therefore, to examine whether short-term modulation of behaviour can be similarly measured and used to come up with interpretations for changes in FC. The spatial correspondence of ICNs to behavioural domains such as vision, motor, and cognition (Smith et al., 2009)indicates that they can be modulated by tasks. The present chapter attempts to explore the effect of continuous task performance on ICN connectivity (known as "steady-state" tasks, in contrast to periodic tasks traditionally employed in block-design experiments). This was accomplished by the collection of a unique visual and motor steady-state task dataset, along with a block-design task localiser for comparison purposes, and the use of a number of traditional and novel analyses.

3.1 Introduction

A number of studies have shown that the FC of ICNs can still be measured during task in addition to rest (Shirer et al., 2012; Sun, Miller, Rao, & D'Esposito, 2007). For instance Sun et al. found by seeding certain areas of the motor cortex during a motor task that they could reproduce a FC pattern similar to the sensory-motor ICN. However, there are several unresolved issues raised by measuring FC during task conditions. The first is that while ICNs can be measured during tasks, there is no systematic characterization of their increases and decreases in internal and external coupling strength during them.

Furthermore, much of this research has been conducted on ICNs involved in higher-level cognition (Greicius & Menon, 2004; Hampson, Driesen, Skudlarski, Gore, & Constable, 2006; Newton et al., 2011; Sakoğlu et al., 2010; Shirer et al., 2012; Yeo et al., 2011) with only a few studies addressing motor and visual ICNs (Hampson et al. 2004; Jiang et al. 2004; Newton et al. 2007; Sun et al., 2007) which are simpler to understand and interpret. Cognitive studies exploring the relationship between task conditions and resting states have focused mostly on the DMN. These studies demonstrated that the DMN stays functionally connected amongst its nodes during non-demanding task conditions. It has also been found that the simultaneous decoupling of the DMN from the active network and increased coupling within itself is correlated to the intensity of the task (Greicius & Menon, 2004). Of the studies mentioned above focusing on ICNs other than the DMN and cognitive networks, none have systematically examined task modulation and resulting patterns of brain-wide ICN changes. In other cases, two modalities have been used in the steady-state at once—an example being motor and auditory (Newton et al., 2007), precluding the possibility of studying tasks which affect particular ICNs.

Another issue is whether brief stimuli or task intervals such as those employed in traditional block designs can accurately capture brain-wide changes in ICNs. Studies have tried to use block designs to measure the effects of such changes (for example, T. Jiang et al., 2004; Schölvinck, Friston, & Rees, 2011; Sun et al., 2007). These block-design functional connectivity studies are also known as Psychophysiological Interaction (PPI) studies. The PPI analysis procedure involves taking the time course from the entire block

design experiment and using a regressor which is a combination of the task time course and ROI (demeaned) time course. This effectively "stitches together" the task ON time periods and ignores resting times, or vice-versa (O'Reilly, Woolrich, Behrens, Smith, & Johansen-Berg, 2012). The most glaring assumption these studies make is that global FC patterns can be initiated and stabilized within an order of seconds. This can lead to discrepancies resulting from differences in duration for task design. For example, Jiang et al. (2004) had subjects perform a finger-tapping task in epoch sizes of 20 seconds and found a significant change in connectivity only between M1 and the Superior Cerebellum. Another study by Sun et al. (2007) used a very similar task but this time with 58 second epochs. They found increased connectivity between lateral and medial regions. This motivates a look, as done in this work, at the utility of continuous, steady-state tasks in characterizing changes in FC.

Others have employed steady-state task paradigms with the argument that fluctuation characteristics change with time (Duff et al., 2008; Hutchison et al., 2013), and that steady-state tasks are less susceptible to confounding factors than block designs (Hampson, Peterson, Skudlarski, Gatenby, & Gore, 2002). Fair et al. (2007) undertook a systematic study of the differences between block-design and steady-state derived results regarding FC by directly comparing resting-state (not task state) FC derived from steady-state and event-related design conditions (where the "event-related" refers to an image-classification task block interspersed with resting blocks). While they support the conclusion that it may be acceptable to interchange the two, they warn of some distinct differences between the condition types. Specifically, they found that, correlations to

some superior temporal and parietal regions decreased in the block-design analysis and subsequently, network extent during that analysis was diminished compared to that derived from steady-state analysis.

With this very limitation in mind, Shirer et al. used a steady-state approach to assess cognitive states. 10 minute long tasks (memory, music, and arithmetic) and resting states were acquired and examined using ICA and ROI seed analyses. The authors found distinct whole brain connectivity patterns for each of their tasks. This allowed them to design a classifier which achieved an 84% accuracy rate in distinguishing states. They also reported that changes within ICNs sometimes occurred in regions normally activated by the task. This is important as it begins to address the sometimes unclear relationship between changes in FC and BOLD activation, which is one of the questions this work seeks to explore. It would be valuable to extend the whole-brain steady state analysis presented by Shirer et al. to simpler motor and visual tasks in an effort to better understand general principles of task-driven change.

A gap in this and the previously mentioned studies is that they do not specifically address the interaction between BOLD response to a particular stimulus or task and changes in ICNs. In other words, it is not known how task-activation seen in the BOLD signal affects functionally coupled regions in a dynamic fashion. This interaction has not been well characterized at brief intervals or at steady state (Deco et al., 2013). Due to the method of using contrasts in BOLD signal magnitude to investigate activations, it is not possible to make conclusions about underlying connectivity. Do changes in neuronal

firing effected by task performance make up a large percentage of *overall* activity, or are they small in comparison to the background signal? One study found that signals contributions from activation and from intrinsic FC add linearly and that spontaneous fluctuations remain unchanging during task under the assumption that regions functionally connected to the activation site do not change their signal characteristics (Schölvinck et al., 2011). This contradicts findings that power-spectra, and therefore signal properties, in non-activated regions of the motor ICN change (Duff et al., 2008). Additionally, even though Smith et al., (2009) found spatial correspondence between ICNs and behavioural domains, not all task-driven FC changes in the literature reflect changes in activation. Thus, it would be informative to investigate this activation-ICN interaction, or local-global, interaction during steady state conditions to see if such assumptions hold.

In light of this previous work, we sought to systematically investigate the characteristics of some canonical ICNs under a range of steady-state conditions to more fully understand their relation to activation and behaviour. The aim of this would be to aid in the interpretation of stable connectivity changes during simple tasks and their relationship to activation maps. To this end, we studied how continuous non-demanding task conditions with no rest periods (steady-state tasks) modulate FC in ICNs. The key research questions were 1) How are major ICNs modulated during simple, non-demanding tasks in the steady state? 2) How is steady-state functional connectivity in ICNs related to task activation patterns?

For this purpose scans during three different steady-state conditions, visual, motor, and a combined visuo-motor condition, along with a separate resting state scan were acquired and analysed with ICA and correlation analyses.

3.2 Steady-State Task Experiment Methods

To minimize hypothesis-driven bias as much as possible, data-driven analyses such as ICA and automated spatial map parcellation were used. Both seed analyses and covariance matrices were used in the analysis to investigate various aspects of connectivity, both specific and general.

3.2.1 Participants and Experimental Design

16 healthy volunteers without any previous neurological disorders participated in the study after providing written informed consent. Subjects were recruited from the community in accordance with NHS national research ethics service approval (10/H0707/29). Mean age was 27.25; 7 females, 8 males. All subjects underwent steady-state fMRI along with task localizer fMRI, with the order of the scans randomly determined.

Subjects were scanned under five separate seven-minute continuous steady-state conditions involving low-level sensory or motor tasks: rest (eyes open), visual only, motor only, simultaneous (but independent) visual and motor tasks (Fig. 1), and a motor task modulated by cues from the visual condition (this was not analysed further). The

visual conditions consisted of one of three videos (each 6 minutes long) of colorful abstract shapes in motion. The motor conditions involved continuous sequential finger tapping against the thumb, using the right hand. Subjects were asked to maintain a tapping frequency of 1Hz and to switch the direction of tapping every 20-30 seconds. During the combined condition subjects viewed the aforementioned abstract video while simultaneously conducting the self-paced motor tapping task.

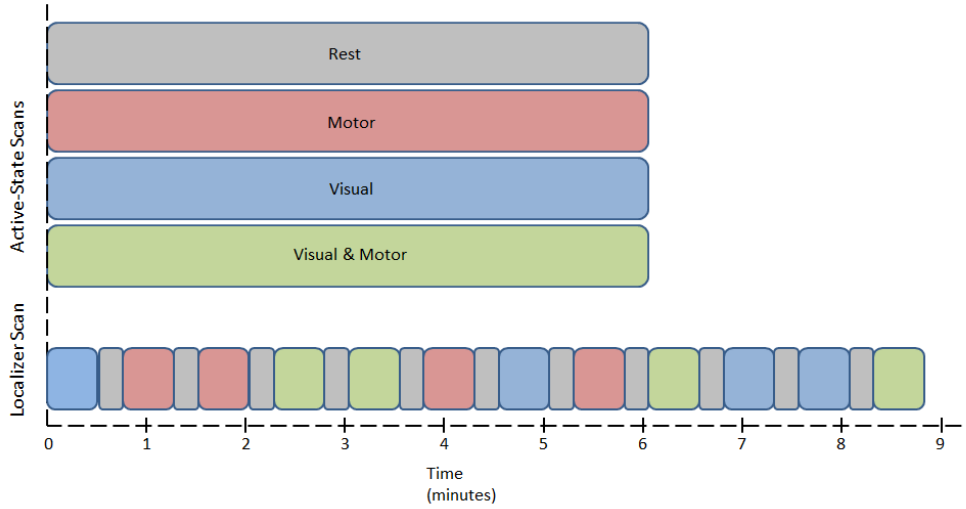


Figure 3.1: Schematic of steady-state and task-localiser scans plotted on timescale.

A further combined visual and motor scan where participants were instructed to identify a cue in the video was acquired but not utilized for this analysis. The order of scans was counter-balanced across participants. An additional task-activation localizer scan, using a pseudo-randomized block design consisting of 30 second task intervals separated by 15 second baseline periods, was performed. The visual, motor, and visual-motor (with cue) conditions were used to enable the identification of brain regions associated with each of the tasks. During the localizer scan, each of the three conditions was repeated four times for a total scan time of 9 minutes and 15 seconds.

3.2.2 Data Acquisition

MRI images were collected by means of a 3-Tesla Verio MRI scanner (Siemens, Erlangen, Germany), using a 32-channel head coil. A Multiband T2*-weighted pulse sequence (Van Essen et al., 2012), exciting and acquiring 6 parallel slices simultaneously, was used for obtaining the functional images pre and post stimulation based on the blood oxygenation level-dependant signal (BOLD; TR: 1300 ms; TE: 40 ms; flip angle: 66°; volumes: 230; FOV: 212 mm transversal slices). Seventy-two slices with slice thickness of 2mm were oriented slightly past AC-PC to cover the whole cortex, with full coverage of the cerebellum. For the task-localiser block design scan an echo-planar T2*-weighted pulse sequence was used to record images based on the BOLD signal (TR: 2000 ms; TE: 30ms; flip angle: 90°; volumes 608; FOV: 192mm transversal slices; 35 slices with slice thickness 3.0 mm, with partial cerebellum coverage). A high-resolution T1-weighted sequence was used to acquire an anatomical image (TR: 2040 ms; TE: 4.7 ms; flip angle 8°; voxel size: 1mm isotropic resolution). Field maps were obtained in order to reduce spatial distortion of the EPI images.

3.2.3 Image pre-processing

All imaging data was processed using FSL 5.1 (www.fmrib.ox.ac.uk/fsl). The resulting scans were field-map corrected using FMRIB's Expert Analysis Tool (FEAT, version 5.98). Scans were corrected for motion using FMRIB's Linear Image Registration Tool (MCFLIRT (Jenkinson, Bannister, Brady, & Smith, 2002)). EPI volumes were spatially realigned to the mean image and co-registered with the structural T1-weighted image

using Boundary-Based Registration (Greve & Fischl, 2009). Time-series pre-whitening was carried out using FILM (FMRIB's Improved Linear Model) with local autocorrelation correction (Smith et al., 2004). Then all structural images were spatially aligned using a nonlinear registration tool (FNIRT) with the resulting warp fields applied to the functional statistical summary images, to the standard template of the Montreal Neurological Institute (MNI, Canada). Images then underwent mean-based intensity normalization, high-pass temporal filtering of 100 seconds for steady-state scans and 180 seconds for localizer scans. Localizer scans only, excluding rest, were subjected to spatial smoothing using a Gaussian kernel of FWHM (full width at half maximum) 5mm.

Steady-state data was further analysed using MELODIC (Multivariate Exploratory Linear Optimized Decomposition into Independent Components, part of FSL http://www.fmrib.ox.ac.uk/fsl/melodic/). Individual scans were temporally concatenated across each task condition and all conditions combined to create 4D datasets and decomposed to 50 independent components. These were then spatially correlated across the whole brain to 10 previously defined network maps (Smith et al., 2009) and the maps with the highest correlation values from each MELODIC output were selected in a winner-takes all paradigm. These 10 network maps were thresholded at Z>3, binarized, and used as regions of interest (ROIs) in the Seed Analysis of steady-state data (described below).

3.2.4 Activation & Seed Analysis

The pre-processed task localizer scans were analysed using FSL's FEAT utility (Version 5.98) for each subject using a voxel-based general linear model (GLM). The block design paradigm was convolved with a gamma function, and its temporal derivative was used to model the activation time-course. The contrasts generated were two contrasts, one for visual and one for motor task condition versus rest.

After individual GLM analyses were generated a high-level group analysis was also performed using mixed effects, assessing mean effects across the group. Z (Gaussianised T/F) statistic images for each subject were thresholded using clusters determined by $Z>2.3$ and a familywise- error-corrected cluster significance threshold of $P<0.05$ was applied to the suprathreshold clusters. The positive activation maps for visual-only and motor-only conditions were binarized and used as ROIs in the Seed Analysis of steady-state data.

Seed analyses were carried out on the steady-state data in an identical manner to that described in Section 2.2.5. Seeds were defined from MELODIC (thresholded at $Z>3$) and GLM output as described above. Here, the main contrasts defined were each task condition with respect to rest (and vice-versa), a contrast to measure the effect of the interaction between the visual and motor task during the combined steady-state condition, and two main effect analyses, one for visual and one for motor conditions. The main effect of the motor task was calculated by subtracting the sum of the rest and visual-only scans from the sum of the visual-motor and motor-scans. The main effect of visual task was derived similarly, with the sum of the resting state and motor-only scan

being subtracted from the sum of the visual-motor and visual-only scans. The interaction contrast was calculated by subtracting the effects from the individual visual and motor scans from the combined-condition scan.

To examine symmetrical changes in ROIs defined from motor activation maps derived from the block design, each of the four clusters activated during the motor condition (in the SMA, hand-area, putamen, and cerebellum) was separated and another ROI was defined by taking its mirror image. Seed analyses were performed on these in the same manner as above, with added GLM contrasts to examine areas which increase and decrease in their connectivity with both left and right ROIs.

3.2.5 Parcellation and Matrix ROI Analysis

In order to analyse the functional connectivity changes with and across ICNs during task conditions with respect to functional nodes, an automatic parcellation method was used to meaningfully parcellate ICNs and generate connectivity matrices. These matrices incorporate information from a larger number of seed-region time courses and allow for their simultaneous comparison. The matrices also simplify the presentation of changes in ICN behaviour by reducing them to a single time course. While this approach may cause us to lose access to some of the finer details of FC changes with task, it allows for a quick summary of overall trends

To generate parcellations, group-level MELODIC output was matched to 10 canonical RSNs as defined by (Smith et al., 2009) via spatial cross-correlation methods as

described above. Thresholds for the ICA maps were set to Z>3. Then the spatial overlap for each FCN was compared to probability structures in the Harvard-Oxford Cortical (probability threshold was set to p>.5) and Subcortical Atlases, as well as with structures in the Cerebellar Atlas. No nodes within networks overlapped. This procedure resulted in each network being parcelled into atlas structures. Additionally, activation maps were thresholded at Z>2 and parcelled using the same algorithm. Average time series for each parcel and for whole ICNs were extracted and correlated, and covaried with one another to generate two sets of correlation and covariance matrices, one with respect to entire RSNs and one with respect to parcelled RSNs, for each of the four task conditions.

Contrasts were generated for each condition with respect to the rest condition using a non-parametric statistical permutation method included in FSL (Randomise v 2.9, 2000 permutations), and an un-thresholded paired t-test to reveal trends. Statistical output thresholds were set to p<.05 with family-wise error correction for multiple comparisons to generate matrices contrasting conditions. Main effects for motor and visual task conditions (calculated in the same manner described above) were also calculated using the same approach as those detailed above.

An identical parcellation and matrix-generating procedure was used on activation statistical maps to generate ROIs within areas of activation derived from the localiser scans described in Section 3.2.2. The parcellation algorithm was used on positive (activated) and negative (deactivation) statistical map output from the FEAT analysis of the task localiser scans at the threshold of Z>2. In the case of the motor activations, each

ROI was also reflected in space left to right for use in an analysis investigating symmetrical changes in connectivity. The average time course for each ROI was calculated, and correlated and covaried with time courses from each other ROI.

The three types of parcellations used are described here. The reason for generating three parcellations was to focus on particular regions of interest or to present clear general results. In other words, the various parcellations reflect varying degrees of spatial specificity and location.

Table 3.1: Parcellation types

Name	**Description**	**Associated Figures**
1-Global Parcellation	ICNs generated by ICA were parcellated using atlas-based algorithm.	A.2
2-Visual Parcellation	Group activation and deactivation maps from visual-task localiser scans were parcellated using atlas-based algorithm.	3.8
3-Motor Parcellation	Group activation maps from motor-task localiser scans were parcellated using atlas-based algorithm. Each parcel was copied across x-axis to generate mirror version.	3.11

3.2.6 Covariance vs. Correlation

To gain better understanding of the difference between the covariance and correlation measures used above, descriptions of the two measures are provided here.

Covariance:

$$C(x,y) = \frac{\sum_{i=1}^{n}(x_i - x_m)(y_i - y_m)}{n-1} \quad \text{Eq. 2.1}$$

Where C is covariance, x_I is an observation of the independent variable, x_m is the mean of the independent variable, y_i is an observation of the dependent variable, y_m is the mean of the dependent variable, and n is the number of observations. Covariance is a measure of how two variables change together, and is affected by the amplitude of the signal. Thus the covariance value of two waveforms will increase if one of their amplitudes is increased. The same is not true of correlation, which is normalized form of covariance:
Correlation:

$$r(x, y) = \frac{C(x,y)}{s_x s_y} \qquad \text{Eq. 2.2}$$

Where r is the correlation coefficient between variables x and y, C is covariance, and s_x and s_y are the standard deviations of x and y respectively. Thus, covariance preserves information regarding amplitude. Another reason for generating covariance matrices for contrasts was to obtain information about intra-node connectivity, which correlation does not provide because correlating a waveform with itself gives a value of 1, while covarying a waveform with itself yields a value (i.e. variance) with a quadratic relationship to the amplitude.

3.2.7 Power, Correlation, and Activation Comparison

In order to investigate whether change in correlation with steady-state task had any general relationship to changes in activation, T-statistic maps were averaged under each node in parcellation (1) and significant changes in activation from zero were determined via a t-test. The reason parcellation (1) was used is because it covers the most spatial area in the brain, and thus allows us to generalize about whole-brain connectivity. Additionally, histograms for directional significant changes were generated by

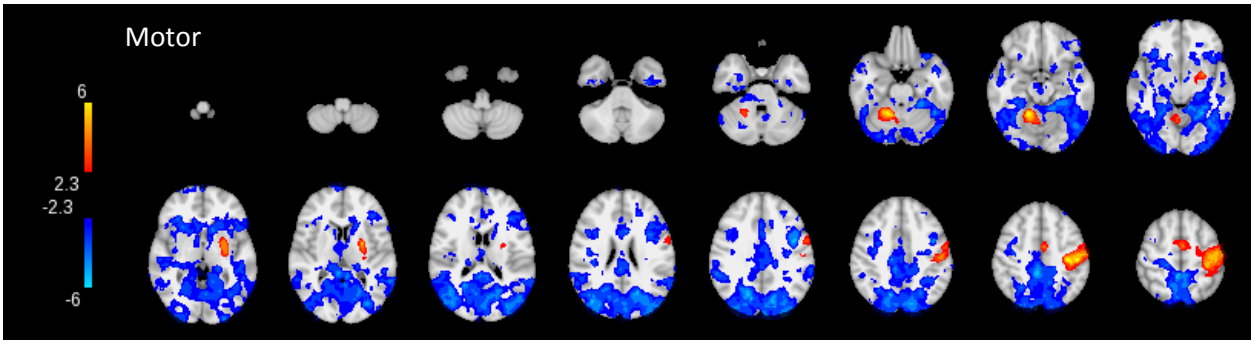
separating nodes which showed significant increases in activation from those showing decreases. All pairings of nodes where none, one, or both regions showed significant changes in average activation were plotted against correlation values between those nodes. Task conditions were combined into one histogram and compared to a histogram of correlations for the same pairings of nodes at rest. The same procedure was repeated for covariances, but since un-contrasted covariance values are difficult to interpret because they are influenced by signal amplitude, which varies intrinsically in various parts of the brain (and since this is a whole-brain analysis), only correlation plots are presented here.

3.3 Steady-State Experiment Results

The aim of the following analyses is to demonstrate and explore the complex nature of FC changes in ICNs during simple, continuous tasks.

3.3.1 Task-localiser scans

Task localiser scans enabled the identification of BOLD amplitude changes for the motor, visual, and combined conditions relative to rest (Figure 3.2).



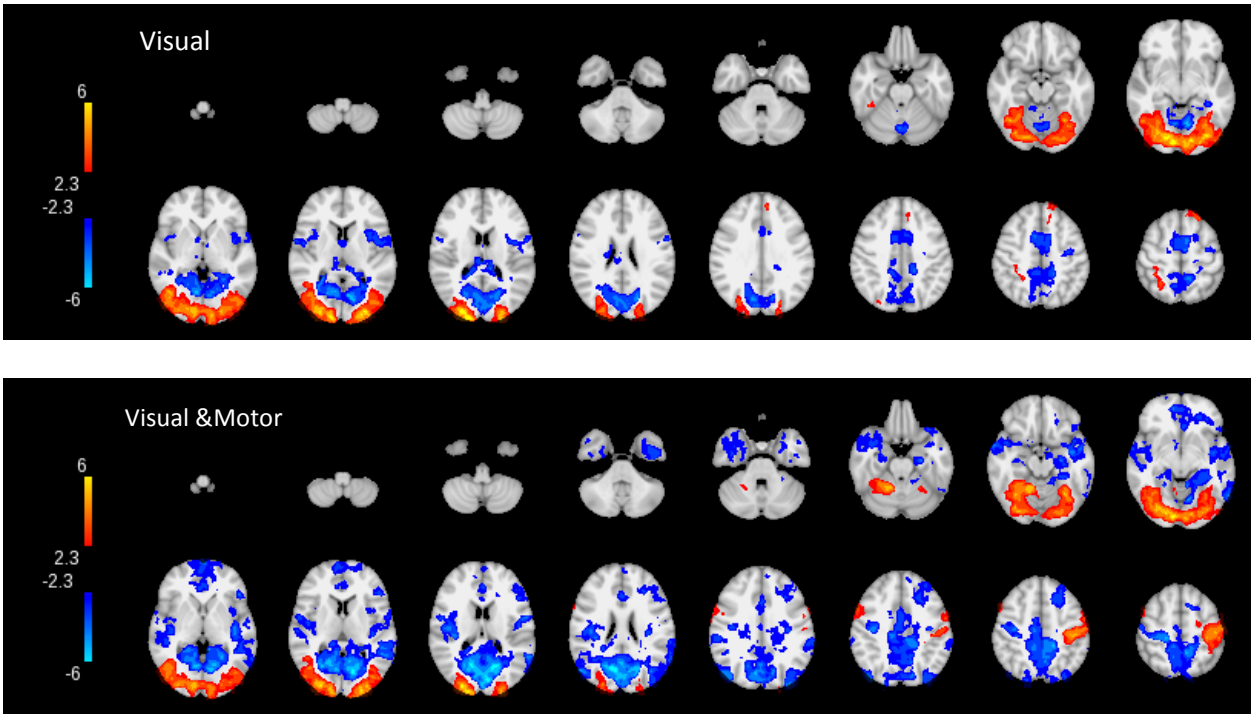


Figure 3.2: Visual (top), motor (middle), and visual & motor (bottom) task activations (red) and deactivations (blue). Z-statistic was thresholded at 2.3.

The top panel in Figure 3.2 shows the group activation map of a two-sided contrast between finger tapping and the baseline condition. Since the finger-tapping motor task was performed using the right hand, the left primary motor and pre-motor cortex and right cerebellum showed increased activation with respect to baseline, as well as the posterior part of the left putamen. Visual areas were deactivated relative to the resting baseline, as were some prefrontal, parietal, and cerebellar areas. The middle panel shows the equivalent contrast maps for the visual condition. The abstract videos, used as visual stimuli, activated low-level foveal visual areas (including the cortical area identified as the occipital visual ICN), as well as higher-level visual areas in the occipitotemporal cortex (e.g. V4, hMT, which overlap with the lateral visual ICN). The task also resulted in deactivations in the medial visual area associated with peripheral low-level visual

processing, as well as medial motor cortex areas (e.g. overlapping the Supplementary Motor Area). The combined condition, involving abstract videos and right-hand finger tapping, largely activated the same areas as described for each condition separately.

3.3.2 ICN Extent and Shape during steady-state task conditions

MELODIC ICA yielded 50 spatial maps, separately for each of the three task conditions and for the resting state, and specified in Section 3.2. We identified the canonical resting-state maps using the same procedure utilized in Chapter 2 (Section 2.2.4).

To demonstrate the extent to which our networks correspond to the Smith 10, the figure below shows correlation coefficients of components found using the spatial correlation algorithm described above. On the x-axis are the Smith 10 and on the y-axis are the networks derived from this dataset.

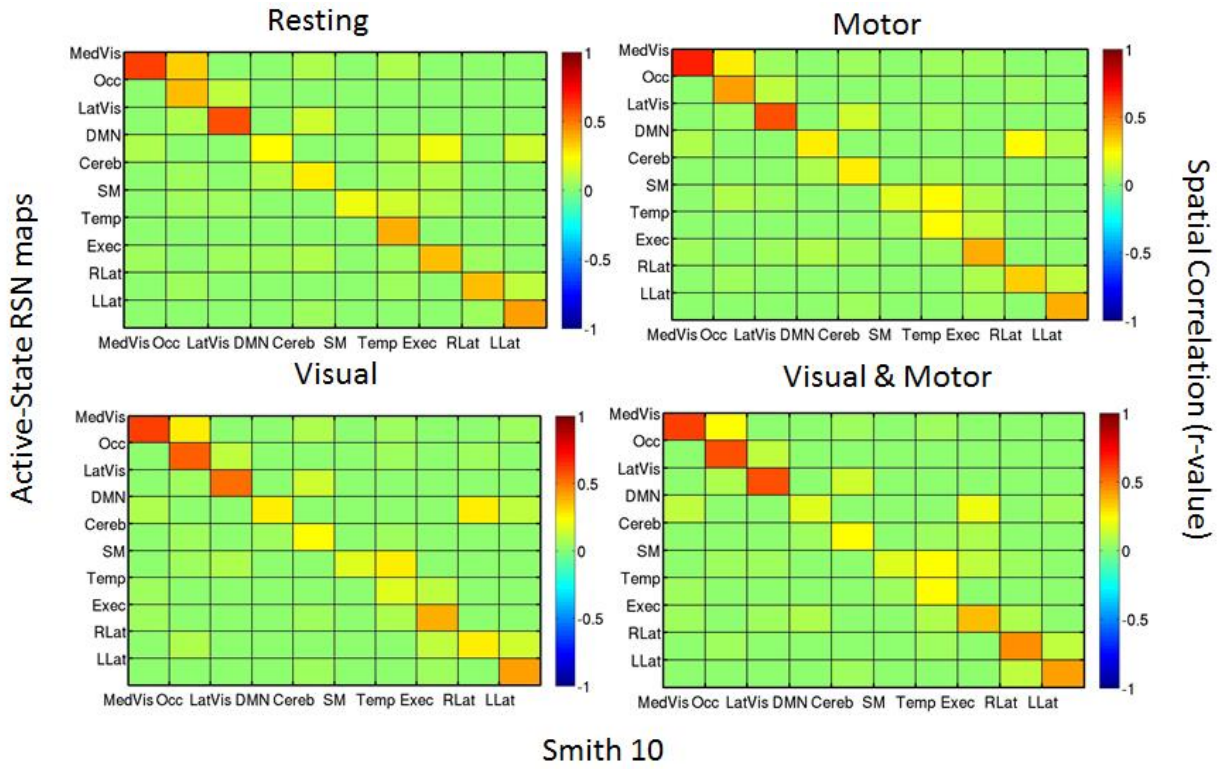


Figure 3.3: Correlation of 10 major networks found through ICA to Smith 10. Each component is correlated to all other components.

For the four conditions shown in Figure 3.3 the main diagonal shows the strongest correlations, with some weaker exceptions amongst cognitive networks such as the DMN and Right Lateral.

To illustrate more clearly the variability between correlations to the Smith 10 and each of the networks we present the correlations in the form of a bar chart.

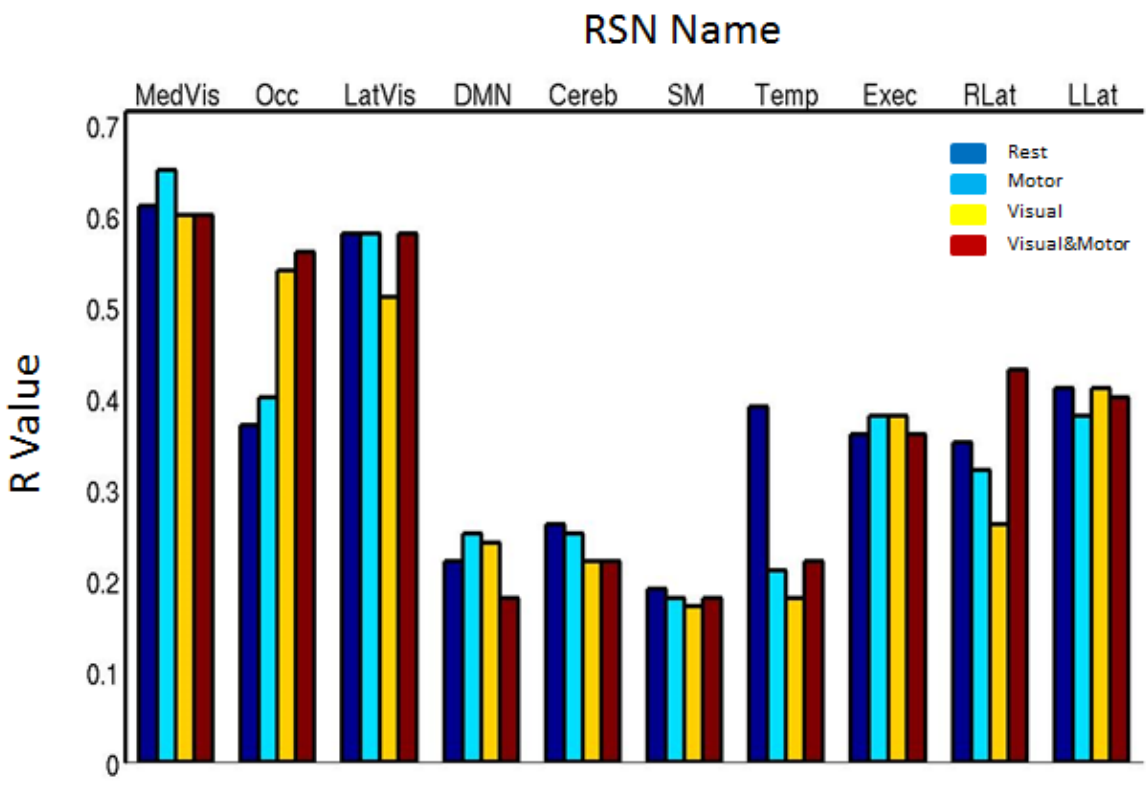


Figure 3.4: Correlation of 10 major networks found through ICA to Smith 10. Each ICN is correlated to its counterpart for four tasks. (R=Rest, V=Visual, T=Task, VT=Visual&Task).

The effects that stands out the most in Figure 3.4 is that there is little variability in spatial correspondence of ICNs across the three task conditions with the exception of the temporal ICN, where the network at rest corresponds most to its Smith 10 counterpart. This might be due to the fact that the regions covered by this ICN are thought to be involved in attention modulation. Another observation is that the occipital ICN becomes more similar to that of the Smith 10 during tasks with a visual component (visual and combined visual & motor). This might be due to stronger network-wide correlations induced by the tasks, increasing the extent of the ICN. The low correspondence of the sensorimotor ICN can be attributed to the differences in spatial coverage used in this

dataset and that used to generate the Smith 10: the two networks are similar in shape but shifted in the z-plane with respect to one another. A similar effect can explain the cerebellar ICA. The reason for the general difference in the DMN between this dataset and the Smith 10 could be associated with the higher spatial and temporal resolution acquisition used here.

Figure 3.5 shows the 10 ICNs generated by running ICA on all steady and resting state scans for all subjects combined overlaid on maps of the Smith 10. Because these combined ICN maps were used in all subsequent connectivity analyses, it is important to verify the similarity between the networks generated in this dataset and those in the literature.

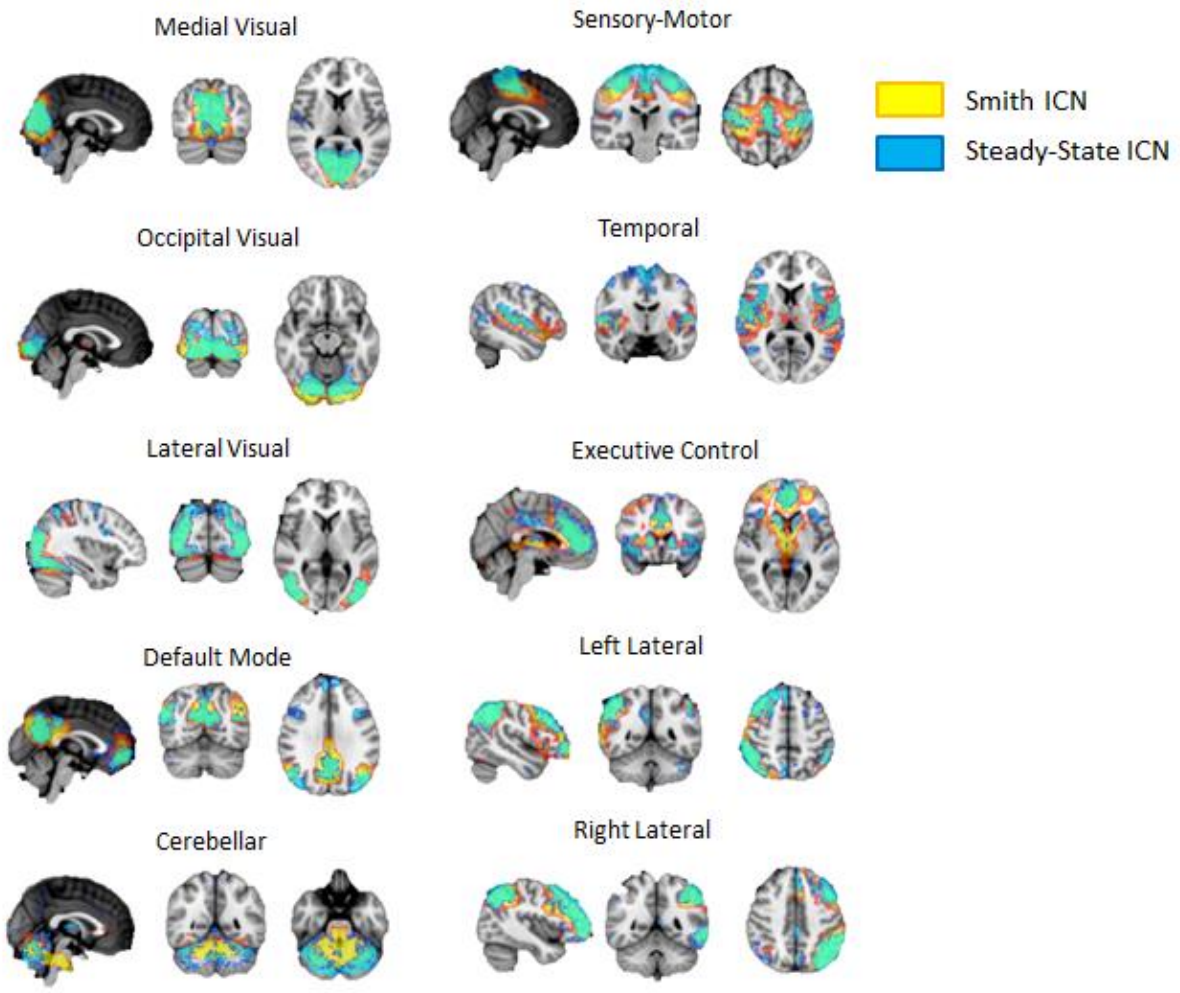
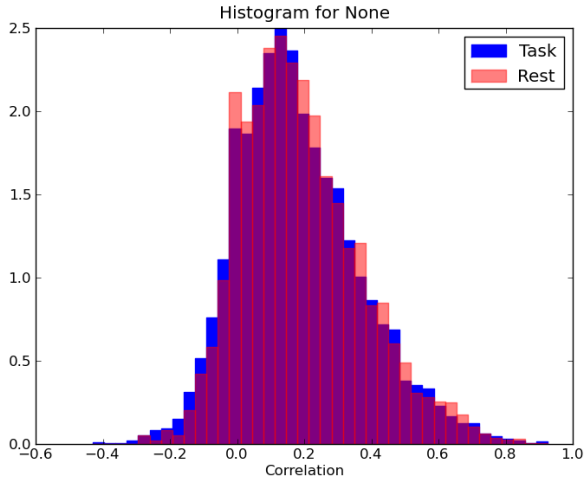


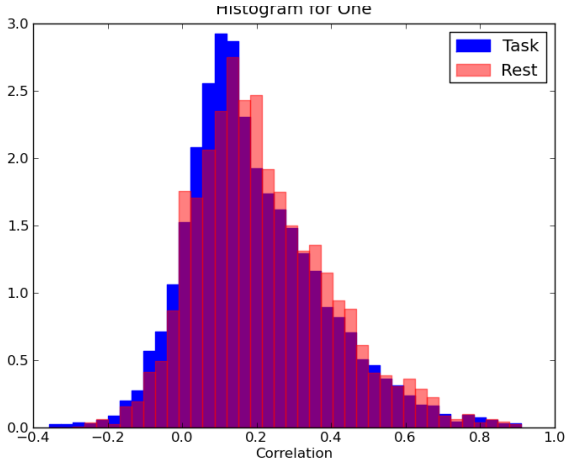
Figure 3.5: Spatial maps of the 10 canonical networks from Smith et al. (2009) (shown in yellow) and combined-condition ICA output (shown in blue)

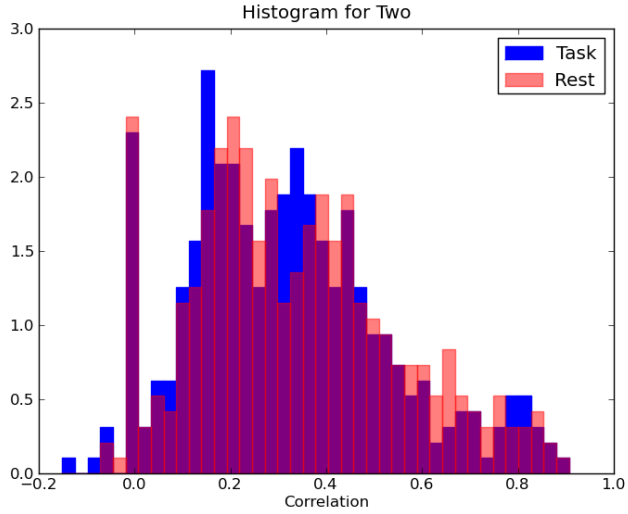
The result above showing strong spatial correlations between ICNs from two datasets supports the claim that canonical ICNs are present in these subjects at a group level across task conditions. This validation allows us to refer to ICNs during task as well as during rest, and justifies the use of task-concurrent ICNs when defining ROIs later in this analysis. It also serves as additional evidence that the strength of ICNs is not diminished during task condition but can even be bolstered (e.g. the occipital ICN in Figure 3.4).

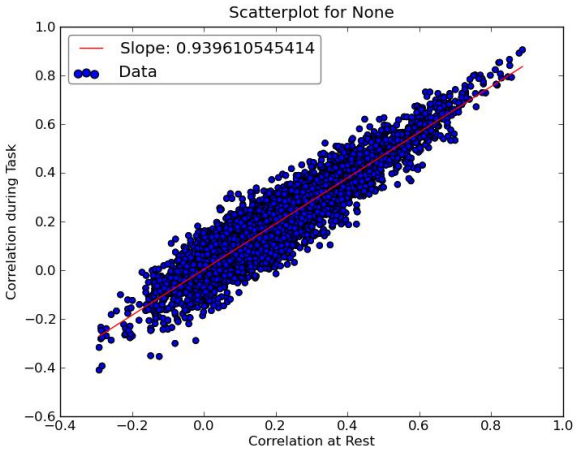
3.3.3 Relationship of Activation to Correlation

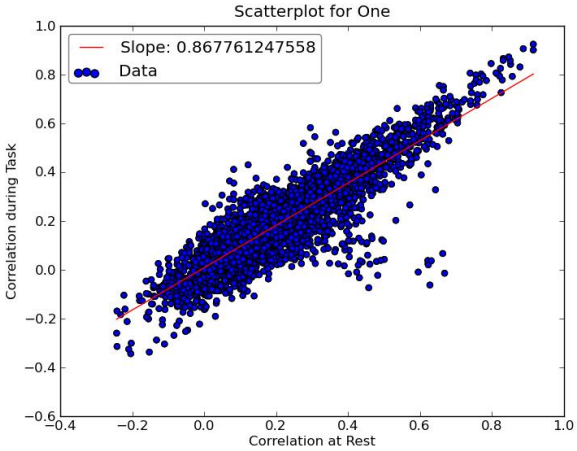
In order to investigate the general relationship of activations to connectivity changes during task, parcellation (1) was employed to generate nodes. Each of the 94 nodes in the whole-brain parcellation was paired with each of the others to yield a 94x94 set of node-pairs. Each of these was sorted based on whether both nodes, one node, or neither of the nodes in the pair were significantly positively activated during the visual or motor task localiser across subjects. Then the correlation values for these nodes during that task and at rest were displayed in a histogram. The results are given below:






Histogram for Two
Task
Rest
Correlation


Scatterplot for None
Slope: 0.939610545414
Data
Correlation during Task
Correlation at Rest


Scatterplot for One
Slope: 0.867761247558
Data
Correlation during Task
Correlation at Rest

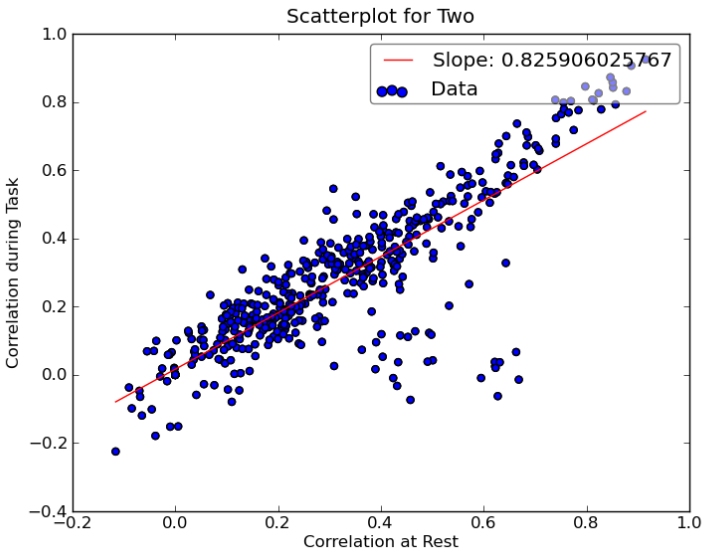

Scatterplot for Two
Slope: 0.825906025767
Data
Correlation during Task
Correlation at Rest

Figure 3.6: (Top set) Normalized histograms showing distribution of correlations for pairs of nodes where none, one, or two of the nodes changes significantly in its level of activation during visual or motor task. These are overlaid on histograms of correlations for the same nodes at rest. (Bottom set) Scatterplots where each point represents a pair of nodes plotted according to correlation at rest (x-axis) and during task (y-axis).

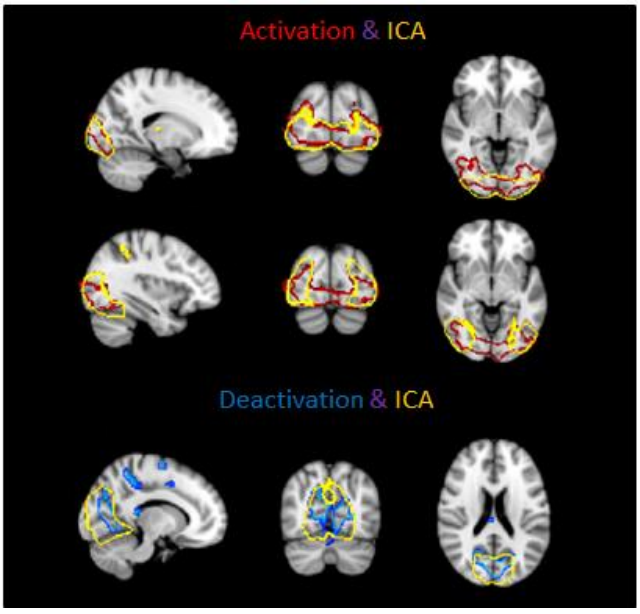
As expected, when neither node in a pair is activated their correlations do not change. When one node is activated, the correlations tend to go slightly down, indicating that perhaps activated regions decrease their shared signal with inactivated or deactivated regions. When both nodes are significantly activated during the tasks, however, there is a change in the distribution of correlations for those nodes, with some tending to go to zero and others tending to increase in value, especially at about r=.8. This means that it is not necessarily true that co-activated ROIs tend to increase in their correlation to one another. Versions of Figure 3.6 featuring deactivated regions, and with separate histograms for visual and motor conditions are shown in the appendix (A.1). To delve deeper into the relationship between activation and FC changes further, various parcellations and task conditions could be investigated using a similar analysis.

3.3.4 Whole-brain changes in connectivity during steady-state tasks

In order to more specifically investigate changes in connectivity, visual and motor seed ROIs were taken from the activation maps shown in Figure 3.2 and from the visual and motor ICA components derived from the MELODIC shown in Figure 3.5. The purpose of this analysis was to better understand and compare how major task-related activated regions and ICNs change in connectivity across the whole brain during steady-state tasks.

3.3.4.1 Visual Task Condition-Seed Analysis

Seed analyses were run on ROIs derived from activation maps as well as from visual ICNs during the visual steady-state task and contrasted with the resting-state condition. Motor ROIs did not show significant changes in FC during this visual task.



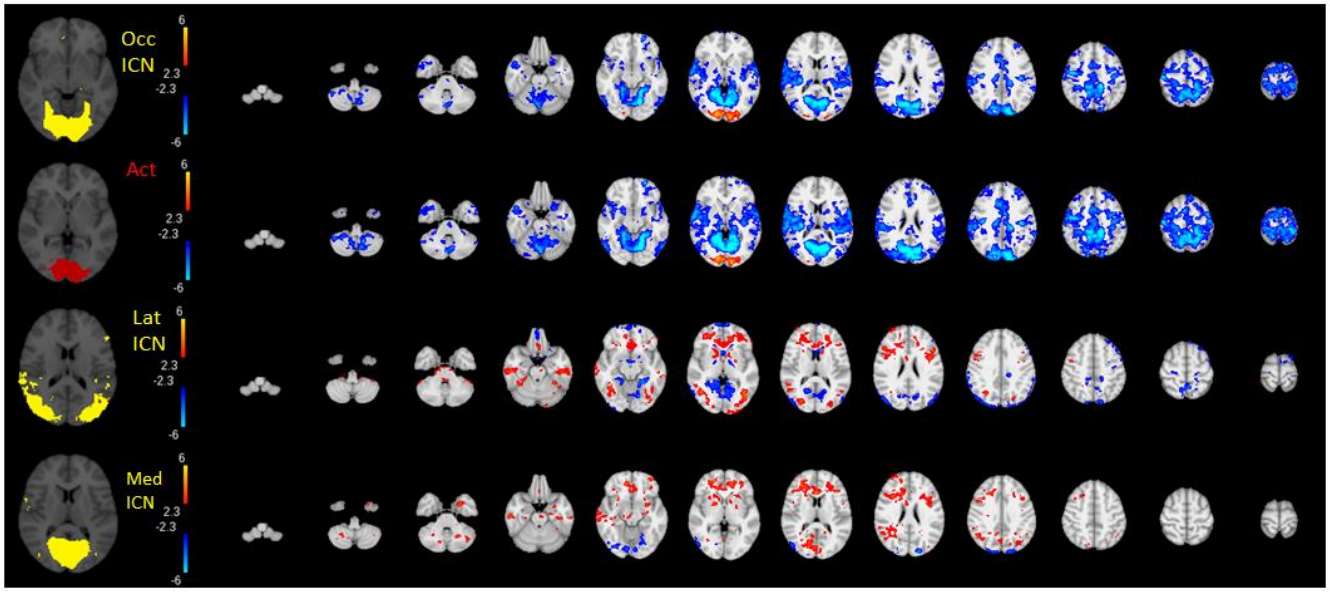


Figure 3.7: (Top) Overlay of task activations/deactivations and ICN maps for comparison. (Bottom) Seed analysis of visual ICNs and area of activation. Seed maps are thresholded at Z>3. Red areas show stronger correlations with the ROI during task and blue areas show weaker correlations during task.

The top two panels in the bottom portion of Figure 3.7 show two-sided contrasts of functional connectivity between the resting-state and visual steady-state when occipital ICN and visual activation seeds are used. The maps appear to be very similar. In both, there is a strong dissociation from medial-visual areas and increased localized association within the ROI in the foveal visual areas. The occipital visual ICN and the activation map, thresholded at Z>2.3 and binarized, have a large spatial overlap (56% and 57% of each map respectively is covered by the other). Therefore it is not surprising that the connectivity changes observed after utilizing each of them as seeds are very similar as well. The third and fourth panels in Figure 3.7 show the same two-sided contrast for the Lateral Visual and Medial Visual ICNs. The Lateral Visual ICN, which also overlaps with the locus of activation, shows decreases in FC to the medial visual areas and increased FC to regions within itself. Additionally, it shows increased FC to pre-frontal areas lying within the executive control ICN. This might be explained by the fact that the Lateral Visual ICN is involved in higher-level visual processing and visual association to other modalities. The Medial Visual ICN also shows increased coupling to prefrontal areas, but becomes dissociated from foveal visual areas (the occipital ICN). Overall, these results suggest most importantly that certain visual ICNs become more connected within themselves and dissociated from other networks during task, and that

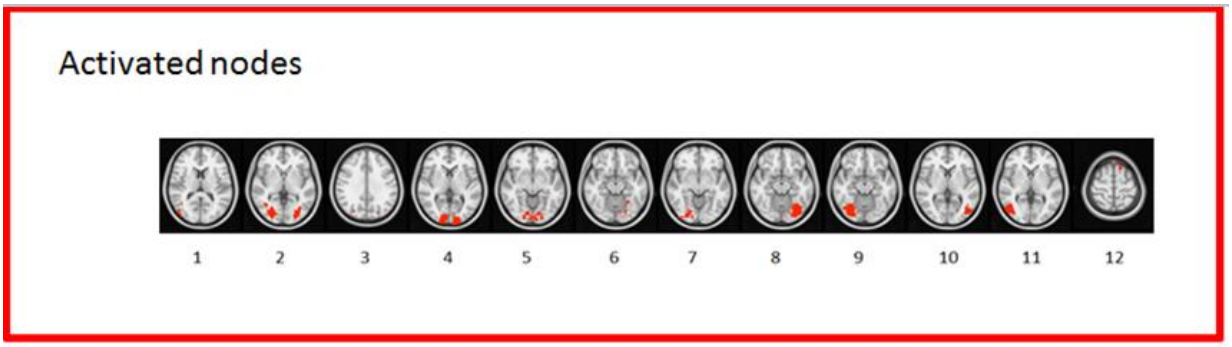
ICNs which overlap with activated areas tend to follow congruent patterns of FC change during the visual task.

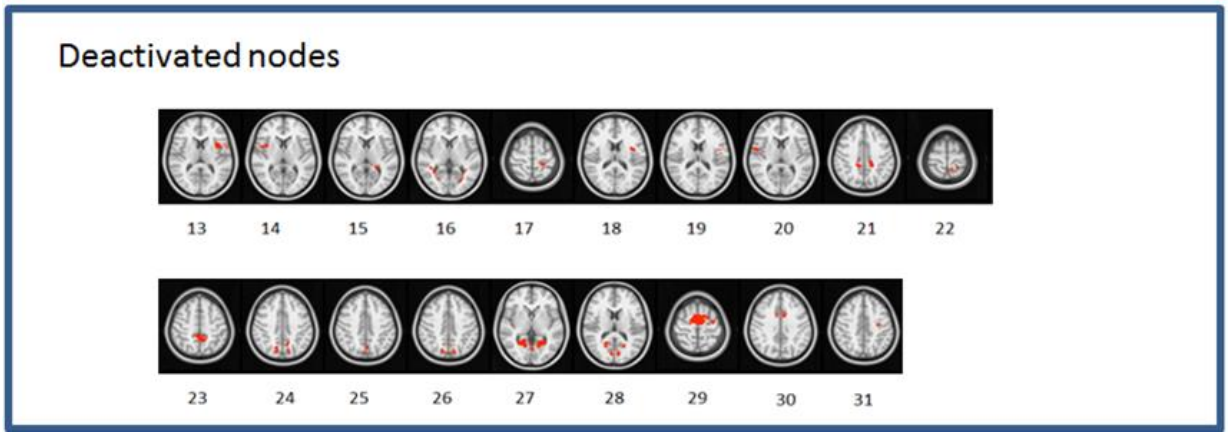
Next, these same changes in FC during the visual steady-state task are investigated using connectivity matrices.

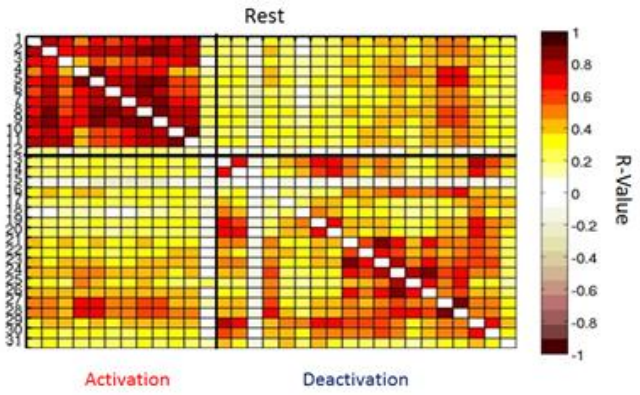
3.3.4.2 Visual Task Condition-Connectivity Matrices

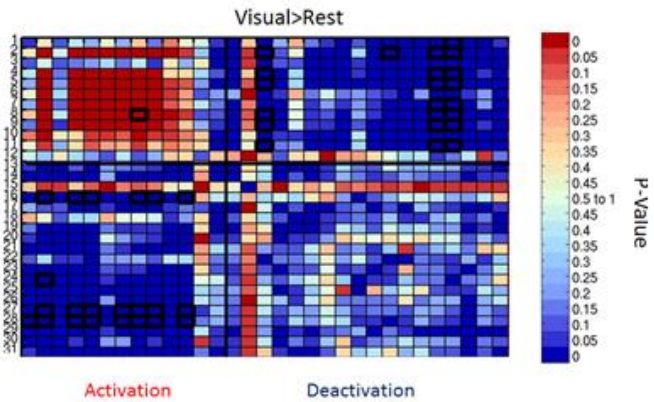
In order to explore the interaction between local activation, ICNs, and FC, activation maps were parcellated into ROIs using an automated technique reliant on the Juelich and Harvard-Oxford probability atlases as described in Section 3.2.5 (Parcellation (2)). The purpose of this analysis was to better understand how activated regions change in connectivity in relation to deactivated regions. The other goal of the analysis was to examine the difference between activation which spatially coincides with ICNs and activation which does not.

Correlation matrices for only visually activated and deactivated regions—derived from task localiser scans—were generated. First, a raw correlation matrix for the rest condition only was generated. Then motor and visual steady-state contrasts with resting conditions were generated. Summary slices showing the various components comprising the parcellation were also generated for ease of interpretation.


Activated nodes
1
2
3
4
5
6
7
8
9
10
11
12


Deactivated nodes
13
14
15
16
17
18
19
20
21
22
23
24
25
26
27
28
29
30
31


Rest
R-Value
Activation
Deactivation


Visual>Rest
P-Value
Activation
Deactivation

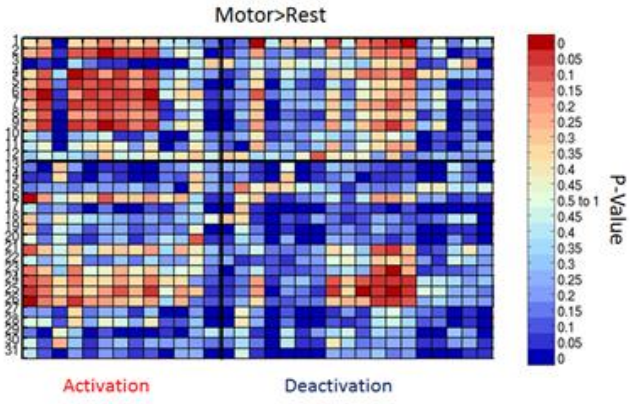

Motor>Rest
P-Value
Activation
Deactivation

Figure 3.8: Visual-activated/deactivated area parcellation corresponding to rows/columns of matrices (top), Raw correlation matrix (second from top), visual steady-state task contrast (bottom left), motor steady-state task contrast (bottom right) for nodes derived from visually activated and deactivated regions from localiser scans. Pairs of nodes which increase in value (covariance) are in red, and decreases are given in blue. Statistics which pass the test for multiple-comparisons are highlighted in black.

The top portion of Figure 3.8 shows the parcellation of the activated and deactivated regions into atlas structures. While the activated regions all lie within the visual cortex, it is important to note that some deactivated regions are in the motor cortex, such as components 29 to 31. Despite this, there are high resting-state correlations amongst visually activated regions and amongst regions which are deactivated together in the visual condition. This may be explained by the fact that the medial visual ICN includes some areas of the motor cortex even at high thresholds and that both motor and medial visual areas are deactivated during the visual steady-state task.

As seen in the bottom left panel in Figure 3.8, visually activated regions tend to have increased functional connectivity amongst themselves (with notable exceptions being components 1 and 3, which are part of the lateral visual ICN) and greatly decreased connectivity to deactivated regions during the visual steady-state condition. The dissociations in particular pass tests for multiple comparisons, reflecting the strong decoupling observed earlier in both the ICN matrix and seed results. Additionally, deactivated regions are less connected amongst themselves, implying perhaps that the visual task condition serves to synchronize fluctuations in activation and desynchronize them in deactivated regions (this can also be seen in activation-correlation histograms—

Figure A.1). There are some activated nodes which decrease their connectivity with other activated nodes, and some deactivated nodes, such as component 15 in the anterior part of the medial visual area, which increase their connectivity with activated regions, though not significantly.

While the Motor>Rest contrast in Figure 3.8 shows some of the same trends (albeit weaker) in connectivity as the Visual>Rest contrast, there are some key differences. These include increases rather than decreases in connectivity between visually activated and deactivated regions, and increases amongst deactivated regions. The trends which remain similar between the two task conditions may be due to common differences in attention from rest.

In order to examine effects of visual task performance on networks across the whole brain, connectivity matrices for ICNs were generated. This is methodologically interesting, as dual regression is such a common analysis method.

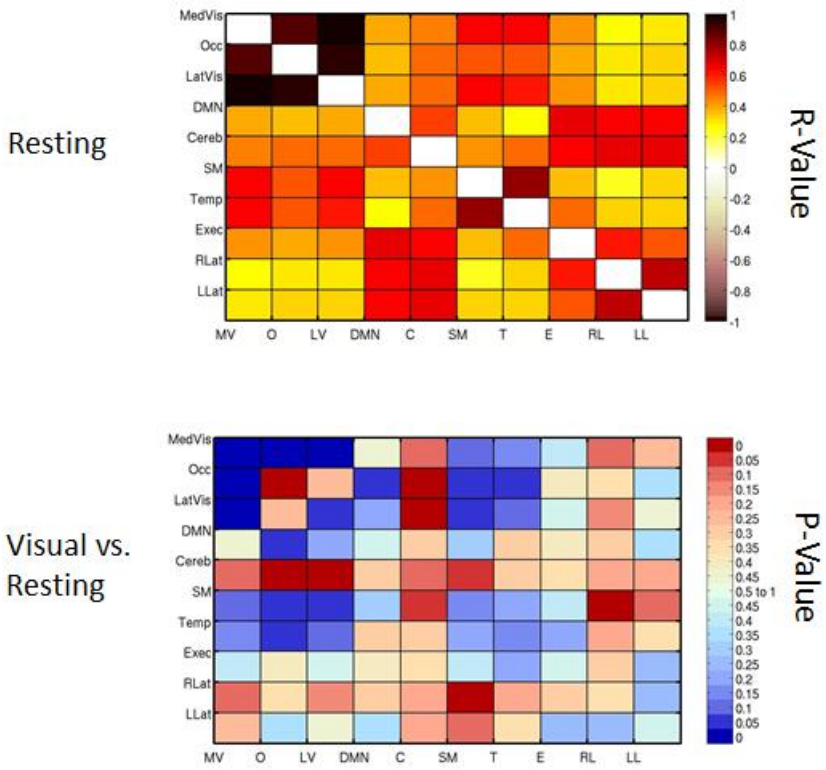


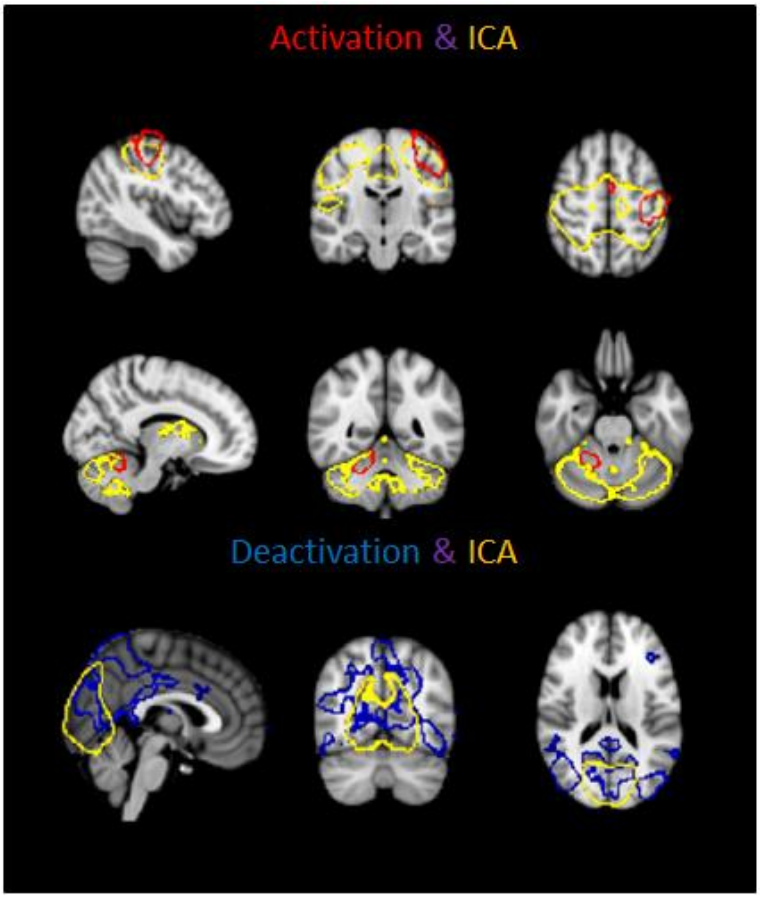
Figure 3.9: Resting correlation values (top) and Visual Task vs. Rest covariance contrasts (bottom) for the 10 canonical ICNs. Increases in connectivity during visual steady-state with respect to rest are shown in red, decreases in blue.

The above figure corroborates the results in Figure 3.8 in that the occipital ICN increases in its connectivity to itself and decreases its connectivity to the medial visual ICN. We also see increases in connectivity by the activated visual networks (occipital and lateral) to the cerebellum. Extended versions of these figures, generated using the 94x94 matrices (Parcellation (1)), are featured in the Appendix.

Next similar changes in motor networks were investigated.

3.3.4.3Motor Task Condition-Seed Analysis

Seed analyses were performed for regions activated during the motor task and the motor ICNs (sensorimotor and cerebellar). One major difference between the visual and motor task is that the motor task asymmetrically activates only part of the motor and cerebellar ICNs, while the visual task activation and occipital ICN are both symmetric and overlapping. An additional ROI was created using the motor activation map flipped left to right and run through a seed analysis. Statistical maps were generated from contrasting motor steady-state scans with the baseline resting state and were thresholded at Z>2.3. The results are shown Figure 3.10:



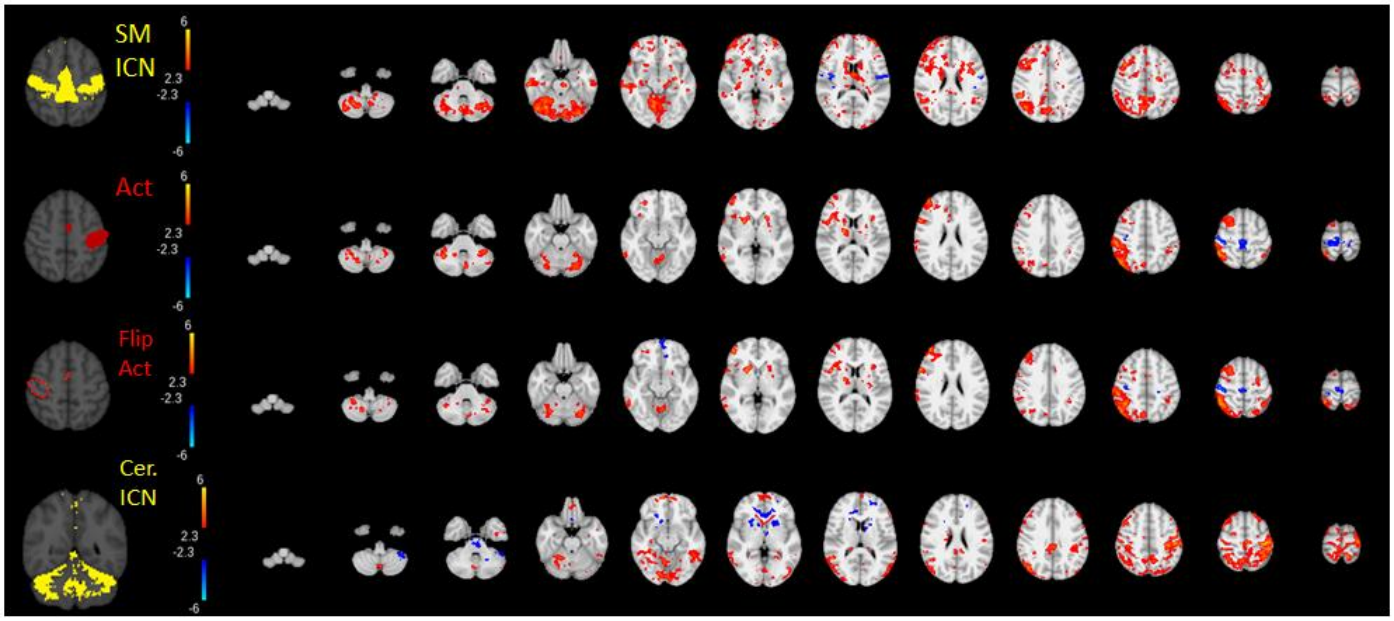


Figure 3.10: Seed analysis results for sensorimotor and cerebellar ICNs as well as flipped and non-flipped areas activated by the motor task. Threshold is at Z>2.3. Red areas are more correlated with the ROI during task and blue areas are less correlated during task.

The top and bottom panels of the figure above show changes in FC for the Sensorimotor and Cerebellar ICN comparing the resting-state the motor steady-state. For the Sensorimotor ICN, the motor steady-state task produces increases in connectivity to a wide range of regions, most notably the cerebellum, the right superior parietal lobe, the right premotor cortex and SMA. Connectivity to some regions of the insular cortex is decreased. Despite the lateral nature of the steady-state tapping task, the changes in connectivity involve both hemispheres (though the ipsilateral hemisphere has more pronounced changes). The same is not true of the cerebellar ICN, which increases its connectivity preferentially with the left motor cortex. The middle panels show changes in FC for ROIs comprised of regions activated during the motor task, as defined during the task localiser scans. One surprising result here is that the changes in connectivity

observed after using the flipped activation map as a seed are very similar to those of the non-flipped activation map seed. During the steady-state unilateral finger tapping task, both ROIs increase in their connectivity to the cerebellum , the right Superior Parietal Lobe and the right premotor cortex. They both show decreases in connectivity to medial parts of the sensorimotor ICN. This interesting symmetrical response in FC with respect to a unilateral task and therefore unilateral activation pattern is explored further in Section 3.3.4.4. Considering overall changes in connectivity, the motor ROIs during motor task modulation present a much more complex set of changes in FC than do the visual ROIs during visual task modulation. Connectivity within the sensorimotor ICN region seems to decrease or not change at all, while connectivity increases with a wide range of regions outside of the motor cortex. Similarly to the visual steady-state task, the motor task did not produce significant changes in connectivity for the visual ROIs described above.

Effects of FC change during the motor steady-state condition are further explored through connectivity matrices in the next section.

3.3.4.4Motor Task Condition-Connectivity Matrices

To explore the relationship between activation and changes in FC during the motor steady-state condition in motor regions, matrices were generated in the same way as those in Figure 3.8, but the nodes used this time were activated motor areas and their flipped counterparts, which were not activated (but not necessarily deactivated) by the motor task. In the matrix, each node is placed next to its mirror image to better visualize

the symmetry of effects. Our hypothesis before performing this analysis was that only nodes which were part of the activated regions during the finger tapping task would increase in their connectivity to one another over rest, and that they would decrease in connectivity to their mirrored counterparts, which were not activated, similar to what we observed during the visual steady-state condition.

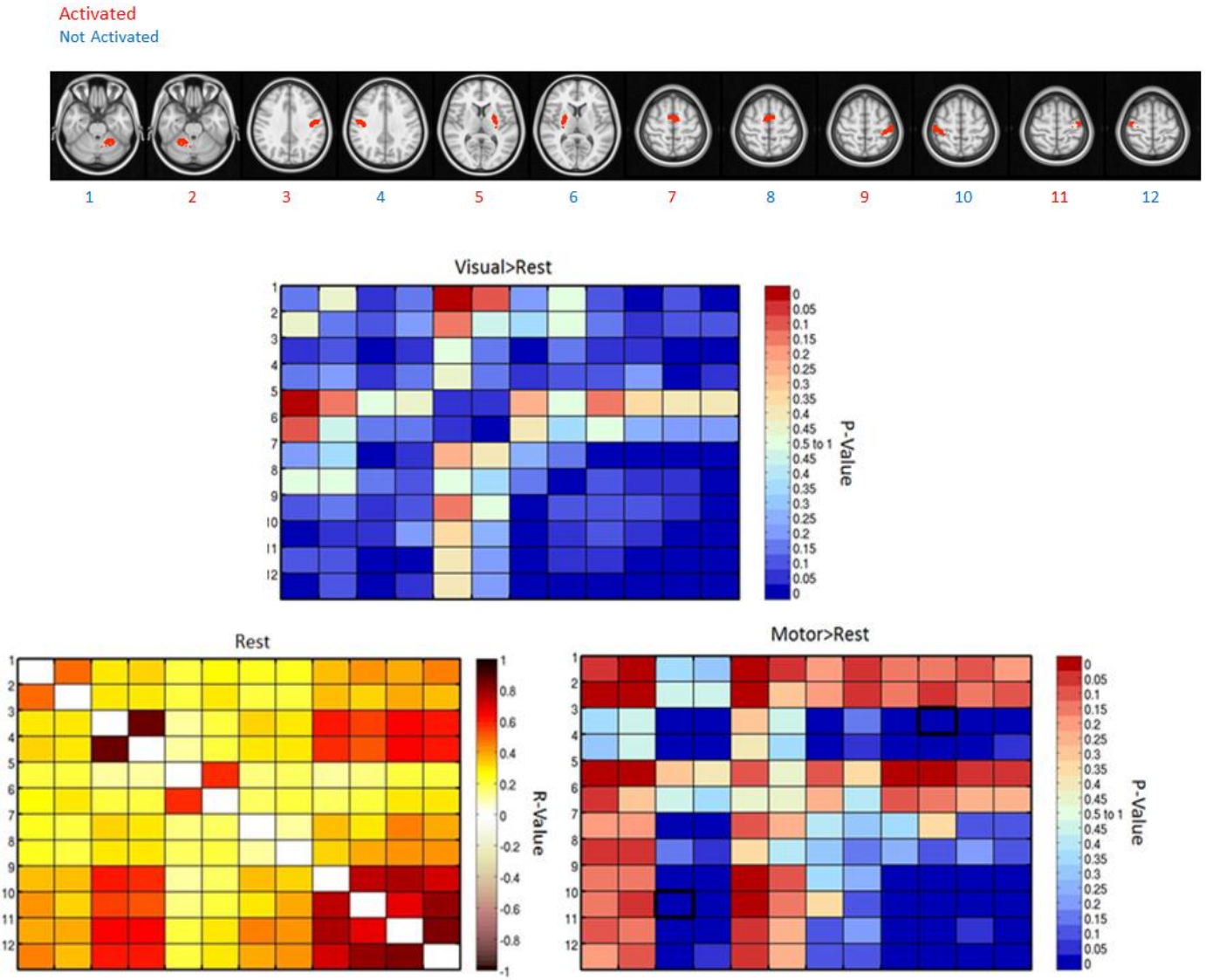


Figure 3.11: Overview of parcellation nodes (top), Raw correlation matrix (bottom left), visual task contrast (middle), motor task contrast (bottom right) for nodes in activated region and their mirrors. Pairs of nodes

which increase in value (covariance) are in red, and decreases are given in blue. Statistics which pass the test for multiple-comparisons are highlighted in black.

The bottom left panel in Figure 3.11 suggests that nodes are strongly connected to their mirror counterparts at rest. Every pair of regions except for the SMA, which was only partially lateralized to begin with, has a correlation value at or above .6. This fits with the fact that the cerebellar and sensorimotor ICNs are symmetrical, implying that regions in the left and right hemispheres are strongly correlated to one another during rest. During the visual steady-state condition these motor regions tend to decrease in functional connectivity to one another (with the exception of the putamen to the cerebellum)—a result seen before in Figure 3.9 amongst motor regions deactivated during the visual task. Additionally, during the motor steady-state condition the nodes which are in the lateral motor cortex (components 9-12) decrease in connectivity to one another. Interestingly, the results shown in the matrix extend the observation made concerning symmetry during the seed analysis (Figure 3.10) to all sub-nodes in the motor activation parcellation. In other words, flipped nodes which are not activated tend to closely mirror the changes in connectivity by their activated counterparts. To explore this phenomenon further, the activation map identified in Figure 3.2.2 was split into of the four loci of motor-task activated regions: hand area (as shown above in figure 3.11), SMA, left putamen, right cerebellum. Each was seeded along with its flipped version in the opposite hemisphere. These seed maps are shown below:

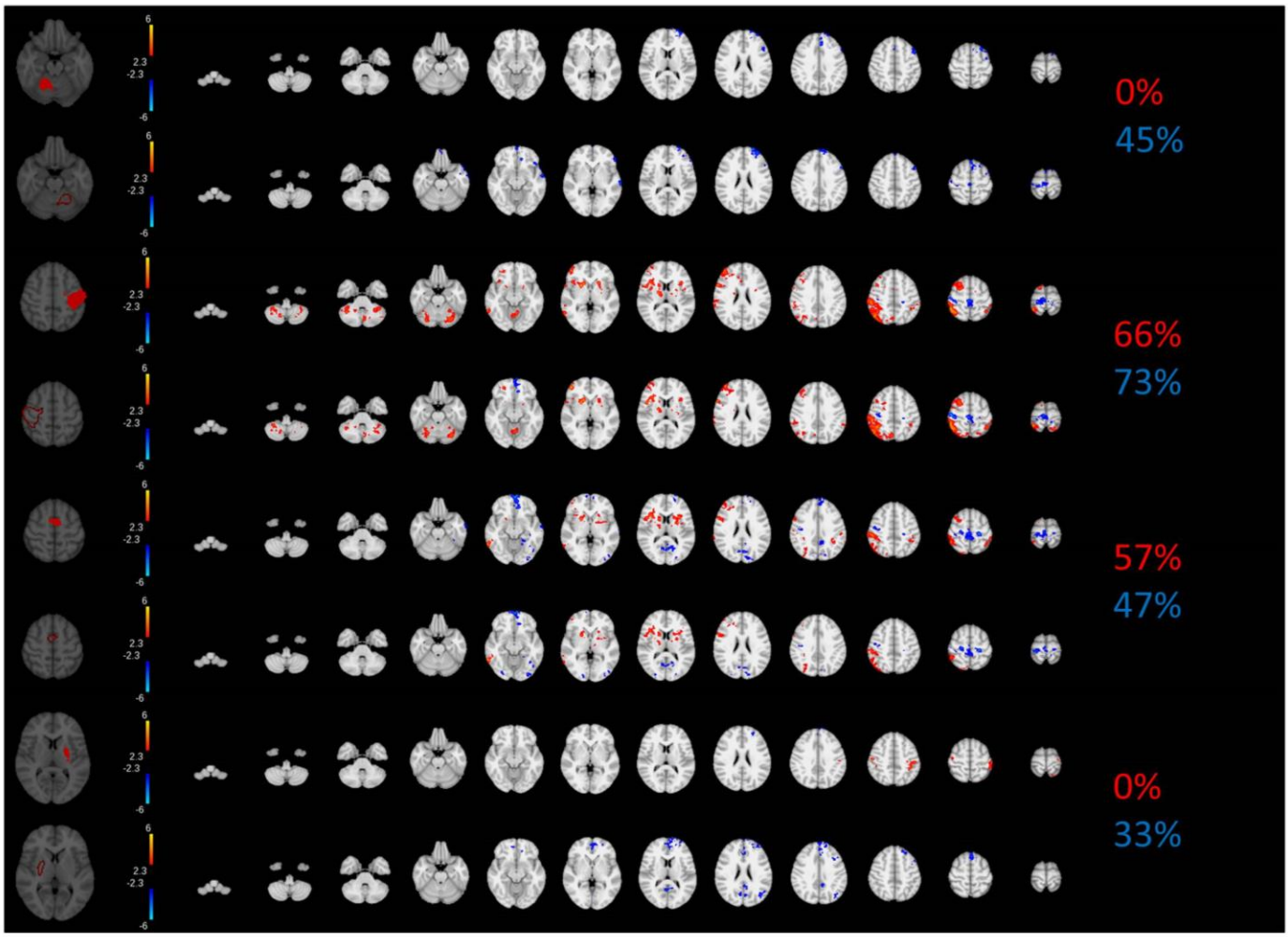


Figure 3.12: Changes in FC for four different loci of motor activation (cerebellum, M1, SMA, Putamen) and their mirror counterparts. Activations are shown in red, deactivations in blue. Z statistic was thresholded at 2.3. Percentage spatial overlap between FC changes (positive=red; negative=blue) with respect to the activated node are given for each set on the right.

The seed maps for each flipped and non-flipped locus mostly show a surprisingly high degree of correspondence, confirming the results shown in Figure 3.10. The activated portion of the putamen does not change in connectivity during the motor task in the same way that its flipped counterpart does, and the FC changes for the cerebellum node

seed do not show major similarity to its mirror node. The flipped and non-flipped hand area and SMA nodes share a high degree of similarity in their FC changes. It must be noted here, however, that the SMA was not purely lateralized and that there is spatial overlap in the two mirrored seeds. In short, the fact that a unilateral motor task shows bilateral changes in connectivity could mean that ICN structure influences changes in connectivity in nodes even when they are not directly activated.

We now investigate how these changes affect measurements of interactions between the SMN and other major RSNs:

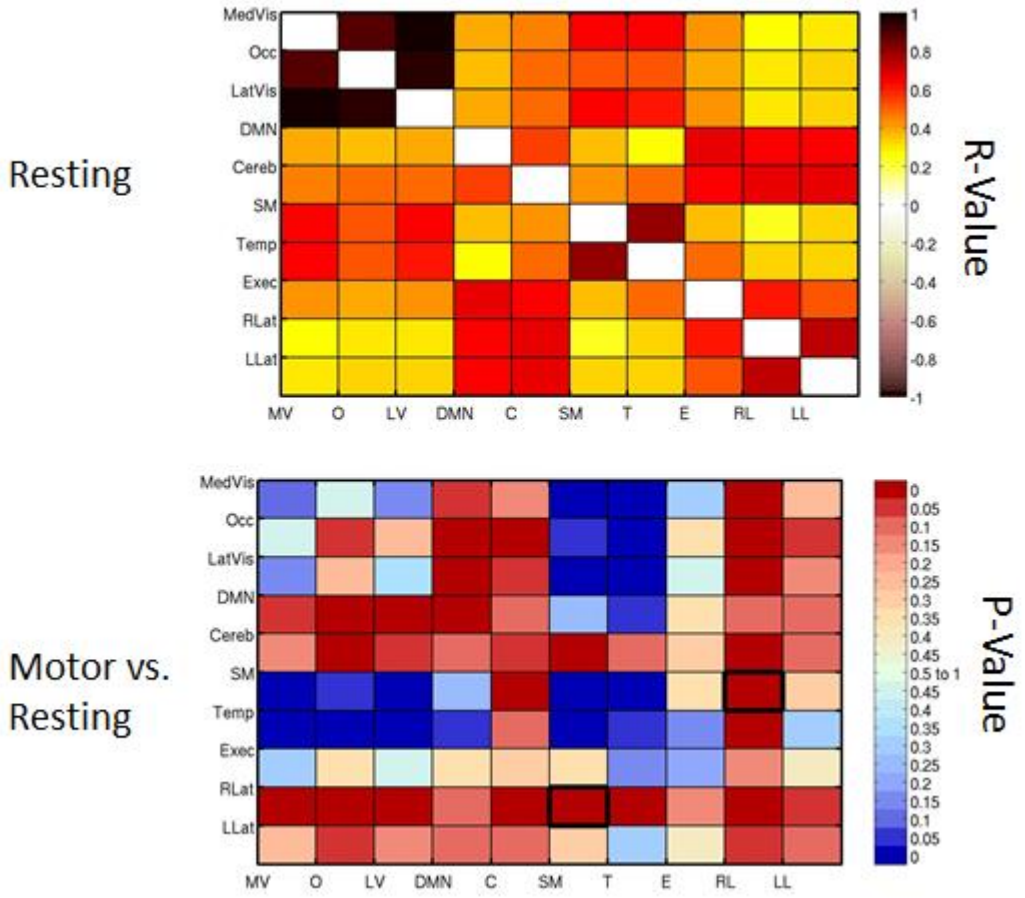


Figure 3.13: Resting correlation values (top) and Motor Task vs. Rest covariance contrasts (bottom) for the 10 canonical ICNs. Increases in connectivity during visual steady-state with respect to rest are shown in red, decreases in blue.

These matrices allow us to quickly visualize brain-wide changes in connectivity. The main results corroborate those seen in the activation matrices above (Figure 3.10). The sensorimotor ICN becomes dissociated from itself and the temporal ICN, and more connected to the right lateral ICN. Additionally, we observe that the cerebellum increases its connectivity with almost every ICN and that the DMN becomes more connected to visual areas. Extended versions of these figures, generated using the 94x94 matrices (Parcellation (1)) are featured in the Appendix (section A.2).

3.3.4.5 Combined Visual and Motor Task Steady-State

Finally, the changes of connectivity during the concurrent visual and motor task condition described in Section 3.2.1 were examined using both the visual and motor ROIs presented above. The contrast between visual-motor combined steady-state and rest appeared to simply superimpose the changes in FC seen during the individual task conditions (Appendix). Since we were interested in the effects unique to the combined condition and not simply those which resulted from linear addition of the effects of the two conditions, we also assessed maps generated using the interaction contrast described in Section 3.2.4, in which the effects of individual visual and motor steady-state tasks were subtracted from the effect of the visual-motor combined steady-state task condition.

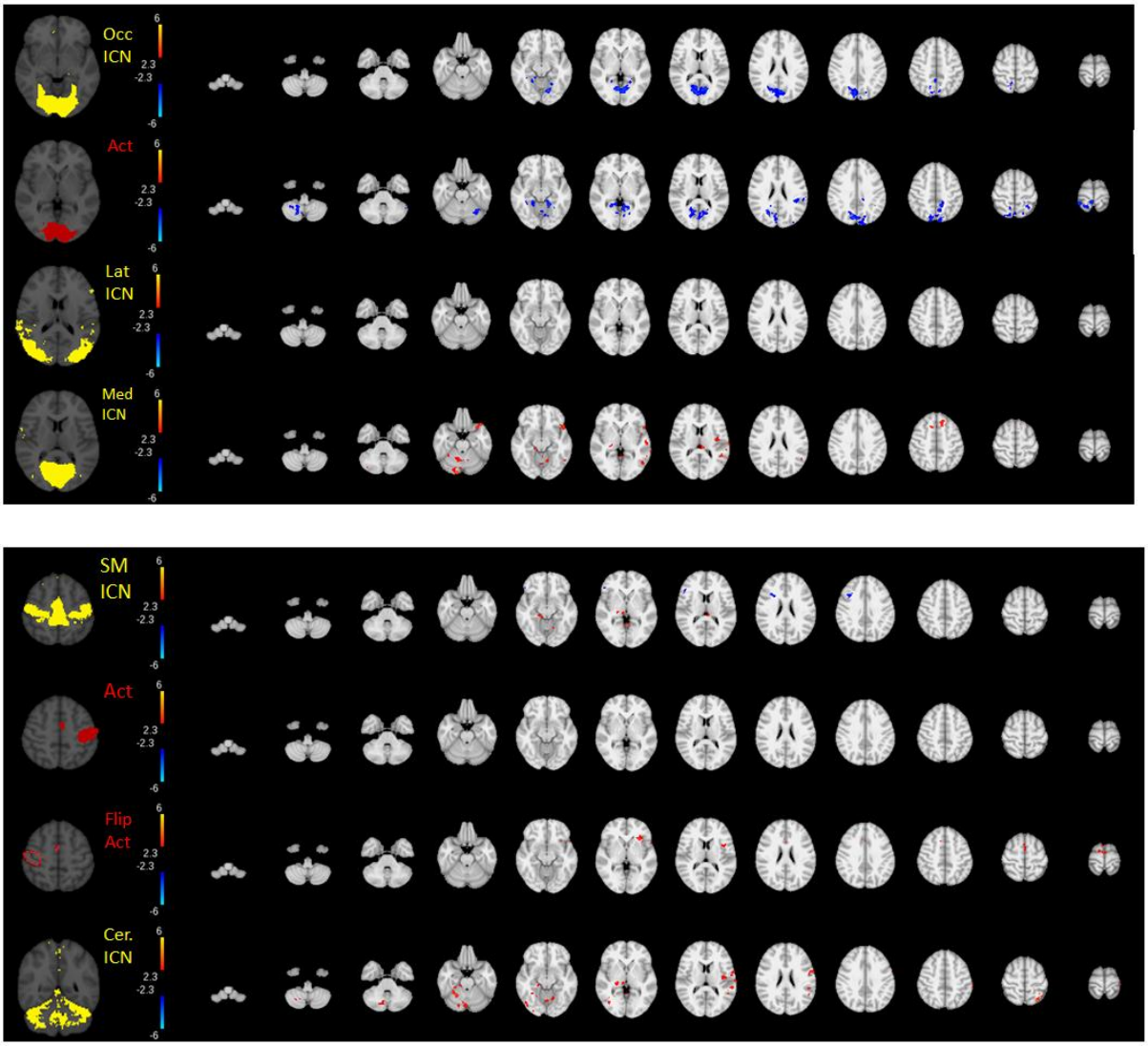


Figure 3.14: Seed analysis results for visual (top) and motor (bottom) ROIs during combined visual & motor steady-state task condition contrasted with separate motor and visual conditions. Threshold is at Z>2.3. Red areas are more connected with the ROI during task than rest and individual visual and motor task conditions, and blue areas less connected.

The top panel in Figure 3.14 shows the effects of interaction between visual and motor tasks in the combined condition for visual ROIs. The visual activation seed and occipital visual ICN show dissociation from the area covered by the medial visual ICN, implying that the combined condition serves to increase the amount of dissociation between the

foveal and medial visual areas compared to the visual-only steady state task. The medial visual ICN increases its connectivity with pre-frontal areas during the combined condition compared to either the visual or motor condition. It should be noted that this effect disappears upon raising the threshold of the statistical map to Z>3.

The effect of interaction between the visual and motor steady-state is shown in the bottom panel of Figure 3.14 for motor ROIs. While there are some patches showing effects, these changes were modest.

The sparseness of interactions between the motor and visual conditions means that the motor and visual steady-state tasks interact in a largely linear fashion. This finding confirms the reliability of the effects and shows that in the case of visual and motor steady-state tasks, FC changes interact in a simple, linear way. Since this was also observed in connectivity matrices, they are not presented here but are given in the Appendix.

3.4 Discussion

The aim of this section of the thesis is to investigate the effects of steady-state task modulation on ICN characteristics, functional connectivity, and relationship to task-activation. Previous research has shown that ICNs relating to cognitive domains such as the DMN and the executive control network not only persist during task performance, but alter their connectivity amongst one another in task-relevant ways (Shirer et al., 2012). However, this analysis has not been extended to other canonical ICNs unrelated to

cognition. Our work contributes to the understanding of the relationship between task and ICN connectivity by examining in detail the effects of visual and motor steady-state tasks on connectivity changes in major visual and motor ICNs.

3.4.1 ICN robustness and task-activation patterns

The first important result presented in Section 3.3 concerned the robustness of ICNs during task conditions. We found that ICNs remain undiminished and sometimes even strengthened during motor, visual, and motor-visual combined task conditions. This is analogous with the finding first put forth by Greicius & Menon (2004) that the DMN can be resolved through the use of ICA during a cognitive-processing block-design experiment and later extended to steady-state cognitive-processing paradigms by studies such as the one by Hampson et al. (2006). This finding provides additional support for the idea that ICNs remain coupled within themselves during task conditions and shows for the first time that this is true for *steady-states* (Sun et al, (2007) showed that the motor network persists during motor task conditions, but only during block-design bimanual motor experiments). The reason that showing ICNs persist during continuous task performance is important is that these are the only conditions under which conclusions about persistent ICN behaviour can be drawn—measurements of connectivity during transient states during block-designs might be confounded by time-dependent effects. Those networks which did not show excellent correlation to the canonical Smith 10 in Figure 3.3—namely the DMN, cerebellum, and sensorimotor network—still showed excellent correlation when task-state ICNs were compared to the resting-state ICN for the steady-state dataset.

Localiser scans taken during traditional block-design experiments involving the visual, motor, and visual-motor combined condition showed classical activation patterns (Allison, Meador, Loring, Figueroa, & Wright, 2000). The combined visual and motor condition proved to be essentially a summation of visual and motor activations, an effect which has also been observed previously (Calhoun, Adali, & Pekar, 2004). Exploring the linearity of the addition of the visual task to the motor task further in Section 3.3.4.5 (Figure 3.14), we saw that there is very little interaction between the two conditions with respect to changes in connectivity. One strong interaction during the combined condition is that the occipital ICN becomes even more dissociated from regions in the medial visual ICN. In general however, changes in connectivity by visual ROIs are very similar regardless of the presence or absence of a concurrent motor task, and vice versa. This additive property of visual and motor tasks has not been reported in the literature to our knowledge—it allows all the interesting results to be captured in the analysis of the motor and visual conditions separately.

3.4.2 Changes in FC during visual and motor tasks—relationship to activations

The goal of Section 3.3.4 was to investigate changes in functional connectivity between major ICNs and activation-based ROIs during steady-state motor and visual task performance. A detailed analysis of these changes for visual and motor-related networks is lacking in the literature. The sections below discuss results during the visual and motor tasks:

3.4.2.1 Visual Steady-State Condition

Figures 3.9 and 3.13 show the effects of visual and motor steady-state tasks on coupling between and within major ICNs. Though very few values in the matrices passed tests for multiple comparisons, some strong trends are present. The occipital visual and lateral visual ICNs tend to become more connected amongst and within themselves, while becoming strongly disconnected from the medial visual ICN. Because the visual task was designed to stimulate foveal areas, the task activation map overlaps with the occipital and partly with the lateral visual ICNs but not with the medial visual ICN. This implies that it is activated areas that become stronger in their FC to one another. To explore this further, activation and deactivation maps for the visual task were parcellated and used to generate correlation matrices (Figure 3.8). These matrices showed increased connectivity among most visually activated areas and decreased connectivity not only between activated and deactivated areas, but also amongst deactivated areas. These results strongly suggest that for the visual task, activation shapes changes in connectivity. Since activation coincided with the occipital and lateral visual ICNs, these networks increased their connectivity, and since the medial visual ICN coincided with deactivation, that network decreased in its connectivity. Many studies have examined the relationship between structural connectivity and functional connectivity (J. S. Damoiseaux & Greicius, 2009), but we could find none which specifically looked at the relationship between activation and FC. Therefore, we cannot be sure if our results are generalizable in the literature. More work will have to be carried out to firmly establish the results.

3.4.2.2 Motor Steady-State Condition & Activation-Connectivity Relationship

The pattern of changes in FC was rather different during motor task conditions. The motor ICN becomes less connected to itself during motor task and more connected to the cerebellum. Since parts of the motor cortex and the cerebellum are both activated during the motor task, this pattern of FC change suggests an effect similar to the seen in the visual system—activated areas become more connected to one another (one important caveat is that the cerebellum activation locus does not entirely overlap with the cerebellum ICN). The dissociation of the motor ICN amongst its own nodes might be a result of the lateralized activation accompanying a finger tapping task. This neither agrees with nor contradicts previous findings in the literature concerning connectivity in the motor cortex during task, which reported no changes in connectivity during unilateral or bilateral finger tapping tasks (Morgan & Price, 2001; Sun et al., 2007). Additionally, it has been reported by Newton et al. (2007) that finger tapping rate does not affect connectivity between the SMA and M1, while coupling between the cerebellar ROI and M1 increases with tapping rate, going along with our finding of increased connectivity between the cerebellar and sensorimotor ICNs (though Newton et al.'s study is not strictly equivalent because it combined finger tapping with auditory input). To explore this further, activated motor areas as well as their contra-lateral counterparts were parcellated and used to make connectivity matrices. Surprisingly, while activated areas did generally increase in their connectivity to one another (parts of the cerebellum, putamen, and M1), parts of the motor cortex which were also activated during task decreased in their connectivity to one another (i.e. M1, S1, and SMA) regardless of their hemisphere location. This indicates that, analogous to the situation between structural

and functional connectivity, it is not the case that regions which activate together connect together during task. In order to confirm this, the histograms in Figure 3.6 were generated. These plots show average correlation values across all subjects across all tasks and across all nodes (in the 94-node parcellation from Table 2.1) where no, one, or two nodes in each pairing increased in average activation value (determined by taking the average value under each node). The results, again, show that some pairings nodes increase and some decrease if they are activated together. Closer examination (A.1) showed that on average, visual and motor tasks elicit different sorts of changes in connectivity, with visual-task activated nodes tending to increase in their correlation to one another and motor-task activated nodes decreasing, with some increases. All this serves to corroborate the notion that changes in functional connectivity cannot be predicted simply from changes in activation as these changes are task and region-dependent, as first postulated by Morgan & Price (2001), who found after analysing three ROIs in the motor cortex that activation does not help predict changes in connectivity. While it is not clear what makes the motor and visual systems different, a main factor could be that the visual task is an input task while the motor is an output task. What this means is that the visual ICN may not need to communicate with other parts of the brain to process low-level images but to produce timed movement, the motor regions may need to interface with other networks. The difference between visual and motor FC changes might also have resulted from difference in laterality—the visual input was bilateral while the motor task was unilateral. Lateral inhibition could very well lead to dissociation of one side of the motor cortex from the other and has been observed in healthy patients using brain stimulation techniques (Ferbert et al., 1992). More

complex reasons for the differences could include varying intrinsic characteristics of visual and motor ICNs, including quantity and origin of neuronal inputs.

Going back to the changes in regional coupling observed during the motor steady-state task, another key result was that activated motor loci, when parcellated and used as seed ROIs, showed similar changes in connectivity to their contralateral counterparts. To investigate in more detail, each locus and its mirror image was seeded in a whole-brain seed analysis to produce statistical brain maps showing changes in connectivity (Figure 3.12). Surprisingly, M1 and the SMA show very similar changes in connectivity to their contralateral versions. Likewise, the seed in the cerebellum mirrored the deactivations of its flipped image. This result seems to indicate that regions not activated by task in the motor ICN are still influenced by regions that are perhaps reflecting that the coupling between nodes in the ICN does not disappear when one set is activated. This could be due to lasting structural links with the sensorimotor ICN, or common input pathways. In order to generalize this across networks, the effects of lateral task activation should be studied with other ICNs, most saliently the visual ICN. What we might expect to see in a hemi-field visual stimulus experiment is that changes in un-activated foveal areas match those in activated areas. Additional experiments could be conducted to further explore this very interesting symmetry effect seen in the motor ICN. Specifically, a bimanual steady-state motor task should be carried out in addition to a hemi-field visual task. Following the conclusions drawn from our results, we might expect to see an increase in overall motor ICN connectivity during the bimanual task, and a decrease in occipital visual ICN connectivity resulting from partial activation. Then contralateral seeds could

be taken in the visual cortex and connectivity could be assessed for similarity. The reason we might see this is due to the "fire together, wire together" principle. Since at rest bilateral regions within the sensorimotor ICN (for example) are coupled to one another, they also exhibit strong structural coupling (this was reviewed in Section 3.1). The changes in connectivity which take place on one side could mirror the other due to these structural connections, and even perhaps due to common neuronal inputs (which drive the resting state fluctuations).

Finally, we can consider the findings in Chapter 2 of this thesis in a new light based on the results in this section. The divergence of the results regarding the sensorimotor ICNs in the two studies—with one showing decreased connectivity and the other increased connectivity—also suggests that there is a fundamental difference between observing long-term and short-term changes in connectivity, and that care must be taken in applying findings from one to analyse another. Because there is a difference in the phenomena underlying long-term and short-term changes in behaviour and FC, changes across time-scales may not be scalable. However at a very fundamental level, both studies show strong links between changes in connectivity, no matter the direction, and behaviour.

4 Overall Summary & Future Directions

This thesis examined the effects of long-term and short-term modulation on Intrinsic Connectivity Networks in order to improve understanding of the relationship of connectivity to behaviour and task. The first study investigated long-term effects of motor rehabilitation on resting-state functional connectivity in stroke patients, and the second looked at the effects of more transient modulation in healthy subjects. In summary, our analysis of changes in ICN connectivity with continuously performed tasks did not provide support for the idea that ICNs are simply connected regions following a basic set of principles. Rather, ICN connectivity is a dynamic, complex, and task-dependent phenomenon. Long-term unilateral motor behaviour modulation in the form of therapy, for example, resulted in increased connectivity within the motor network while short-term unilateral continuous motor task performance resulted in decreased connectivity. Long-term modulation also resulted in changes in connectivity between the visual and motor ICNs, while short-term modulation did not result in any significant interaction between these two networks. These results may imply two fundamentally different mechanisms by which ICNs change over different time scales, both within and amongst themselves.

In these datasets alone there are many other analyses yet to be done: in depth analysis of the DMN, Temporal ICN, and higher-level cognitive ICNs was not carried despite their sometimes marked changes in connectivity. The additional steady-state attention task mentioned in the Section 3.2 was not analysed at all. Some of the reasons for this

included limited time and scope, and a realization after finding complex changes in motor and visual networks that instead of becoming easier, analysis of additional and more abstract ICNs could become even more complicated and opaque. Analysis of the stroke data in Chapter 2 using the matrix-parcellation methods utilized in Chapter 3 could also result in new insights missed in seed analyses. The issues which must be solved to conduct such an analysis include ways of spatially parcellating the areas around lesions and decisions regarding alignment of lesions to produce meaningful group effects.

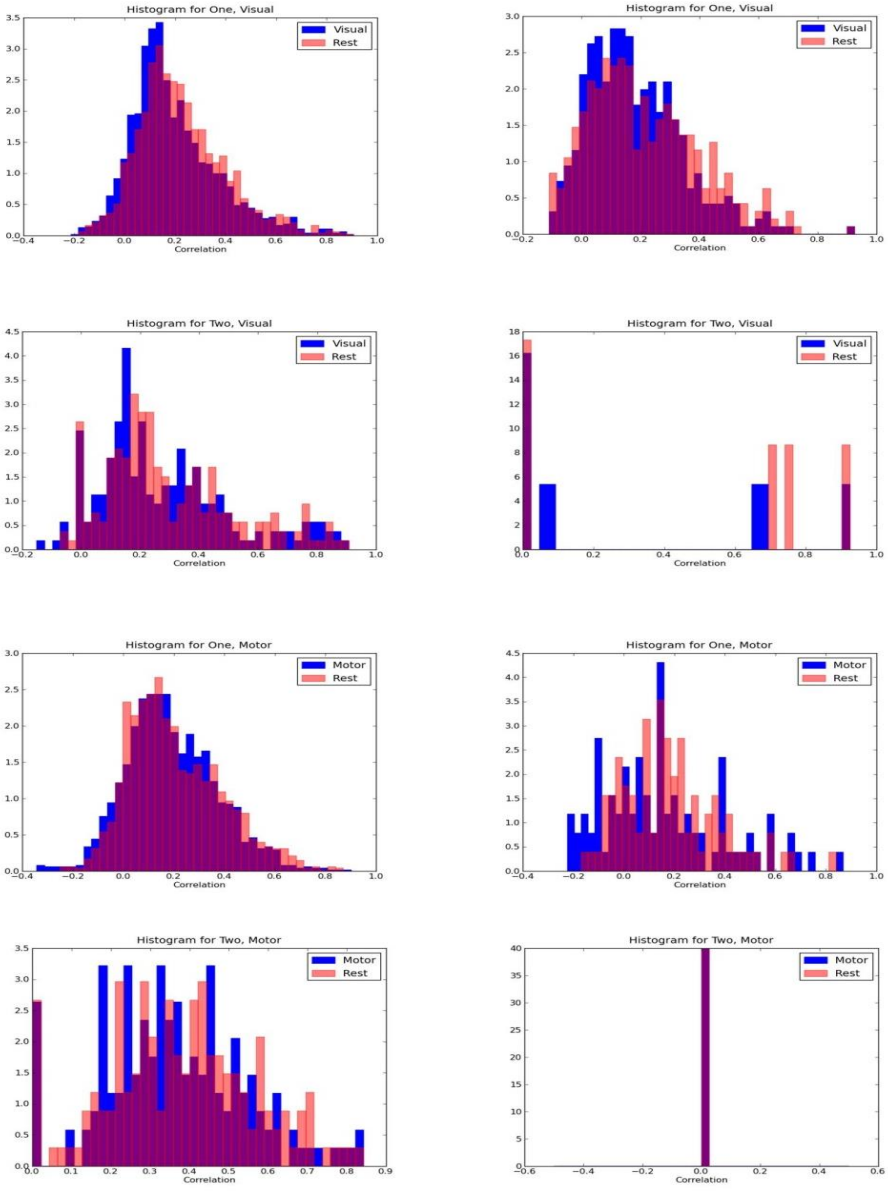
Another major direction that would be suitable for a larger work would be to investigate modulation of connectivity as a result of Transcranial Direct-Current Stimulation (tDCS). tDCS involves applying low direct-current to regions of the brain on the size order of several square centimetres. This changes neuronal activation thresholds depending on location and stimulation duration. It follows that tDCS can induce changes in both activation and functional connectivity in controlled ways. Several groups have done work in this field; for example Keeser et al. (2011) have found that application of tDCS to the dorsolateral prefrontal cortex increases resting-state connectivity of the DMN to the left and right "frontal-parietal" networks as the authors refer to them. During a block-design task, Alon, Roys, Gullapalli, & Greenspan (2011) found that applying cathodal tDCS over M1 actually *decreases* FC in the motor network. No tDCS experiments have been done during steady-state task, and none have used the ICA parcellation approached touted in this paper. With these methods, a systematic and global understanding of the effects of controlled connectivity modulation on rest and task performance could be

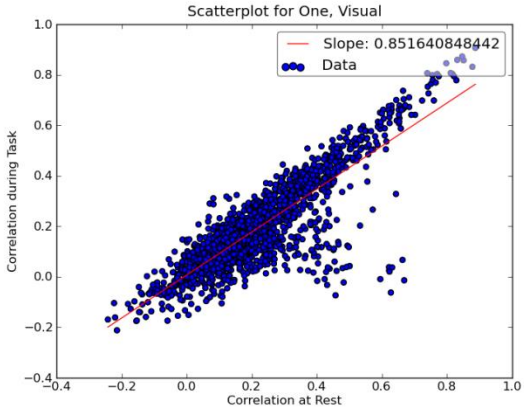
gained. The reason this would be valuable is because the significance of particular connectivity patterns observed in steady-state tasks might be ascertained through external perturbation. Similarly, the implied importance of FC as a either a marker or driver of recovery during stroke rehabilitation suggests an application for tDCS during therapy for stroke. A future study might assess the effects of tDCS in modulating connectivity in the motor cortex and correlation to behavioural outcomes.

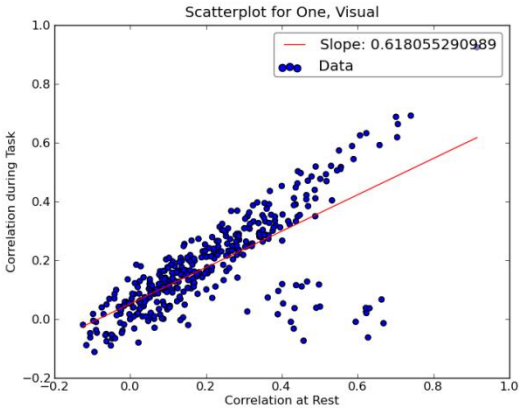
Overall, developing an understanding of how these networks, constantly communicating and fluctuating in the brains of every person (and indeed perhaps most animals) could greatly increase our understanding of this marvellous organ. The hope is that characterization of ICNs could reveal things regarding their origin and their purpose. Do they play a role in neuronal readiness? Consolidation? Memory? Or maybe do the eternal fluctuations allow sensory input to be processed slightly differently at different points in time, giving us multiple angles of input from the outside world? We also may be able to learn why and how disease and external modulation by drugs and current affect these networks, and what it means to our ability to process information and perform tasks. With the explosion of research in the field, there is no doubt the answers will soon be within our grasp.

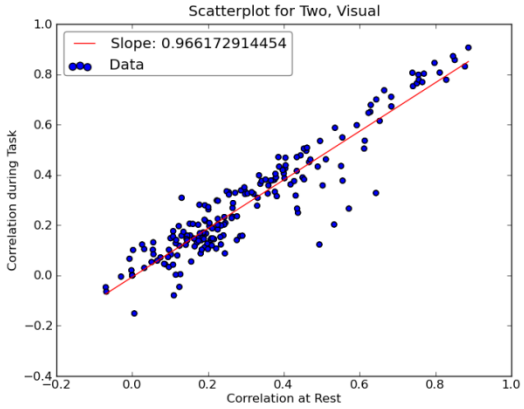
Appendix

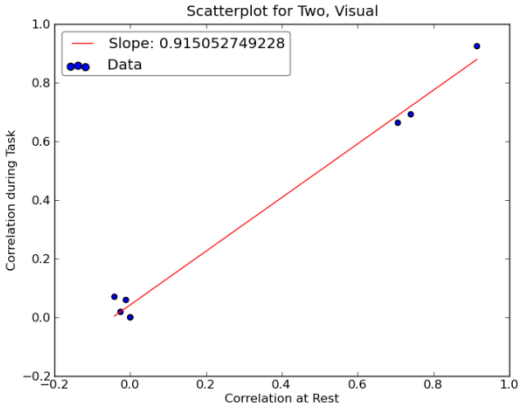
Figure A.1: (Top set) Histograms of correlations between pairings of nodes during task **activation (left column)** and **deactivation (right column)** of one or two nodes during each of the three task conditions (visual, motor, and visual & motor combined). (Bottom set) Scatterplots corresponding to the histograms in the top set (activation and deactivation in left and right column respectively) where each point represents a pair of nodes plotted according to correlation at rest (x-axis) and during task (y-axis).

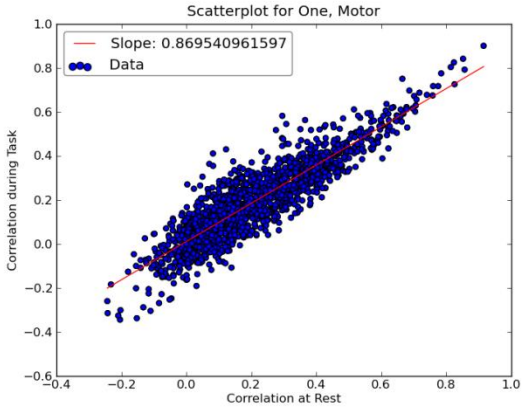


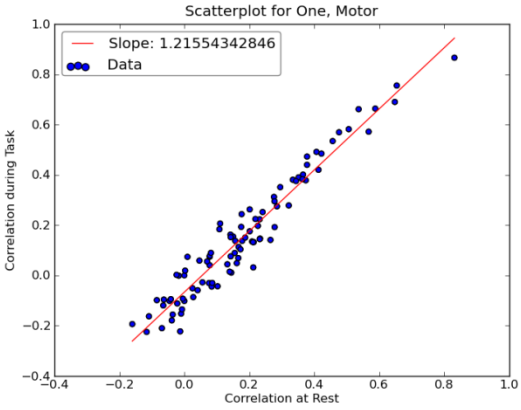

Scatterplot for One, Visual
Slope: 0.851640848442
Data
Correlation during Task
Correlation at Rest


Scatterplot for One, Visual
Slope: 0.618055290989
Data
Correlation during Task
Correlation at Rest


Scatterplot for Two, Visual
Slope: 0.966172914454
Data
Correlation during Task
Correlation at Rest


Scatterplot for Two, Visual
Slope: 0.915052749228
Data
Correlation during Task
Correlation at Rest


Scatterplot for One, Motor
Slope: 0.869540961597
Data
Correlation during Task
Correlation at Rest


Scatterplot for One, Motor
Slope: 1.21554342846
Data
Correlation during Task
Correlation at Rest

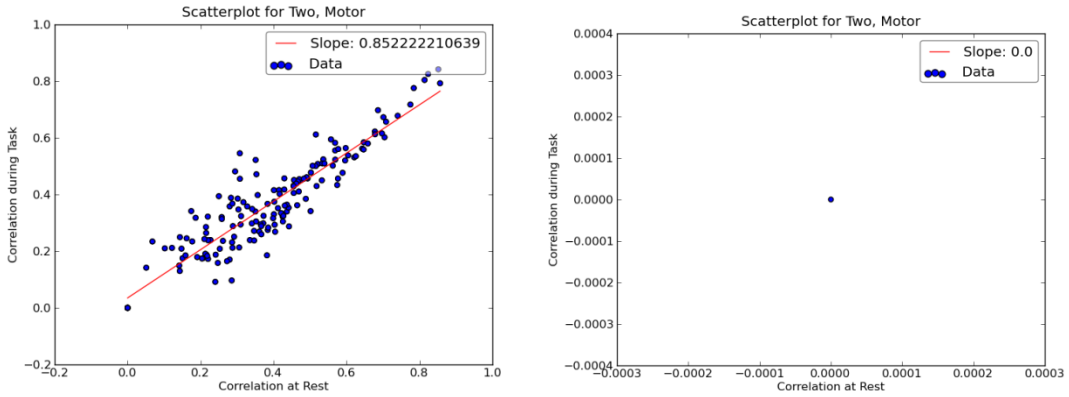
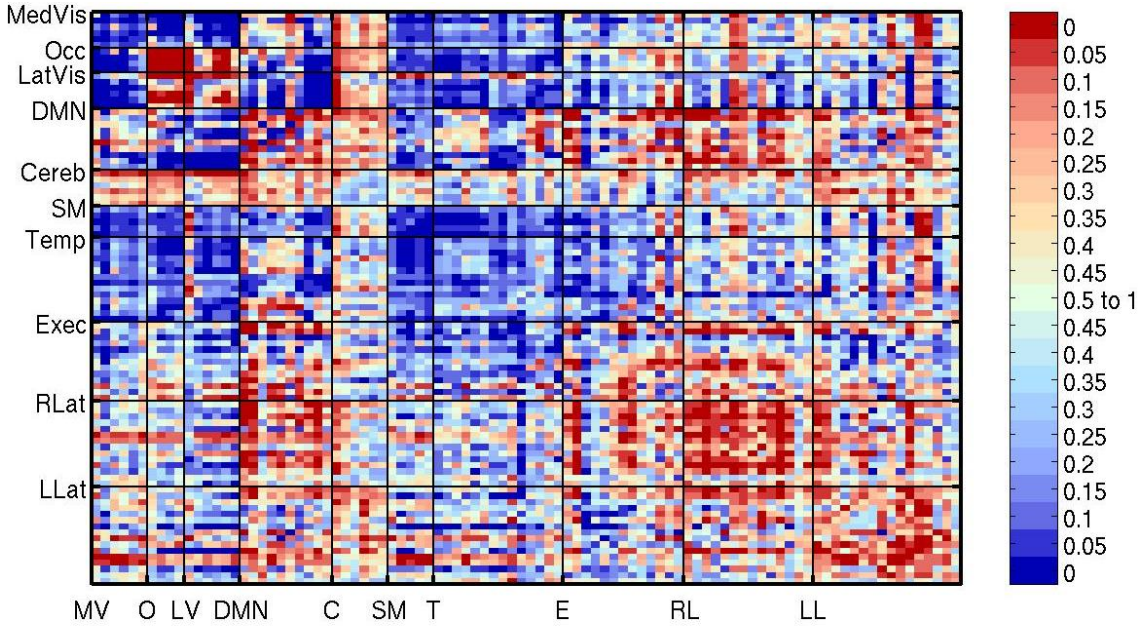
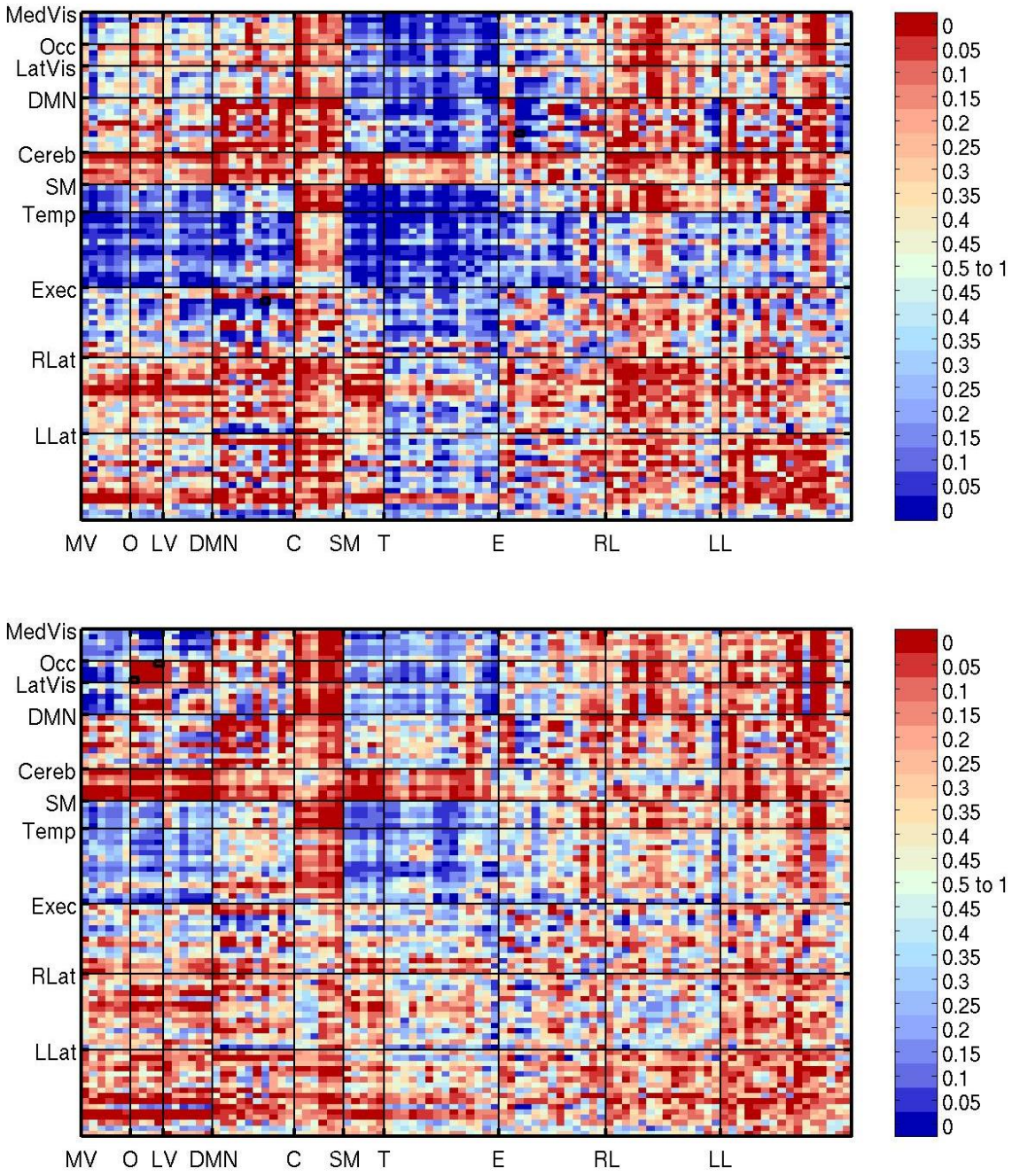


Figure A.2: Covariance matrix contrasts generated using the 94x94 Parcellation (1) for visual (top), motor (middle), and combined visual-motor steady-state task (bottom) conditions with respect to rest.





References

Achard, S., Salvador, R., Whitcher, B., Suckling, J., & Bullmore, E. (2006). A resilient, low-frequency, small-world human brain functional network with highly connected association cortical hubs. *The Journal of neuroscience : the official journal of the Society for Neuroscience*, *26*(1), 63–72. doi:10.1523/JNEUROSCI.3874-05.2006

Allison, J. D., Meador, K. J., Loring, D. W., Figueroa, R. E., & Wright, J. C. (2000). Functional MRI cerebral activation and deactivation during finger movement. *Neurology*, *54*(1), 135–135. doi:10.1212/WNL.54.1.135

Alon, G., Roys, S. R., Gullapalli, R. P., & Greenspan, J. D. (2011). Non-invasive electrical stimulation of the brain (ESB) modifies the resting-state network connectivity of the primary motor cortex: a proof of concept fMRI study. *Brain research*, *1403*, 37–44. doi:10.1016/j.brainres.2011.06.013

Beckmann, C. F., DeLuca, M., Devlin, J. T., & Smith, S. M. (2005). Investigations into resting-state connectivity using independent component analysis. *Philosophical transactions of the Royal Society of London. Series B, Biological sciences*, *360*(1457), 1001–13. doi:10.1098/rstb.2005.1634

Biswal, B., Yetkin, F. Z., Haughton, V. M., & Hyde, J. S. (1995). Functional Connectivity in the Motor Cortex of Resting. *Magnetic Resonance in Medicine*, *34*(9), 537–541.

Bolognini, N., Vallar, G., Casati, C., Latif, L. A., El-Nazer, R., Williams, J., … Fregni, F. (2011). Neurophysiological and behavioral effects of tDCS combined with constraint-induced movement therapy in poststroke patients. *Neurorehabilitation and neural repair*, *25*(9), 819–29. doi:10.1177/1545968311411056

Buckner, R. L., Krienen, F. M., & Yeo, B. T. T. (2013). Opportunities and limitations of intrinsic functional connectivity MRI. *Nature Neuroscience*, *16*(7), 832–837. doi:10.1038/nn.3423

Calhoun, V. D., Adali, T., & Pekar, J. J. (2004). A method for comparing group fMRI data using independent component analysis: application to visual, motor and visuomotor tasks. *Magnetic resonance imaging*, *22*(9), 1181–91. doi:10.1016/j.mri.2004.09.004

Carter, A. R., Astafiev, S. V, Lang, C. E., Connor, L. T., Rengachary, J., Strube, M. J., … Corbetta, M. (2010). Resting interhemispheric functional magnetic resonance imaging connectivity predicts performance after stroke. *Annals of neurology*, *67*(3), 365–75. doi:10.1002/ana.21905

Cordes, D., Haughton, V. M., Arfanakis, K., Carew, J. D., Turski, P. a, Moritz, C. H., … Meyerand, M. E. (2001). Frequencies contributing to functional connectivity in the cerebral cortex in "resting-state" data. *AJNR. American journal of neuroradiology*, *22*(7), 1326–33. Retrieved from http://www.ncbi.nlm.nih.gov/pubmed/11498421

Cordes, D., Haughton, V. M., Arfanakis, K., Wendt, G. J., Turski, P. a, Moritz, C. H., … Meyerand, M. E. (2000). Mapping functionally related regions of brain with functional connectivity MR imaging. *AJNR. American journal of neuroradiology*, *21*(9), 1636–44. Retrieved from http://www.ncbi.nlm.nih.gov/pubmed/11039342

Cudeck, R. (1989). Analysis of correlation matrices using covariance structure models. *Psychological Bulletin*. Retrieved from http://psycnet.apa.org/journals/bul/105/2/317/

Damoiseaux, J., & Rombouts, S. (2006). Consistent resting-state networks across healthy subjects. *Proceedings of the National Academy of Sciences of the United States of America*, *103*(37), 13848–13853. doi:10.1073/pnas.0601417103

Damoiseaux, J. S., & Greicius, M. D. (2009). Greater than the sum of its parts: a review of studies combining structural connectivity and resting-state functional connectivity. *Brain structure & function*, *213*(6), 525–33. doi:10.1007/s00429-009-0208-6

Deco, G., Ponce-Alvarez, a., Mantini, D., Romani, G. L., Hagmann, P., & Corbetta, M. (2013). Resting-State Functional Connectivity Emerges from Structurally and Dynamically Shaped Slow Linear Fluctuations. *Journal of Neuroscience*, *33*(27), 11239–11252. doi:10.1523/JNEUROSCI.1091-13.2013

Dimyan, M. a, & Cohen, L. G. (2011). Neuroplasticity in the context of motor rehabilitation after stroke. *Nature reviews. Neurology*, *7*(2), 76–85. doi:10.1038/nrneurol.2010.200

Doyon, J., & Benali, H. (2005). Reorganization and plasticity in the adult brain during learning of motor skills. *Current opinion in neurobiology*, *15*(2), 161–7. doi:10.1016/j.conb.2005.03.004

Duff, E. P., Johnston, L. a, Xiong, J., Fox, P. T., Mareels, I., & Egan, G. F. (2008). The power of spectral density analysis for mapping endogenous BOLD signal fluctuations. *Human brain mapping*, *29*(7), 778–90. doi:10.1002/hbm.20601

Eickhoff, S. B., Stephan, K. E., Mohlberg, H., Grefkes, C., Fink, G. R., Amunts, K., & Zilles, K. (2005). A new SPM toolbox for combining probabilistic cytoarchitectonic maps and functional imaging data, *25*, 1325–1335. doi:10.1016/j.neuroimage.2004.12.034

Fair, D. a, Schlaggar, B. L., Cohen, A. L., Miezin, F. M., Dosenbach, N. U. F., Wenger, K. K., … Petersen, S. E. (2007). A method for using blocked and event-related fMRI data to study "resting state" functional connectivity. *NeuroImage*, *35*(1), 396–405. doi:10.1016/j.neuroimage.2006.11.051

Ferbert, A., Priori, A., Rothwell, J. C., Day, B. L., Colebatch, J. G., & Mardsden, C. D. (1992). INTERHEMISPHERIC INHIBITION OF THE HUMAN MOTOR CORTEX. *Journal of Physiology*, (D), 525–546.

Friston, K J, Frith, C. D., Fletcher, P., Liddle, P. F., & Frackowiak, R. S. (1996). Functional topography: multidimensional scaling and functional connectivity in the brain. *Cerebral cortex (New York, N.Y. : 1991)*, *6*(2), 156–64. Retrieved from http://www.ncbi.nlm.nih.gov/pubmed/8670646

Friston, K. J. J., Frith, C. D., Liddle, P. F., & Frackowiak, R. S. J. (1993). Functional Connectivity: The Principal-Component analysis of Large (PET) Data Sets.

Friston, Karl J. (1994). Functional and effective connectivity in neuroimaging: A synthesis. *Human Brain Mapping*, *2*(1-2), 56–78. doi:10.1002/hbm.460020107

Gerstein, G L, Bedenbaugh, P., & Aertsen, M. H. (1989). Neuronal assemblies. *IEEE transactions on bio-medical engineering*, *36*(1), 4–14. doi:10.1109/10.16444

Gerstein, George L ., & Perkel, D. H. (1969). Simultaneously Recorded Trains of Action Potentials : Analysis and Functional Interpretation. *Science*, *164*(3881), 828–830.

Grefkes, C., Nowak, D. a, Eickhoff, S. B., Dafotakis, M., Küst, J., Karbe, H., & Fink, G. R. (2008). Cortical connectivity after subcortical stroke assessed with functional magnetic resonance imaging. *Annals of neurology*, *63*(2), 236–46. doi:10.1002/ana.21228

Greicius, M. D., & Menon, V. (2004). Default-mode activity during a passive sensory task: uncoupled from deactivation but impacting activation. *Journal of cognitive neuroscience*, *16*(9), 1484–92. doi:10.1162/0898929042568532

Greicius, M. D., Srivastava, G., Reiss, A. L., & Menon, V. (2004). Default-mode network activity distinguishes Alzheimer ' s disease from healthy aging : Evidence from functional MRI.

Greicius, M. D., Supekar, K., Menon, V., & Dougherty, R. F. (2009). Resting-state functional connectivity reflects structural connectivity in the default mode network. *Cerebral cortex (New York, N.Y. : 1991)*, *19*(1), 72–8. doi:10.1093/cercor/bhn059

Greve, D. N., & Fischl, B. (2009). Accurate and robust brain image alignment using boundary-based registration. *NeuroImage*, *48*(1), 63–72. doi:10.1016/j.neuroimage.2009.06.060

Hampson, M., Driesen, N. R., Skudlarski, P., Gore, J. C., & Constable, R. T. (2006). Brain connectivity related to working memory performance. *The Journal of neuroscience : the official journal of the Society for Neuroscience*, *26*(51), 13338–43. doi:10.1523/JNEUROSCI.3408-06.2006

Hampson, M., Olson, C. A. I. R., Leung, H., Skudlarski, P., & Gore, J. C. (2004). Changes in functional connectivity of human MT / V5 with visual motion input, *15*(8), 1315–1319. doi:10.1097/01.wnr.0000129997

Hampson, M., Peterson, B. S., Skudlarski, P., Gatenby, J. C., & Gore, J. C. (2002). Detection of functional connectivity using temporal correlations in MR images. *Human brain mapping*, *15*(4), 247–62. doi:10.1002/hbm.10022

Hodics, T., Cohen, L. G., & Cramer, S. C. (2006). Functional imaging of intervention effects in stroke motor rehabilitation. *Archives of physical medicine and rehabilitation*, *87*(12 Suppl 2), S36–42. doi:10.1016/j.apmr.2006.09.005

Honey, C J, Sporns, O., Cammoun, L., Gigandet, X., Thiran, J. P., Meuli, R., & Hagmann, P. (2009). Predicting human resting-state functional connectivity, *106*(6), 1–6.

Honey, Christopher J, & Sporns, O. (2008). Dynamical consequences of lesions in cortical networks. *Human brain mapping*, *29*(7), 802–9. doi:10.1002/hbm.20579

Hutchison, R. M., Womelsdorf, T., Allen, E. a., Bandettini, P. a., Calhoun, V. D., Corbetta, M., … Chang, C. (2013). Dynamic functional connectivity: Promises, issues, and interpretations. *NeuroImage*. doi:10.1016/j.neuroimage.2013.05.079

Jafri, M. J., Pearlson, G. D., Stevens, M., & Calhoun, V. D. (2008). A method for functional network connectivity among spatially independent resting-state components in schizophrenia. *NeuroImage*, *39*(4), 1666–81. doi:10.1016/j.neuroimage.2007.11.001

James, G. A., Lu, Z.-L., VanMeter, J. W., Sathian, K., Hu, X. P., & Butler, A. J. (2009). Changes in resting state effective connectivity in the motor network following rehabilitation of upper extremity poststroke paresis. *Topics in stroke rehabilitation*, *16*(4), 270–81. doi:10.1310/tsr1604-270

Jenkinson, M., Bannister, P., Brady, M., & Smith, S. (2002). Improved Optimization for the Robust and Accurate Linear Registration and Motion Correction of Brain Images. *NeuroImage*, *17*(2), 825–841. doi:10.1006/nimg.2002.1132

Jiang, L., Xu, H., & Yu, C. (2013). Brain connectivity plasticity in the motor network after ischemic stroke. *Neural plasticity*, *2013*, 924192. doi:10.1155/2013/924192

Jiang, T., He, Y., Zang, Y., & Weng, X. (2004). Modulation of functional connectivity during the resting state and the motor task. *Human brain mapping*, *22*(1), 63–71. doi:10.1002/hbm.20012

Johansen-Berg, H., Dawes, H., Guy, C., Smith, S. M., Wade, D. T., & Matthews, P. M. (2002). Correlation between motor improvements and altered fMRI activity after rehabilitative therapy. *Brain : a journal of neurology*, *125*(Pt 12), 2731–42. Retrieved from http://www.ncbi.nlm.nih.gov/pubmed/12429600

Johansen-Berg, H., Rushworth, M. F. S., Bogdanovic, M. D., Kischka, U., Wimalaratna, S., & Matthews, P. M. (2002). The role of ipsilateral premotor cortex in hand movement after stroke. *Proceedings of the National Academy of Sciences of the United States of America*, *99*(22), 14518–23. doi:10.1073/pnas.222536799

Johnston, J. M., Vaishnavi, S. N., Smyth, M. D., Zhang, D., He, B. J., Zempel, J. M., … Raichle, M. E. (2008). Loss of resting interhemispheric functional connectivity after complete

section of the corpus callosum. *The Journal of neuroscience : the official journal of the Society for Neuroscience*, *28*(25), 6453–8. doi:10.1523/JNEUROSCI.0573-08.2008

Kandel, E. R., Schwartz, J. H., Jessell, T. M., Siegelbaum, S. A., & Hudspeth, A. J. (2012). *Principles of Neural Science, Fifth Edition*. McGraw-Hill Medical.

Keeser, D., Meindl, T., Bor, J., Palm, U., Pogarell, O., Mulert, C., … Padberg, F. (2011). Prefrontal transcranial direct current stimulation changes connectivity of resting-state networks during fMRI. *The Journal of neuroscience : the official journal of the Society for Neuroscience*, *31*(43), 15284–93. doi:10.1523/JNEUROSCI.0542-11.2011

Kim, Y. H., You, S. H., Kwon, Y. H., Hallett, M., Kim, J. H., & Jang, S. H. (2006). Longitudinal fMRI study for locomotor recovery in patients with stroke. *Neurology*, *67*(2), 330–3. doi:10.1212/01.wnl.0000225178.85833.0d

Kreisel, S. H., Hennerici, M. G., & Bäzner, H. (2007). Pathophysiology of stroke rehabilitation: the natural course of clinical recovery, use-dependent plasticity and rehabilitative outcome. *Cerebrovascular diseases (Basel, Switzerland)*, *23*(4), 243–55. doi:10.1159/000098323

Laible, M., Grieshammer, S., Seidel, G., Rijntjes, M., Weiller, C., & Hamzei, F. (2012). Association of activity changes in the primary sensory cortex with successful motor rehabilitation of the hand following stroke. *Neurorehabilitation and neural repair*, *26*(7), 881–8. doi:10.1177/1545968312437939

Lowe, M. J., Dzemidzic, M., Lurito, J. T., Mathews, V. P., & Phillips, M. D. (2000). Correlations in low-frequency BOLD fluctuations reflect cortico-cortical connections. *NeuroImage*, *12*(5), 582–7. doi:10.1006/nimg.2000.0654

Morgan, V., & Price, R. R. (2001). Dependence of Functional Connectivity on Functional State of the Brain, *9*, 2001.

Murphy, K., Birn, R. M., Handwerker, D. a, Jones, T. B., & Bandettini, P. a. (2009). The impact of global signal regression on resting state correlations: are anti-correlated networks introduced? *NeuroImage*, *44*(3), 893–905. doi:10.1016/j.neuroimage.2008.09.036

Newton, A. T., Morgan, V. L., & Gore, J. C. (2007). Task demand modulation of steady-state functional connectivity to primary motor cortex. *Human brain mapping*, *28*(7), 663–72. doi:10.1002/hbm.20294

Newton, A. T., Morgan, V. L., Rogers, B. P., & Gore, J. C. (2011). Modulation of steady state functional connectivity in the default mode and working memory networks by cognitive load. *Human brain mapping*, *32*(10), 1649–59. doi:10.1002/hbm.21138

Nir, Y., Mukamel, R., Dinstein, I., Privman, E., Harel, M., Fisch, L., … Malach, R. (2008). Interhemispheric correlations of slow spontaneous neuronal fluctuations revealed in human sensory cortex. *Nature Neuroscience*, *11*(9), 1100–1108. doi:10.1038/nn.2177

O'Reilly, J. X., Woolrich, M. W., Behrens, T. E. J., Smith, S. M., & Johansen-Berg, H. (2012). Tools of the trade: psychophysiological interactions and functional connectivity. *Social cognitive and affective neuroscience*, *7*(5), 604–9. doi:10.1093/scan/nss055

Park, C., Chang, W. H., Ohn, S. H., Kim, S. T., Bang, O. Y., Pascual-Leone, A., & Kim, Y.-H. (2011). Longitudinal changes of resting-state functional connectivity during motor recovery after stroke. *Stroke; a journal of cerebral circulation*, *42*(5), 1357–62. doi:10.1161/STROKEAHA.110.596155

Pettersson-Yeo, W., Allen, P., Benetti, S., McGuire, P., & Mechelli, A. (2011). Dysconnectivity in schizophrenia: where are we now? *Neuroscience and biobehavioral reviews*, *35*(5), 1110–24. doi:10.1016/j.neubiorev.2010.11.004

Sakoğlu, U., Pearlson, G. D., Kiehl, K. a, Wang, Y. M., Michael, A. M., & Calhoun, V. D. (2010). A method for evaluating dynamic functional network connectivity and task-modulation: application to schizophrenia. *Magma (New York, N.Y.)*, *23*(5-6), 351–66. doi:10.1007/s10334-010-0197-8

Sawaki, L., Butler, A. J., Leng, X., Wassenaar, P. a, Mohammad, Y. M., Blanton, S., … Wittenberg, G. F. (2008). Constraint-induced movement therapy results in increased motor map area in subjects 3 to 9 months after stroke. *Neurorehabilitation and neural repair*, *22*(5), 505–13. doi:10.1177/1545968308317531

Schölvinck, M. L. L., Friston, K. J. J., & Rees, G. (2011). The influence of spontaneous activity on stimulus processing in primary visual cortex. *NeuroImage*, *59*(3), 2700–8. doi:10.1016/j.neuroimage.2011.10.066

Seeley, W. W., Menon, V., Schatzberg, A. F., Keller, J., Glover, G. H., Kenna, H., … Greicius, M. D. (2007). Dissociable intrinsic connectivity networks for salience processing and executive control. *The Journal of neuroscience : the official journal of the Society for Neuroscience*, *27*(9), 2349–56. doi:10.1523/JNEUROSCI.5587-06.2007

Seitz, R. J., Azari, N. P., Knorr, U., Binkofski, F., Herzog, H., & Freund, H.-J. (1999). The Role of Diaschisis in Stroke Recovery. *Stroke*, *30*(9), 1844–1850. doi:10.1161/01.STR.30.9.1844

Sergi, F., Krebs, H. I., Groissier, B., Rykman, A., Guglielmelli, E., Volpe, B. T., & Schaechter, J. D. (2011). Predicting efficacy of robot-aided rehabilitation in chronic stroke patients using an MRI-compatible robotic device. *Conference proceedings : ... Annual International Conference of the IEEE Engineering in Medicine and Biology Society. IEEE Engineering in Medicine and Biology Society. Conference*, *2011*, 7470–3. doi:10.1109/IEMBS.2011.6091843

Sharma, N., Baron, J.-C., & Rowe, J. B. (2009). Motor imagery after stroke: relating outcome to motor network connectivity. *Annals of neurology*, *66*(5), 604–16. doi:10.1002/ana.21810

Shirer, W. R., Ryali, S., Rykhlevskaia, E., Menon, V., & Greicius, M. D. (2012). Decoding Subject-Driven Cognitive States with Whole-Brain Connectivity Patterns. *Cerebral Cortex*, *22*(1), 158–165. doi:10.1093/cercor/bhr099

Shmuel, A., & Leopold, D. a. (2008). Neuronal correlates of spontaneous fluctuations in fMRI signals in monkey visual cortex: Implications for functional connectivity at rest. *Human brain mapping*, *29*(7), 751–61. doi:10.1002/hbm.20580

Shmuel, A., Yacoub, E., Pfeuffer, J., Van de Moortele, P. F., Adriany, G., Hu, X., & Ugurbil, K. (2002). Sustained negative BOLD, blood flow and oxygen consumption response and its coupling to the positive response in the human brain. *Neuron*, *36*(6), 1195–210. Retrieved from http://www.ncbi.nlm.nih.gov/pubmed/12495632

Smith, S. M., Fox, P. T., Miller, K. L., Glahn, D. C., Fox, P. M., Mackay, C. E., … Beckmann, C. F. (2009). Correspondence of the brain's functional architecture during activation and rest. *Proceedings of the National Academy of Sciences of the United States of America*, *106*(31), 13040–5. doi:10.1073/pnas.0905267106

Smith, S. M., Jenkinson, M., Woolrich, M. W., Beckmann, C. F., Behrens, T. E. J., Johansen-Berg, H., … Matthews, P. M. (2004). Advances in functional and structural MR image analysis and implementation as FSL. *NeuroImage*, *23 Suppl 1*, S208–19. doi:10.1016/j.neuroimage.2004.07.051

Sridharan, D., Levitin, D. J., & Menon, V. (2008). A critical role for the right fronto-insular cortex in switching between central-executive and default-mode networks. *Proceedings of the National Academy of Sciences of the United States of America*, *105*(34), 12569–74. doi:10.1073/pnas.0800005105

Sun, F. T., Miller, L. M., Rao, A. a, & D'Esposito, M. (2007). Functional connectivity of cortical networks involved in bimanual motor sequence learning. *Cerebral Cortex*, *17*(5), 1227–1234. doi:10.1093/cercor/bhl033

Tombari, D., Loubinoux, I., Pariente, J., Gerdelat, A., Albucher, J.-F., Tardy, J., … Chollet, F. (2004). A longitudinal fMRI study: in recovering and then in clinically stable sub-cortical stroke patients. *NeuroImage*, *23*(3), 827–39. doi:10.1016/j.neuroimage.2004.07.058

Tyszka, J. M., Kennedy, D. P., Adolphs, R., & Paul, L. K. (2011). Intact bilateral resting-state networks in the absence of the corpus callosum. *J Neurosci*, *%19;31*(42), 15154–15162. doi:10.1523/JNEUROSCI.1453-11.2011

Ungerleider, L. (1995). Functional MRI evidence for adult motor cortex plasticity during motor skill learning. *Nature*, (377), 155–158. Retrieved from http://lbcnimh.nih.gov/Ungerleider/Publications/Karni_et_al_Nature_1995.pdf

Vahdat, S., Darainy, M., Milner, T. E., & Ostry, D. J. (2011). Functionally specific changes in resting-state sensorimotor networks after motor learning. *The Journal of neuroscience : the official journal of the Society for Neuroscience*, *31*(47), 16907–15. doi:10.1523/JNEUROSCI.2737-11.2011

Van Dijk, K. R. a, Hedden, T., Venkataraman, A., Evans, K. C., Lazar, S. W., & Buckner, R. L. (2010). Intrinsic functional connectivity as a tool for human connectomics: theory, properties, and optimization. *Journal of neurophysiology*, *103*(1), 297–321. doi:10.1152/jn.00783.2009

Van Essen, D. C., Ugurbil, K., Auerbach, E., Barch, D., Behrens, T. E. J., Bucholz, R., … Yacoub, E. (2012). The Human Connectome Project: a data acquisition perspective. *NeuroImage*, *62*(4), 2222–31. doi:10.1016/j.neuroimage.2012.02.018

Vincent, J. L., Patel, G. H., Fox, M. D., Snyder, a Z., Baker, J. T., Van Essen, D. C., … Raichle, M. E. (2007). Intrinsic functional architecture in the anaesthetized monkey brain. *Nature*, *447*(7140), 83–6. doi:10.1038/nature05758

Wang, L. E., Fink, G. R., Diekhoff, S., Rehme, A. K., Eickhoff, S. B., & Grefkes, C. (2011). Noradrenergic enhancement improves motor network connectivity in stroke patients. *Annals of neurology*, *69*(2), 375–88. doi:10.1002/ana.22237

Wang, L., Yu, C., Chen, H., Qin, W., He, Y., Fan, F., … Zhu, C. (2010). Dynamic functional reorganization of the motor execution network after stroke. *Brain : a journal of neurology*, *133*(Pt 4), 1224–38. doi:10.1093/brain/awq043

Westlake, K. P., & Nagarajan, S. S. (2011). Functional connectivity in relation to motor performance and recovery after stroke. *Frontiers in systems neuroscience*, *5*(March), 8. doi:10.3389/fnsys.2011.00008

White, T. P., Joseph, V., Francis, S. T., & Liddle, P. F. (2010). Aberrant salience network (bilateral insula and anterior cingulate cortex) connectivity during information processing in schizophrenia. *Schizophrenia research*, *123*(2-3), 105–15. doi:10.1016/j.schres.2010.07.020

Wittenberg, G. F., & Schaechter, J. D. (2009). The neural basis of constraint-induced movement therapy. *Current opinion in neurology*, *22*(6), 582–8. doi:10.1097/WCO.0b013e3283320229

Wolf, S. L., Catlin, P. a., Ellis, M., Archer, a. L., Morgan, B., & Piacentino, a. (2001). Assessing Wolf Motor Function Test as Outcome Measure for Research in Patients After Stroke. *Stroke*, *32*(7), 1635–1639. doi:10.1161/01.STR.32.7.1635

Wolf, Steven L, Winstein, C. J., Miller, J. P., & Morris, D. (2006). Effect of Constraint-Induced Movement, *296*(17), 2095–2104.

Xiong, J., Parsons, L. M., Gao, J. H., & Fox, P. T. (1999). Interregional connectivity to primary motor cortex revealed using MRI resting state images. *Human brain mapping*, *8*(2-3), 151–6. Retrieved from http://www.ncbi.nlm.nih.gov/pubmed/10524607

Yeo, B. T. T., Krienen, F. M., Sepulcre, J., Sabuncu, M. R., Lashkari, D., Hollinshead, M., … Buckner, R. L. (2011). The organization of the human cerebral cortex estimated by intrinsic functional connectivity. *Journal of neurophysiology*, *106*(3), 1125–65. doi:10.1152/jn.00338.2011